On the Techno-Economic Merits and Challenges of Clean Hybrid Energy Systems in Contemporary Power Systems

by

James William Hurtt

B.S., Virginia Polytechnic Institute and State University, 2007

M.S., Virginia Polytechnic Institute and State University, 2012

A thesis submitted to the

Faculty of the Graduate School of the

University of Colorado in partial fulfillment

of the requirement for the degree of

Doctor of Philosophy

Department of Electrical, Computer, and Energy Engineering

2024

Committee Members:

Prof. Kyri Baker

Prof. Lucy Pao

Prof. Bri-Mathias Hodge

Prof. Michael Walker

Prof. Mark Deinert

Hurtt, James William (Ph.D., Electrical Engineering)

On the Techno-Economic Merits and Challenges of Clean Hybrid Energy Systems in Contemporary Power Systems

Thesis directed by Assistant Professor Kyri Baker

One of the principal challenges of the 21st century is the reduction of human generated greenhouse gas emissions (GHG). The modern electric power sector is a large contributor to GHG due to its high utilization of fossil fuel-based sources. Fossil fuels have the benefit of high flexibility and relatively low cost (both capital and operating), with the drawback of high lifecycle emissions. Clean energy sources exist in the form of renewable and nuclear energy, but they are constrained operationally and financially. This thesis evaluates a hybrid energy system (HES) employing solar photovoltaics (PV) and wind turbine generators (WTG) electrically coupled with a small modular reactor (SMR) to provide flexible and cost-effective clean energy. Energy storage in the form of a battery energy storage system (BESS) for ramp rate regulation & frequency response and hydrogen (H2) via electrolysis as a co-product are employed to optimize these sources. A high-fidelity power model, using minute-scale environmental data, utilizing a detailed SMR plant model was developed to evaluate the dynamic operation, annual energy production, and financial viability of multiple HES configurations. Additionally, a transient model with sub-second time sampling was built to ensure the optimal economic solution can also meet bounding transient cases. As the result of this thesis show, an HES can meet the contemporary demands of contemporary power systems, but the financial viability is dependent on government subsidies, or significant progress being made on reducing SMR capital cost, or improving the value of hydrogen storage.

Dedication

To the countless people who have offered a helping hand and words of encouragement throughout my life.

Acknowledgements

First and foremost, I need to acknowledge my advisor, Dr. Kyri Baker, for patiently putting up with me while I slowly worked on my research topic at a remarkably slow pace. Kyri has been a source of motivation and positive feedback throughout my studies. I do not believe I would have been able to complete a part time PhD program with anyone else as my advisor.

I'd also like to acknowledge my committee members: Dr.'s Pao, Walker, Deinert and Hodge. All of whom took time out of their respective busy schedules to sit on my committee and all went above and beyond to provide feedback and support to me outside of the typical expectations as a committee member.

I also want to acknowledge the support of my friends and colleagues who took an interest in my research and provided thoughtful feedback, and the occasional thought-provoking debate on the topic. I am also grateful and indebted to all the brilliant minds I've encountered both professionally and academically that instilled in me a high standard of engineering excellence and a strong work ethic. They include Michael Ozpolat (deceased), Lou Larkin (deceased), Jonathan Hexter, Dr. Lamine Mili, Dr. Yilu Liu, Chris Wright, Dr. Marija Markovic, Dr. Jennifer Atteberry, Silvia Giron Viesca, and Charlie Hamp.

Finally, I need to acknowledge my family. From my parents, Thomas (deceased) and Dorothy Hurtt, for they always encouraged me in my studies. My grandfather, G. Daniel Hembree (deceased), who saw something in me from a young age and always encouraged me. My brother Tom, for being a great role model for me throughout my life. My wife, Barbara, for putting up with my long nights of running simulations and writing papers, as well as endless encouragement. Finally, my children, Daniel and Amelia, for inspiring me to make a minor contribution towards making the world a better place for them.

Table of Contents

List of Tables

List of Figures

List of Acronyms and Abbreviations

AC	Alternating Current
AOI	Angle of Incidence
BESS	Battery Energy Storage System
CF	Capacity Factor
DC	Direct Current
DHI	Diffused Horizontal Irradiance
DNI	Direct Normal Irradiance
DOD	Depth of Discharge
EIA	Energy Information Administration
FR	Frequency Response
GHG	Greenhouse Gas Emissions
GHI	Global Horizontal Irradiance
H2	Hydrogen
HES	Hybrid Energy System
HOPP	Hybrid Optimization and Performance Platform
IAEA	International Atomic Energy Administration
IEEE	Institute of Electrical and Electronics Engineers
IES	Integrated Energy System
INL	Idaho National Laboratory
IRA	Inflation Reduction Act
IRR	Internal Rate of Return
ITC	Investment Tax Credit
LCOE	Levelized Cost of Energy
MIDC	Measurement and Instrumentation Database Center
NASA	National Aeronautics and Space Administration
NERC	North American Electric Reliability Corporation
NPV	Net Present Value
NREL	National Renewable Energy Laboratory
NSRDB	National Solar Radiation Database
PEM	Proton Exchange Membrane
PGE	Portland Gas & Electric
PID	Proportional Integral Differential
POA	Plane of Array
PPA	Power Purchase Agreement
PSS/E	Power System Simulation for Engineering
PTC	Production Tax Credit
PV	Photovoltaic
PWR	Pressurized Water Reactor
RF	Rainflow

RR	Ramp Rate
SMA	System, Mess and Anlagentechnik
SMR	Small Modular Reactor
SOC	State of Charge
UK	United Kingdom
UO	University of Oregon
USGS	United States Geological Survey
WACM	Western Area Power Administration – Rocky Mountain Region
WECC	Western Electricity Coordinating Council
WTG	Wind Turbine Generator

List of Symbols and Variables

a	Wind speed adjustment factor based on terrain (set to 0.34)
α_{PV}	PV cell power temperature coefficient in %/°C
β	Delayed neutron fraction (0.007)
Δh	Change in turbine enthalpy in kJ/kg
ΔT	Temperature delta from module to cell (selected to be +3°C for polycrystalline)
δV	Incremental change in wind speed due to wake effects in m/s
η_{elec}	SMR synchronous generator efficiency in %
η_{elec_f}	Electrolyzer electrical efficiency in %
η_f	Faraday conversion efficiency in %
η_{turb}	Turbine efficiency in %
$\eta_{inv}(P_{dc})$	Inverter efficiency as a function of input DC power in %
η_{mod}	Module efficiency in %
θ_A	Solar azimuth angle in degrees
$\theta_{A,array}$	Solar array azimuth angle in degrees
θ_T	Solar array tilt angle in degrees
θ_z	Solar zenith angle in degrees

λ	Neutron decay constant (0.1 s^{-1})
Λ	Prompt neutron lifetime constant ($2x10^{-5}$ s)
ρ	Net reactor core reactivity in per unit
ρ_{air}	Air density in kg per cubic meters
ρ_{inlet}	Inlet steam pressure into turbine
τ	Thermal power fraction (0.97)
φ_f	Average fractional reactor flux in per unit
ψ_d, ψ_q, ψ_0	Park transform d-axis, q-axis, 0 sequence flux linkage in Wb
ω_{base}	Base radial frequency in rad/sec
a	PV panel first thermal coefficient (selected -3.56 for polycrystalline)
A	Constant term for the battery curve fit from life test plot (set to 19,817)
A_1	Area of a WTG rotor hub in m^2
$A_{overlap}$	Area of WTG rotor hub overlap in m^2
AOI	Angle of incidence in angular degrees
A_{cond}	Condenser heat exchanger area in m^2
A_{arr}	Total active PV array area in m^2
A_{fc}	Fuel to coolant heat transfer area in m^2
A_{ms}	Metal lump to secondary coolant heat transfer area in m^2

A_{pm}	Primary coolant to metal lump heat transfer area in m^2
A_{WTG}	Swept area of the wind turbine in m^2
b	PV panel exponential thermal coefficient (selected -0.075 for polycrystalline)
B	Exponential term for the battery curve fit from life test plot (set to -0.763)
C	Delayed neutron precursor for fission reaction
c_m	Metal lump specific heat capacity in J/kg-˚C
c_p	Primary coolant heat transfer coefficient in W/m²-˚C
c_{pc}	Primary coolant in core region specific heat capacity in W/m²-˚C
c_{pf}	Primary coolant near fuel rods specific heat capacity in W/m²-˚C
$C_p(v)$	Wind turbine coefficient of power
C_T	Thrust coefficient for WTG wake effects
CF_{DC}	Capacity factor of a PV system, normalized to DC energy output in %
$Cycle(t_i)$	Cycle duration in DOD in minutes
$\frac{dU_v}{dp}$	Change in enthalpy in saturated vapor in kJ/kg-sec

$\frac{dU_w}{dp}$	Change in enthalpy in the saturated liquid in kJ/kg-sec
$\frac{dv_g}{dp}\frac{U_{wv}}{v_{wv}}$	Enthalpy over water density times change in specific volume
D_0	Distance between WTG rows in multiples of rotor area
D_{annual}	Annual BESS degradation in %/year
$D_{calendar}$	Calendar aging effects on the BESS in %/day
$DCAC_{ratio}$	DC to AC ratio of the PV subsystem
DHI_{beam}	Diffused Horizontal Irradiance vector at the POA in W/m^2
DNI_{beam}	Direct Normal Irradiance vector at the POA in W/m^2
e_d, e_q, e_0	Park transform d-axis, q-axis, 0 sequence voltages in V
E_{HES_t}	HES energy production for year t
F_t	Condenser fouling factor
$F_{constant}$	Faraday constant 96,485.3 in A-s/mol
GHI_{beam}	Global Horizontal Irradiance vector at the POA in W/m^2
$H2_{price}$	Hydrogen production value in $/kg
$H2_{prod_t}$	Hydrogen production quantity for year t in kg-H2

$h_1 - h_{17}$	Enthalpy along the Rankine cycle of the SMR in kJ/kg
h_{fc}	Reactor fuel to coolant heat transfer coefficient in W/m²-˚C
h_{ms}	Metal lump to secondary coolant heat transfer coefficient in W/m²-˚C
h_{pm}	Primary coolant to metal lump heat transfer coefficient in W/m²-˚C
$height_{actual}$	Actual turbine height in m
$height_{measured}$	Height at measured wind speed in m
i_q, i_q, i_0	Park transform d-axis, q-axis, 0 sequence currents in A
I_F	Electrolyzer stack current in A
k	Wind turbine model wake-decay constant (typical value is 0.07)
m_{cp}	Mass flow of water through the primary coolant loop in kg/sec
m_{cw}	Mass flow of cooling water through the primary coolant loop in kg/sec
$m_1 - m_7$	Mass flow of secondary cycle coolant flows through the SMR in kg/sec
m_c	Mass of core coolant in kg

m_f	Reactor fuel mass in kg
m_m	Metal lump mass in kg
m_p	Mass of primary coolant in steam generator in kg
m_{sv}	Mass saturated vapor liquid in secondary in kg
m_{sw}	Mass of saturated liquid in secondary in kg
n	Number of cycles in BESS time interval
P_{BESS}	BESS power in kW
P_{comp}	Hydrogen compressor losses in kW
P_{H2}	PEM power demand in kW
$P_{HES}(AOI, T_c, POA_{IRR}, v, T_{ci}, t)$	Net-HES power as a function of multivariable input in kW
$P_{PVac}(AOI, T_{cell}, POA_{IRR})$	PV AC power as a function of multivariable input in kW
$P_{PVdc}(AOI, T_{cell}, POA_{IRR})$	PV DC power as a function of multivariable input in kW
P_r	Rated reactor thermal power in kW
P_{sat}	Saturation pressure in the secondary loop of the SMR in kPa
P_{SMR}	Net-electrical SMR power in kW
P_{th}	Reactor nameplate thermal power in kW
P_{turb}	Steam turbine mechanical power in kW
P_{WTG}	Aggregate WTG power in kW

POA_{IRR}	The irradiance seen at the PV panel plane in W/m²
PPA	Power purchase agreement price in $/MWh
$Q_{cond,1}$, $Q_{cond,2}$, $Q_{cond,3}$	Balance equations for the condenser model in kJ/kg
R_a	Synchronous generator stator resistance in Ω
$R_x(t_i)$	Initial rainflow segment in half (0.5) or full (1.0) cycles
$R_y(t_i)$	Final rainflow segment in half (0.5) or full (1.0) cycles
$RF(t_i)$	Rainflow equivalent half (0.5) or full (1.0) cycles
RR_{limit}	Predefined ramp rate limit for the system in %-change/min
STD_{IRR}	Standard Irradiance at 1000W/m²
t_k	Time step interval for finance model in years
T	Total life for finance model in years
$T_{\theta 1}$	Temperature in reactor at node 1 in ˚C
$T_{\theta 2}$	Temperature in reactor at node 2 in ˚C
$T_1 - T_{13}$	Temperature values along the Rankine cycle of the SMR in ˚C
T_a	Ambient air temperature in ˚C
T_{ci}	Inlet steam condenser temperature in ˚C
T_{CL}	SMR primary coolant cold leg temperature in ˚C
T_{cell}	Static solar cell derived temperature in ˚C

$T_{cell}(t_i)$	PV cell previous cell temperature measurement in ^{o}C
$T_{cell}(t_{i-1})$,	PV current cell temperature measurement in ^{o}C
T_{co}	Outlet steam condenser temperature in ˚C
T_f	Reactor fuel temperature in ˚C
T_{HL}	SMR primary coolant hot leg temperature in ˚C
T_{inlet}	Steam turbine inlet temperature in ˚C
T_m	Reactor metal lump heat exchange temperature in ˚C
T_{mod}	Solar module/panel derived temperature in ˚C
T_p	Primary coolant temperature in ^{o}C
T_{ref}	PV cell reference temperature in ^{o}C
T_{sat}	Saturation temperature in ^{o}C
T_{shell}	Shell outlet temperature in ˚C
U	Heat transfer coefficient of the SMR condenser in W/m^2-K
U_{const}	Turbine enthalpy constant in kJ/kg
v	Wind speed at hub height, wind speed at 10 meters above the ground in m/s
$v_{measured}$	Wind speed at 10 meters above the ground in m/s
V_{stack}	Electrolyzer stack voltage
W_{lump}	Working power for the steam lump in kW

$W_{turbine}$	Working power for the steam turbine in kW
$W_{pump,1}$	Working power for the first steam loop pump in kW
$W_{pump,2}$	Working power for the second steam loop pump in kW
x_{01}	Horizontal distance between the upstream and downstream WTG in multiples of rotor diameter
z	Number of electrons per electrolyzer splitting

CHAPTER 1

INTRODUCTION

This thesis covers research into the unique challenges and opportunities offered by combining clean energy resources together into an aggregate hybrid energy system (HES) to offset traditional fossil fuel power generation. This topic is just one aspect in the larger effort to decarbonize energy production for the sake of reducing the impacts of human caused climate change. The key challenge with this topic is pursuing the clean energy transition, without compromising power system reliability and maintaining the lowest possible cost of energy. For this thesis, the contribution to this topic is the dynamic modeling of an equivalent linear time invariant HES of multiple energy sources operating in parallel based on empirical inputs. The model considers practical limitations and environmental constraints to find an optimal HES configuration that meets contemporary power demands with the highest return on investment.

In 2021, approximately 25% of GHG emissions in the United States came from the electric power industry [1]. Furthermore, for other industries to decarbonize (e.g. transportation, buildings, manufacturing), increased demand for electricity is required through efforts like the expansion of electric vehicles, electric heating, and electric drive motors for industrial processing, to name a few. The current challenge in pivoting away from traditional energy sources are the operational constraints of the alternatives: nuclear and renewable energy sources

(primarily, wind and solar). Renewable sources are constrained by their limited resource availability and flexibility with curtailment being the only practical regulation method. Nuclear sources are primarily constrained by their economics and secondarily by their relatively slow response rates. Combining these constrained sources together with energy storage to form an HES has the potential to meet contemporary energy reliability requirements while maintaining the lowest possible cost. The proposed HES, with all sources considered, is shown in a single line diagram in Figure 1. This study uses dynamic power modeling to evaluate the frequency response of the HES. With the model developed, power production cases are simulated to determine the number of ramp rate violations, period of energy surplus, energy deficits, and transient support. From this analytical work, the practical limits of HES are found, balancing energy storage with curtailment, and future cost points for economic viability. Finally, an optimal configuration for an HES in different regions is found based on the relative nameplate capacity of each resource considered and normalized to their economic return on investment.

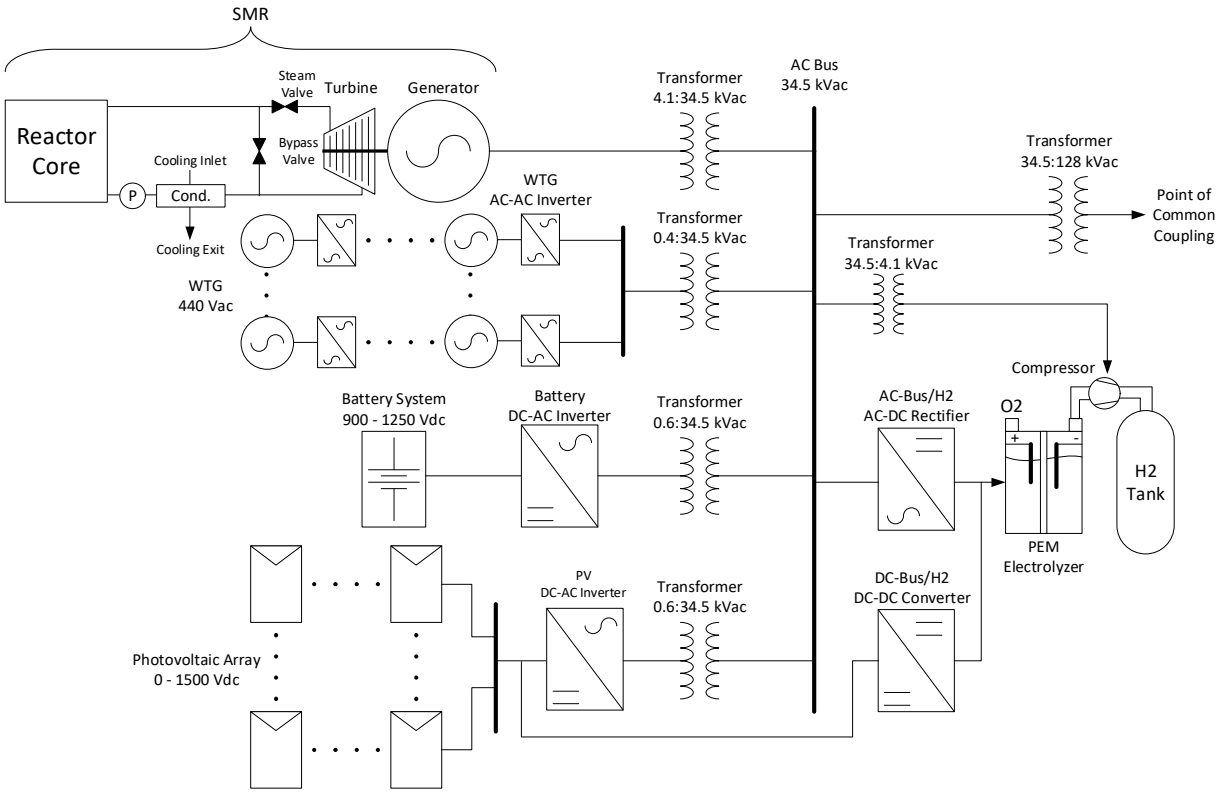

Figure 1: The full HES considered in this study.

1.1 Why a Hybrid System?

There are many ways to represent the interoperability of nuclear, renewable, and energy storage systems. They can be considered as multiple standalone energy sources tied to unique feeders over a large geographical area. This can be modeled as a large IEEE Bus model on separate nodes for each resource. This is particularly useful for modeling distributed renewable resources. While this gives a robust network solution, it is very process intensive and requires non-trivial computational power for analyzing annual energy production at a high sample rate. Furthermore, and particularly in the case of PV and WTG generation, weather patterns over a

large geographical can be quite diverse and cannot be accurately represented by empirical data from a single location. The primary advantage in studying a single plant model HES is that the results are generally worst case from a dynamic standpoint as local conditions are generally more extreme than the average weather conditions over a larger geographical area. Finally, modeling multiple sources as an HES gives a "best of both worlds" approach, where energy production from a PV system is complimentary to a WTG system, and vice versa. This is also true for nuclear energy production, when considering the effects of cooling water temperature on power output, as shown in Chapters 3 and 4. Finally, while outside the scope of this research, black start is an interesting topic for an HES that merits further study. The coupling of an SMR that utilizes a synchronous generator can support black start capabilities and the ability to parallel grid following power converters from PV and WTG systems from that, without the need for sophisticated grid forming converter control systems.

1.2 Scope of Study

This study focuses on the development of a model to accurately represent short (e.g. sub-second) and long-term (e.g. minutes, hours, months, seasonal) interactions of multiple generating resources electrically coupled to form an HES. This is accomplished by a linear time invariant system model developed in MATLAB/Simulink®. The inclusion of practical constraints gives further fidelity to the model. These include the impact of time varying environmental inputs for all

generating resources. It also includes degradation factors and life limiting constraints in the case of storage devices. The modeling effort follows an incremental development approach with each source developed independently and integrated into the final model.

The development of an HES for this study takes the form of an incremental modeling approach. The first step is developing a dynamic model of the solar PV subsystem to accurately emulate its relatively fast transient effects and ways to passively mitigate them. The second step is to combine the PV model with a battery energy storage system (BESS) model to regulate ramp rate and network transients. Third is the development of the SMR with multiple modeling approaches evaluated. Fourth is the addition of WTG and PEM with the initial development of the HES. Finally, an IEEE 9 bus model is utilized to evaluate the transient response of an HES over and under frequency events on a power network.

The study also considers the financial viability of HES. Based on referenced contemporary estimates for capital, operating, and recycling costs to find net present value (NPV) and internal rate of return (IRR) over a 4-year construction phase and 30-year operational life. The financial assessment is used to normalize the various HES configurations to find a solution that is bounded by revenue generation, energy demand met, and reducing excess curtailed energy. The financial model for this study normalizes the tradeoff between revenue, energy curtailed, and

deficit energy (i.e. load demand not met) to IRR. For curtailed energy, the result is reduced CF for the curtailed resources. For demand not met by the HES, an energy penalty based on the market energy rates for the region evaluated is applied to the results per kilowatt hour not met. The overlap of revenue, curtailment, and energy deficit is shown in Figure 2.

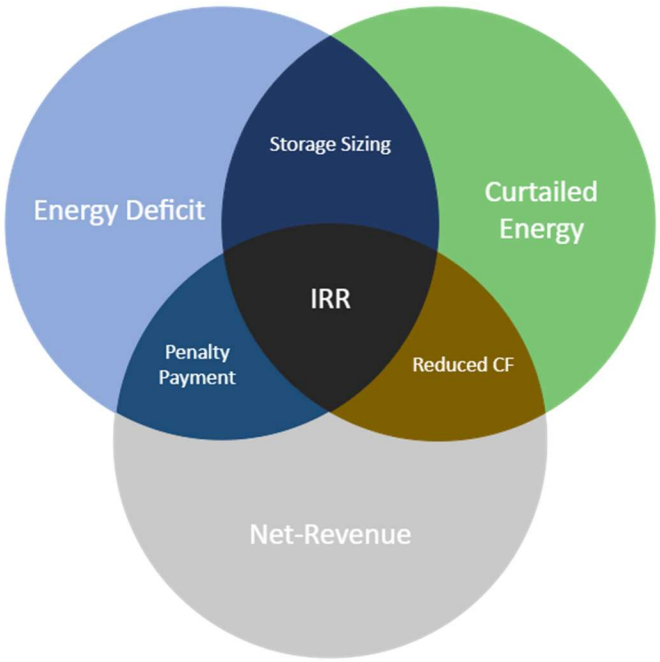

Figure 2: Venn diagram between revenue, curtailed energy, and energy deficit for the proposed HES financial model.

1.3 Contributions

Several key findings were uncovered as part of this research. Some of which are novel, while others reaffirm existing conclusions from past literature on the topic. A summary of the key contributions to this research topic is presented here:

- **Contribution 1. Evaluating passive methods to mitigate ramp rates in a PV system (Section 3.1).** Relatively fast changes in power production are an inherent characteristic of PV systems due to resource variability. Mitigating ramp rates is typically performed actively through inverter controls and/or an energy storage device. The first part of this thesis used a modified PV power model to consider tilt & azimuth angles, along with DC:AC ratio as input parameters. The variation of these parameters led to the result that a significant number of ramps from a PV system can be mitigated by varying these design parameters, particularly the DC:AC ratio. While these benefits come at an economic penalty for reducing energy production, they can still provide a more economical alternative than adding energy storage to fully mitigate ramps.
- **Contribution 2. Developing a minimum battery sizing algorithm based on a 10-year operational life for coupling BESS and PV systems (Section 3.2).** Previous research used rainflow analysis to determine the useful life of a battery based on variable charge and discharge cycles. This contribution built on the previous work and developed an optimization loop to determine the minimum battery kilowatt hour size to support 10 years of operation based on multiple operational scenarios (active ramp rate regulation, peak shifting, and reserve margin).
- **Contribution 3. Modeling nuclear SMR power as a function of steam bypass and cooling water temperature (Section 3.3.2).** For an HES,

modeling the SMR output to vary as the inlet cooling water temperature varies provides a unique complimentary relationship in SMR power output and PV output. When PV output is zero or relatively low, that typically corresponds to lower water temperature, which increases SMR power. The combined effects of these two environmental inputs results in a complimentary relationship that reduces the curtailment and energy storage requirements of the HES.

- **Contribution 4. Annual energy model of an HES using minute-level data (Section 4.2).** This model was constructed to accurately capture source variation from the renewable sources and couple them with load variation from the load following patterns. Previous studies evaluated as part of this work considered longer time intervals and generalized conditions, such as global horizontal irradiance and ambient air temperature for PV power estimates, which skewed the results from ramp rate and energy deficits. This research takes a more granular approach and considers an environmental dependency for each source that makes up the HES.
- **Contribution 5. Evaluation of multiple sources operating in parallel to provide frequency support (Section 4.4.1).** This thesis looks at frequency triggers for the various resources and their coordinated response. The results show that an HES can offer autonomous frequency support for over, and under, frequency excursions. A short duration BESS can provide near instantaneous frequency support for seconds to minutes, while the

slower responding sources (e.g. SMR) have time to adjust to the new operating point.

- **Contribution 6. Evaluating the tradeoff between curtailment versus storing excess renewable energy (Section 6.5).** One of the more interesting results of the full HES evaluation is the optimal PEM size is approximately 30% to 40% of the HES nameplate power (e.g. the total nameplate of the SMR and renewable generation). This ratio is dependent on the tax credits applied but indicates an optimal point between the capital cost of adding more PEM capacity versus the value of the excess energy stored.
- **Contribution 7. Reaffirming the need for low-cost energy storage and/or lower SMR capital costs (Section 6.5).** The results of this thesis show that current unsubsidized costs do not favor a clean HES over traditional fossil fuel sources, even for the most economical configurations. With subsidies considered, they do favor a clean HES but are likely not the solution for large scale roll out of such systems. The key area of cost improvement for an HES, or clean energy systems in general, is reducing the capital cost of SMRs and/or decreasing the cost of energy storage. Without significant cost reductions in those areas, the economics of clean energy sources remains challenging.

1.4 Arrangement of the Thesis

This thesis is arranged into seven chapters. The main technical content is in Chapters 3 through 6. The following is a summary of each research chapter:

- Chapter 3 provides an overview of the incremental models developed and tailored as part of this effort. This encompasses the PV, BESS, WTG, SMR, and PEM models. It also includes energy conversion device models for generators, power electronics, and electrolyzers. It further includes the incremental developments of passive/active ramp rate control and battery sizing loop.
- Chapter 4 covers the fully integrated HES model and IEEE 9 Bus model. The integrated models cover the linearized models of the complete HES. An annual energy simulation based on minute-level data is constructed, configuration evaluated, to determine the period of energy deficit and surplus. Sources operate in parallel and are controlled based on SMR steam bypass regulation and renewable curtailment for cases where storage is not considered. For cases with storage, the setpoint on the PEM is varied to store excess power from the generation sources. For the IEEE 9 Bus model, voltage regulation is managed by the field excitation of the SMR synchronous generator with renewable sources operating at a fixed power factor. Additionally, for the 9 Bus model, an example of worst-case change in source and load is evaluated over multiple minutes of a sub-second sample rate.
- Chapter 5 covers the financial assumptions, tax credits, project life cash flow, and model setup. The assumptions are based on the most recently available data for capital and operating costs for the resources. However, in the case of the SMR, since it's a new technology, a nominal cost projection is used for

capital cost and heritage information on existing nuclear plants for operating costs. An annual cashflow is constructed for each year of the project life that considers things such as construction phase, SMR refueling, BESS and PEM replacement, and decreased performance of aging resources.

- Chapter 6 provides the modeling results and the optimal configurations found. The results are broken into three parts: the results from the network model, the results from the annual energy analysis, and the financial results from the optimization loop. The best configuration for each region and each set of financial assumptions is provided. The results from this highlight the technical and financial limits of an HES and where opportunities for improvement lie.

Lastly, the Appendix includes images of the model constructed and raw data output for each configuration evaluated.

1.5 Summary of Publications

The main publications that serve as the foundation for this thesis are listed below in chronological order. Each section that is derived from one of the below publications is identified at the beginning of each chapter. This thesis covers their work and expands on them in areas where less detailed information was provided in the publication, typically due to page count limitations.

[Publication A] J. Hurtt and K. Baker, "Sensitivity Analysis of Photovoltaic System Design Parameters to Passively Mitigate Ramp Rates," in IEEE Journal of Photovoltaics, vol. 11, no. 2, pp. 545-551, March 2021, doi: 10.1109/JPHOTOV.2020.3045679.

[Publication B] J. Hurtt and K. Baker, "Minimum Battery Energy Storage System Sizing Integrated with a Photovoltaic Plant Considering Practical Limitations," 2021 IEEE Madrid PowerTech, Madrid, Spain, 2021, pp. 1-6

[Publication C] J. Hurtt and K. Baker, "Modeling of a Clean Hybrid Energy System Considering Practical Limitations for Techno-Economic Energy Analysis," 2023 IEEE Industry Applications Society Annual Meeting (IAS), Nashville, TN, USA, 2023, pp. 1-11.

[Publication D] J. Hurtt, K. Baker, M. Walker, "Optimal Techno-Economic Configuration of a Clean Hybrid Energy System Considering Environmental Variability and Power System Impacts," in IEEE Transactions on Power Systems, *In Review*.

CHAPTER 2

LITERATURE REVIEW

This chapter summarizes the key literature referenced for this study. It consists of past research into hybrid systems and modeling techniques. Only the key reference models for ramp rates (Section 2.2), environmental resource (Section 2.3), BESS (Section 2.4), SMR (Section 2.5), and transient models (Section 2.6) are reviewed in this section as significant variations of those modules exist in the literature. The full details on the models referenced and tailored are covered further in Chapter 3. Methods of evaluating each resource, along with parallel operation, and network considerations are covered in Chapter 3. From these foundational models, the full HES model in this study is developed and tailored to meet the energy and economical objectives. From the literature review performed, a novel HES research approach is outlined for this thesis.

2.1 Contemporary Research into Hybrid Energy Systems

A search of IEEE Xplore for certain keywords gives an anecdotal evaluation of the volume of research on HES that utilize nuclear and renewable sources. Table 1 summarizes the keyword searches for several combinations of hybrid energy sources captured at the time of writing this thesis. While the combined keywords of "hybrid solar wind" yields 4,148 IEEE publications the keywords "hybrid solar nuclear wind" result in 87 results with "hybrid nuclear hydrogen" being the lowest with 56 publications.

Table 1: Summary of keyword searches on IEEE Xplore.

Keywords	Publication Results
Hybrid Solar Wind	4,148 [2]
Hybrid Renewables Storage	5,856 [3]
Hybrid Renewables Hydrogen	822 [4]
Hybrid Nuclear Renewables	190 [5]
Hybrid Solar Nuclear Wind	87 [6]
Hybrid Nuclear Hydrogen	56 [7]

While research is relatively limited, there have been notable recent developments in HES by Idaho National Laboratory (INL). INL has an ongoing research effort focused on hybrid systems, called the Integrated Energy Systems (IES) program [8]. This program focuses on combined renewable, natural gas, nuclear, and energy storage systems. IES also considers recaptured waste heat from reactors and energy storage options, including hydrogen with research focused on physics-based modeling. Publications to date from this group have been focused on the rationale for HES with limited modeling details, primarily focused on models for thermal and electrically coupled systems [9] – [11]. Figure 3 shows a notional diagram from [9] of a proposed HES with thermal and electrically coupled sources. While thermal coupling offers efficiency advantages, this thesis is focused only on electrically coupled sources and their interoperability.

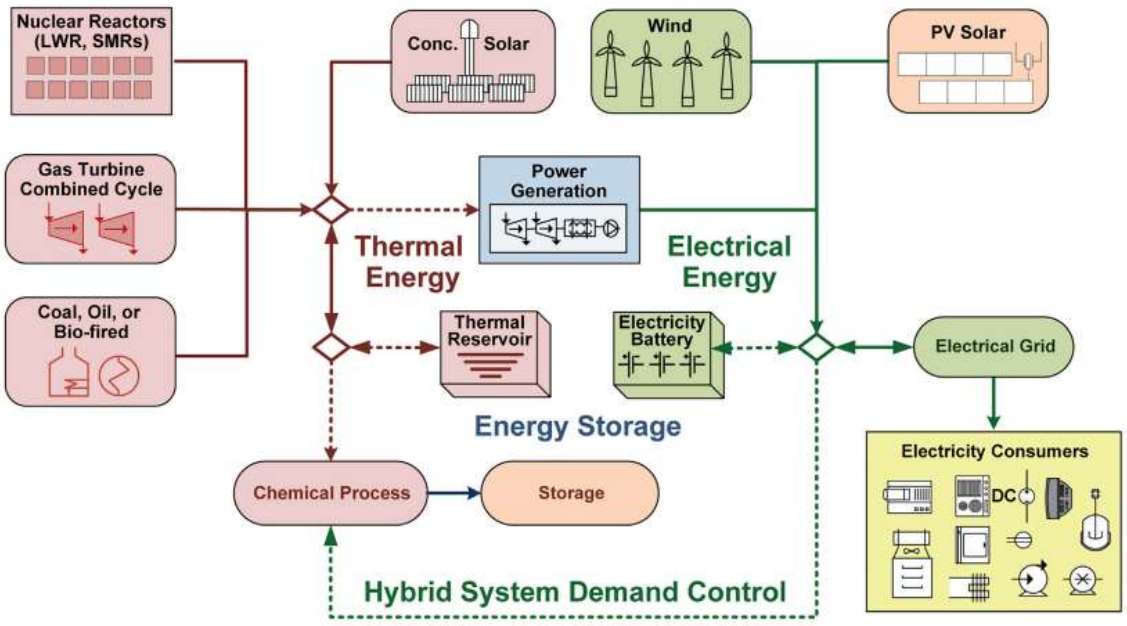

Figure 3: INL notional HES with thermal and electrically coupled sources [9].

Additional research has been performed by other institutions. In [12], different renewable hybrid configurations are coupled with a fossil fuel powered diesel generator for a techno-economic evaluation. In [13], a PV+WTG+BESS system is validated in a laboratory environment for transient response. In [14], a comprehensive overview of the applications, control, and implementation of renewable energy HES (non-nuclear) is evaluated. Clean energy HES using SMRs that are coupled with renewable energy is covered in [15] using low fidelity modeling and 15-minute time data. Finally, a technical evaluation of a PV+SMR hybrid system for a rural distribution feeder, including transient analysis, is covered in [16].

The modeling of HES is a novel research area as well. Analytical tools are being proposed to support their development. One of the most prominent HES modeling tools is from the National Renewable Energy Laboratory (NREL). The Hybrid Optimization and Performance Platform (HOPP) evaluates the optimal renewable HES configurations based on local resources and financial considerations across the United States [17]. The model developed as part of this study differs in by including SMR and aging factors which are not currently part of HOPP [17]. A summary of hybrid electrically coupled systems and software platforms used is given in Table 2.

Table 2: Summary of SMR hybrid studies.

Reference	Sources	Software	Transient Analysis?	Annual Energy Analysis?	Financial Model?
[12]	PV, Wind, BESS, Diesel Generator	HOMER	No	Yes	Yes
[13]	PV, Wind, BESS, Super Capacitors	MATLAB	Yes	No	No
[16]	PV, SMR	PSS/E	Yes	No	No

Reference	Sources	Software	Transient Analysis?	Annual Energy Analysis?	Financial Model?
[18]	PV, SMR, BESS	PSS/E	Yes	No	No
[19]	SMR, Biofuel, Desalination	Not Specified	No	No	Yes
[20]	SMR, Wind	Not Specified	Yes	No	No

This thesis expands on these previous efforts by modeling an HES considering renewable and nuclear resources operating in parallel for evaluation of all criteria: transient, annual energy, and financial. This study evaluates the economics of a renewable and SMR based HES on an annual basis, using minute level empirical data to bound the evaluation to environmental constraints. Finally, the use of aging factors for all resources evaluated improves the fidelity of the results for both real time energy deficits as well as the need for replacements over the 30-year operational life.

2.2 Literature Review of Ramp Rate Modeling

Ramp rate regulation is one of the key pieces of the model development and sets the sample rate of the annual energy model. Much of the research that has been performed in ramp rate mitigation has focused on reducing ramp rate through storage or using inverter controls to limit positive ramps or curtailment. In [21], the most common control strategies for reducing positive ramp rate through inverter controls and negative ramps with BESS are discussed. These approaches are cost effective for reducing positive ramps, but still require a BESS for the negative ramps, which make the economics of implementing them less appealing. Another approach is to forecast cloud cover to pre-emptively reduce solar output to minimize the negative ramp rate. This type of control is discussed in [22] - [23]. The use of cloud cameras is an effective way to mitigate cloud induced transients, but outside the scope of this study as this effort is focused on energy system modeling. In order to accurately measure and estimate the ramp rate resulting from a PV plant design, high-fidelity environmental data for simulations is incorporated.

2.3 Literature Review of Environmental Data Sources

The primary database for empirical data for the renewable power inputs is the National Solar Radiation Database (NSRDB) [24]. The benefit of this database is a broad international repository of five-minute level data of numerous environmental vectors based on satellite data. The dataset runs through 2022, which aligns with the time range used for this study. The only notable drawback is

the time interval of five minutes is longer than the usual ramp rate measure of percent change in power per minute. For this study, minute level data is utilized to provide worst case resource variability (discussed further in Section 6.1).

The use of high-fidelity environmental data has been previously performed to evaluate RR over geographical areas. In [25], environmental data from four sites across Colorado was used to estimate RR in terms of global horizontal irradiance (GHI) variability. This work was extended in [26], where the authors estimated the power output from a hypothetical power plant using averaged GHI across the same four sites. Further analysis performed in [27] shows the variation in RR estimates when using one-minute to fifteen-minute interval datasets and the variation in performance over a region of Northwest India. The results presented as part of this study extend the modeling techniques presented in [25] - [27] and take it a step further from measuring RR to evaluating the change in RR by sweeping these design parameters.

2.4 Literature Review of BESS models

The topic of renewables coupled with a BESS for ramp rate control has been researched extensively, with a significant increase in publications over the last decade. This thesis builds on the previous work performed by a number of selected studies in [28] - [29] and combines a number of practical limits to develop a more

complete capability picture when it comes to planning considerations for a combined system.

Another method that is considered in the coordination of batteries is the augmentation of old batteries. Augmentation is the process of installing new batteries in parallel with older batteries in the BESS, typically isolated from each other through a DC-DC converter. This option is discussed further in [30]. Augmentation is not considered in this thesis as full replacement is considered every 10 year for the financial model. However, this is an option that merits evaluation when developing a plant as an alternative to the approach evaluated in this study.

While other methods and tools for degradation estimates exist, rainflow analysis is selected for its simplicity and existing MATLAB implementation. Rainflow is typically used in mechanical fatigue analysis but has also been proposed in [31] for solar PV variability and further evaluated in [32]. Rainflow analysis for a BESS coupled with a wind farm is also discussed in [33]. This thesis builds on these previous works and uses rainflow for BESS sizing that includes multiple battery charge/discharge constraints, varying ramp rate requirements and multiple use cases to determine the minimum energy size to support a 10-year operational life.

2.5 Literature Review of SMR models

Works considering SMR models are relatively recent with various hybrid systems works covered in [34], with simplified modeling, but no consideration of dynamic and operational cost models. In [35], a SMR model was developed to balance output variation from a wind farm with a changing energy demand pattern. Additionally, in [36] a simplified PV model was coupled with hydrogen electrolysis and BESS due to the PV system not being able to operate in nighttime hours. A dynamic model of an SMR is developed and verified in [37] using PSS/E. The basic methodology of developing the SMR model is based upon [37] and developed for the SMR sub-model in Chapter 3.

2.6 Literature Review of Network Models

There are numerous models of networks for power system studies. The models are typically developed in a standard power system tool, like Siemens PTI PSS/E and based around IEEE standard bus models (3 bus, 9 bus, 13 bus, 33 bus, etc…) [38]. Transient studies with SMR and renewable HES are discussed in previous sections. Another relevant modeling technique with a WTG fault in an IEEE 14 bus model was provided in [39] using hourly sampled load data. Stability models for standalone renewable systems are abundant, including [39] – [40], but only cover the power electronics response. Likewise, nuclear plants have numerous studies performed on their transient stability within an IEEE bus models in [40] – [42] using commercially available software. Models in MATLAB/Simulink have

been recently provided as part of the Simscape toolkit with the IEEE 9 bus model utilized for this study [43]. This study focuses on the dynamic modeling of the SMR generator and steam turbine regulation with the renewable sources modeled as negative loads, as discussed in Section 4.4. The rationale being the time response of the rotating machines is much slower than the power electronic-based generation and is driving the overall response time of the HES.

CHAPTER 3

HES FOUNDATIONAL MODELS

The HES is modeled as an aggregation of foundational models. These are the source and storage models that are electrically coupled to represent the fully integrated HES. These models are discussed in this chapter. The PV, PEM, and initial SMR models are based on literature with some modifications made to support this study. Discussed in this chapter are the PV, WTG, SMR, BESS, and PEM models. The PV model in Section 3.1 was developed as part of [Publication A] to evaluate passive ways to mitigate ramp rates. The BESS model in Section 3.2 was developed in [Publication B] to actively mitigate ramps from a PV system. The SMR and PEM models in Sections 3.3.1 and 3.5 were developed in [Publication C] as part of an initial HES model. The SMR model in Section 3.3.2 was further refined in [Publication D] to account for seasonal variations of inlet cooling water temperature. The WTG model in Section 3.4 was also developed in [Publication D] to evaluate a fully renewable and nuclear, electrically coupled, HES.

3.1 PV Modeling and Passive Ramp Rates

This section covers the PV model that was developed in [Publication A] to determine passive ramp rate mitigation. The PV resource has the highest variability. As such, the modeling effort commenced by utilizing a high-fidelity model to capture the inferred ramp rates. From this effort, the DC:AC ratio impacts are incorporated into the PV sizing of the overall HES model.

3.1.1 PV Multivariable Model

A common way to determine the power output of a PV plant is to use data sets that have hourly global horizontal irradiance (GHI) and ambient air temperature. These parameters are helpful for gross estimation of power output and rely on relatively low-cost instrumentation with minimal data storage. However, these simplified models can differ significantly from actual PV performance when considering the time-based interaction of all irradiance vectors: GHI, Direct Normal Irradiance (DNI), and Diffused Horizontal Irradiance (DHI). Furthermore, the variability of solar production is fast enough that hourly samples provide no meaningful data for analyzing ramp rates. In addition, the power production of a solar plant will be analyzed with respect to the array's irradiance at the plane of array (POA) with wind speed and solar cell level temperature accounted for. To capture this level of detail, further data is needed from the environmental resources set. An illustrative view of these vectors is given in Figure 4. The variables required to capture these dynamics include the following:

- GHI in watts per square-meter (W/m^2)
- DHI in watts per square-meter (W/m^2)
- DNI in watts per square-meter (W/m^2)
- Ambient air temperature in degrees Celsius (^oC)
- Wind speed in meter per second (m/s)
- Solar azimuth angle in degrees (^{o})
- Solar zenith angle in degrees (^{o})

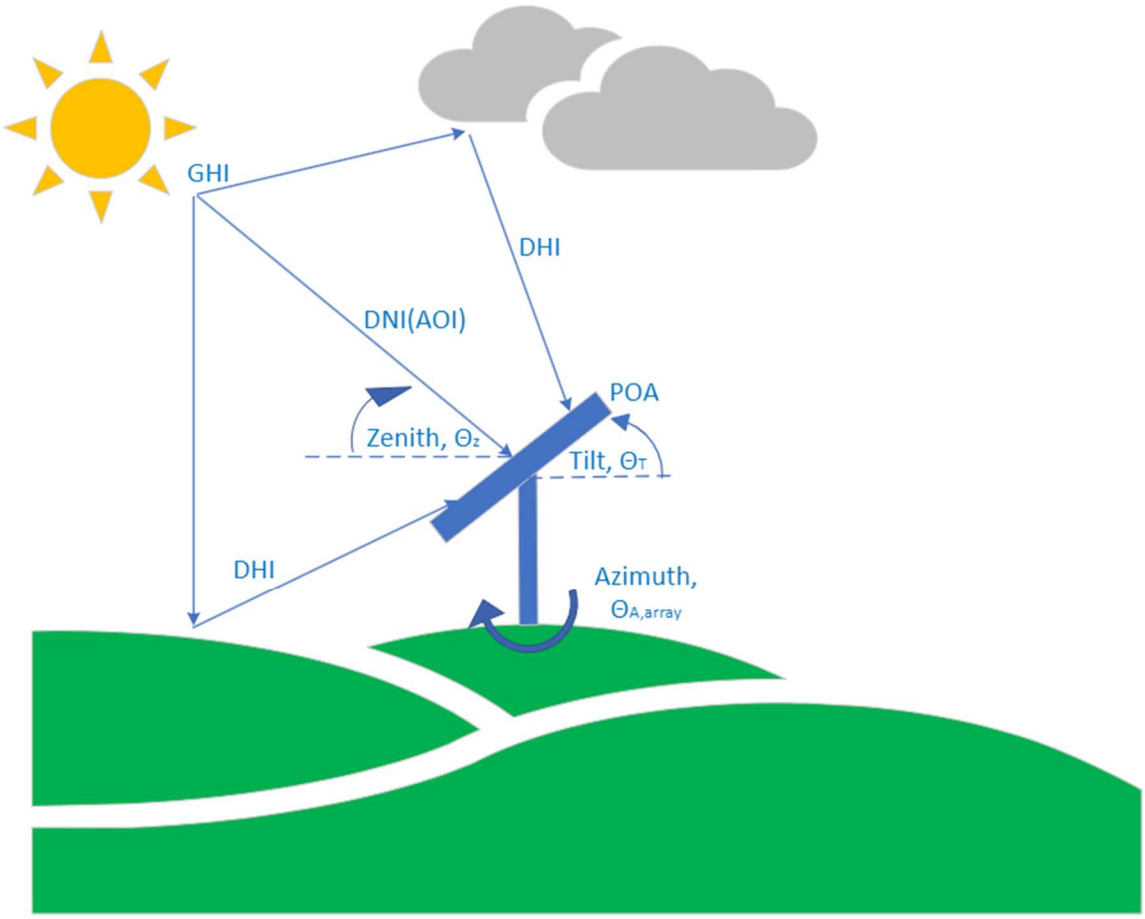

Figure 4: Multivariable approach to PV power production modeling.

The PV environmental performance calculations are referenced from the Sandia modeling collaborative [44]. The derived calculations allow for angular adjusted parameters for irradiance and solar cell temperature that can feed into the PV system power model. To determine POA irradiance, the angle of incidence (AOI) between the irradiance vectors and the orientation of the solar panel is needed. The relationship for AOI is defined as

$$AOI = cos^{-1}[cos(\theta_z)\, cos(\theta_T) + sin\,(\theta_z) sin\,(\theta_T) cos\,(\theta_A - \theta_{A,array})] \quad (1)$$

The relationship between the irradiance vectors GHI, DNI and DHI with the POA are given by the following expression:

$$POA_{IRR} = GHI_{beam} + DNI_{beam} + DHI_{beam} \quad (2)$$

These three vectors give the irradiance contribution on the solar array, from the three sources: ground reflected, direct normal, and cloud reflected. These relationships are defined as:

$$GHI_{beam} = GHI(albedo)\left(\frac{1-cos\,(\theta_T)}{2}\right) \quad (3)$$

$$DNI_{beam} = DNIcos\,(AOI) \quad (4)$$

$$DHI_{beam} = DHI\,\frac{1-cos(\theta_T)}{2} + GHI\,\frac{(0.012\theta_z - 0.04)(1-cos(\theta_T))}{2} \quad (5)$$

Note: all of the parameters are measured from the site instrumentation, except for the tilt angle, which is a design parameter. The GHI_{beam} is a measure of the irradiance reflected from the ground and is also dependent on albedo. The DNI_{beam} is the direct normal irradiance from the sun. The DHI_{beam} is a measure of the irradiance reflected from the clouds and is based on the Sandia cloud irradiance model in [44].

The solar cell temperature is based on one-minute sampled ambient air empirical data. The PV module temperature T_m is defined as the following:

$$T_{mod} = POA_{IRR} e^{(a+bv_{measured})} + T_a \quad (6)$$

From this, the PV cell temperature T_c can be determined to find the actual temperature, and therefore cell efficiency. This is defined as following relationship:

$$T_c = T_{mod} + POA_{IRR} \frac{POA_{IRR}}{STD_{IRR}} \Delta T \quad (7)$$

The solar cell temperature is also impacted by the time constant of the PV panel materials. This is due to the thermal properties of the materials that make up the panel and the time it takes for temperature rises to be absorbed through each layer of a PV module. From [45] - [46], polycrystalline panels were evaluated to measure their time constant in varying test conditions. They concluded a time constant between five to seven minutes. Hence, in this study, a time constant of six minutes is applied. The time constant is implemented into the model using the universal thermal time constant expression from [45] and defined as:

$$T_c(t) = (T_c(t_{i-1}) - T_c(t_i)) e^{\frac{-t}{\tau}} + T_c(t_i) \quad (8)$$

The DC PV power is the product of the plane of array irradiance, array area, temperature coefficients and module efficiency. For AC power, this relationship also includes accommodation for DC:AC ratio and inverter efficiency, which is given as:

$$P_{PVac}(AOI, T_{cell}, POA_{IRR}) = \frac{POA_{IRR} A_{arr}\left(1-\alpha_{PV}\left(T_{cell}-T_{ref}\right)\right)\eta_{mod}\eta_{inv}(P_{PV\_DCdc})}{DCAC_{ratio}} \quad (9)$$

Note the values for PV module coefficients and efficiency are based on the Canadian Solar 330-watt polycrystalline module [47]. Inverter efficiency is a dynamic value that is dependent on the relative level of power output. In order to capture this relationship, the efficiency curve is referenced from an SMA Sunny Central one-megawatt inverter [48].

3.1.2 PV Ramp Rate Sensitivity

3.1.2.1 Single Variable Sensitivity

The optimal tilt angle for energy production varies depending on the latitude of the site. For this analysis, the tilt angle is swept from 10 degrees to 60 degrees, in 5-degree increments, to assess how the annual energy generation and annual number of ramps worse than negative 10% per minute are impacted. This range of variability represents the practical range of tilt without going to extreme angles that results in high panel soiling or excessive structural material needs. All other parameters were held constant at their optimal energy production values for azimuth and DC:AC ratio. Tilt angle sensitivity results for the UO site, which are

normalized against the baseline results in Table 3, are shown in Figure 5. The optimal ramp rate design point is evaluated against the baseline design with the change in energy, ramps, and LCOE captured in Table 4. It can be seen in Figure 5 that the number of ramps is at a minimum at 10-degree tilt angle. Changing tilt angle alone has a significant energy impact with a relatively small reduction in ramps.

Table 3: Baseline energy and ramp rate for optimal PV energy configuration.

Site	Annual Energy Generation (MWh_{AC})	Ramps Worse Than Negative 10%/min	CF_{DC} (%)	LCOE ($/$kWh_{DC}$)
UO	20,941	5,491	15.9	0.076

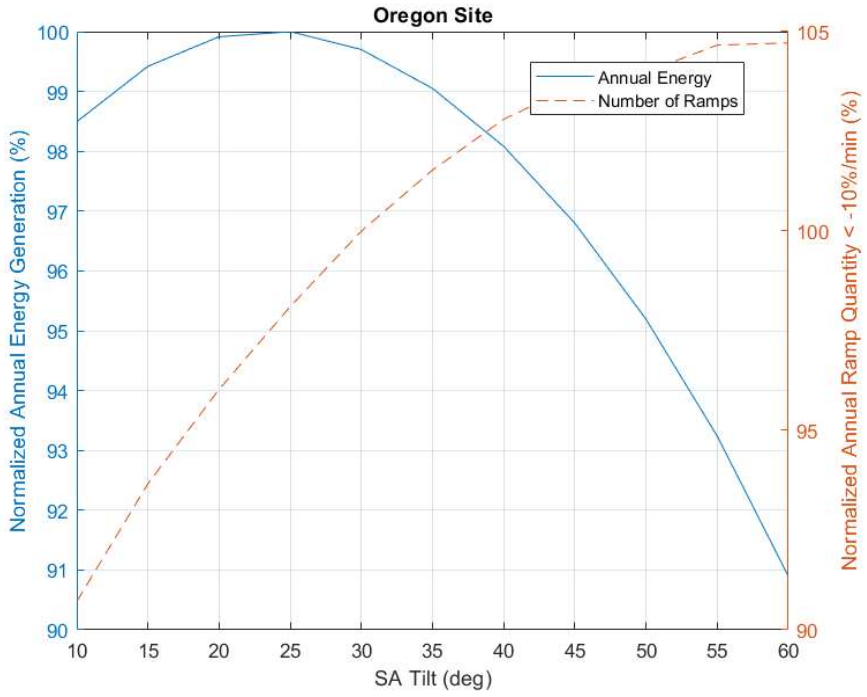

Figure 5: Annual energy generation and ramps as tilt angle is varied.

The azimuth angle of a PV array is used to align the azimuth orientation with the solar azimuth orientation. In the Northern Hemisphere, the optimal PV azimuth angle is close to 180 degrees and corresponds with the average solar azimuth angle. It can be seen from Eq (1) that when these two angles are equal, the minimum AOI is obtained. For this analysis, the azimuth was swept from 90 degrees to 270 degrees in 10-degree increments. This range represents the practical range of azimuth angles in the northern hemisphere from true east (90 degrees) to true west (270 degrees). All other parameters were held constant at their optimal energy production values for tilt angle and DC:AC ratio.

It can be seen in Figure 6 that the number of negative ramps and energy production are closely coupled when varying azimuth angle. Minimum ramping occurs when the azimuth is at 90 degrees. This is consistent with achieving peak energy production early in the day, prior to afternoon cloud cover. The optimal azimuth point for minimum RR quantity is site climate dependent and could occur at either 90 or 270 degrees. Normalized azimuth angle sensitivity results for the UO site are shown in Figure 6. The optimal RR design point is evaluated against the baseline design in Table 3 with the change in energy, ramps, and LCOE captured in Table 4. It can be seen in Figure 6 that the number of ramps is at a minimum at 90-degree azimuth angle. When compared to the tilt angle sensitivity, the azimuth angle variation results in a much more significant decrease in RR with a slight increase in the energy lost from the Table 3 configuration.

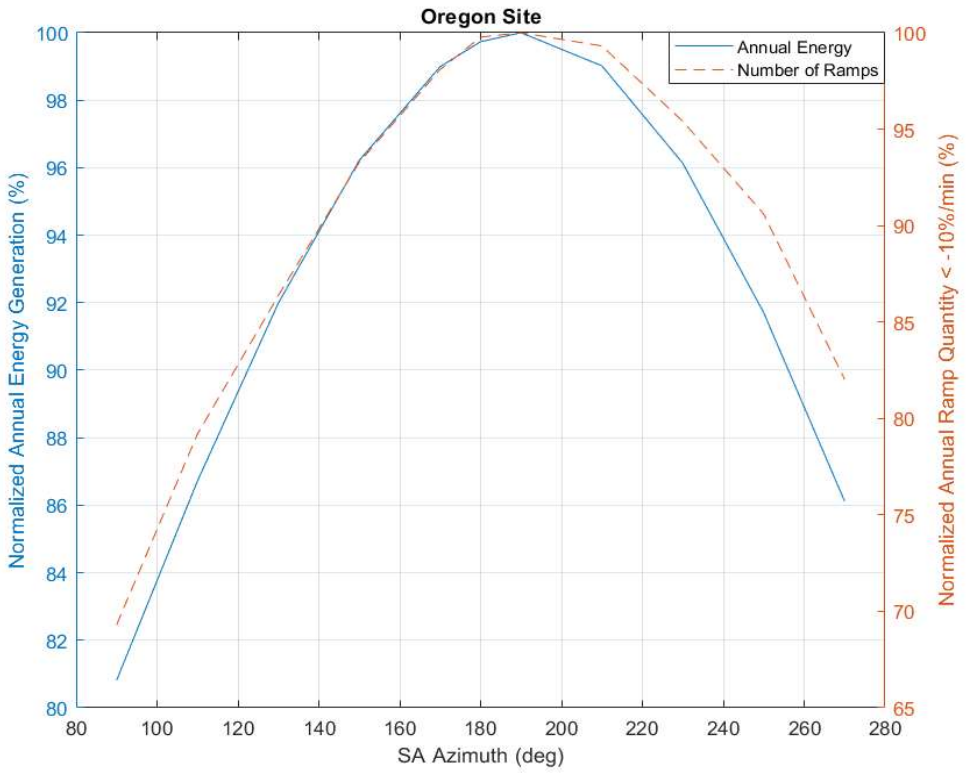

Figure 6: Annual energy generation and ramps as azimuth is varied.

While theoretically there is no limit to the DC:AC ratio, practical issues, particularly the excess energy dissipated on the PV panels, results in the ratio typically being limited to a maximum size of 2.0. For this analysis, the DC:AC ratio was swept from 1.0 to 3.0 in 0.1 increments with clipping losses being accounted for. All other parameters were held constant at their optimal energy production positions for tilt and azimuth. The normalized results compared against the baseline configuration in Table 3 are shown in Figure 7 with the results given in Table 4. The number of ramps peaks at a ratio of 1.4 and then drops as the ratio

increases to 3.0. This is due to the "stretching effect" from the DC:AC ratio clipping more excess energy can reduce the overall ramp magnitude seen at the AC output.

The tradeoff is that the clipped energy (the energy not converted to AC power and left on the PV panels as heat) increases as seen in Figure 7. This lost energy could potentially be stored and used for energy during non-sunlit or low irradiance periods, but this implementation is outside the scope of this study. It can be seen in Figure 7 that the number of ramps is at a minimum at 3.0 DC:AC ratio. When compared to the tilt and azimuth angle sensitivity, the DC:AC variation results in a much more significant decrease in RR, but with a high energy loss as well. One thing to note is that the LCOE is at its maximum with a 3.0 DC:AC ratio. This is due to the reduced CF from overall less DC energy being converted to AC. Tradeoffs between LCOE and reduced RR are situation-dependent design choices, and there exists no optimal one-size-fits-all solution.

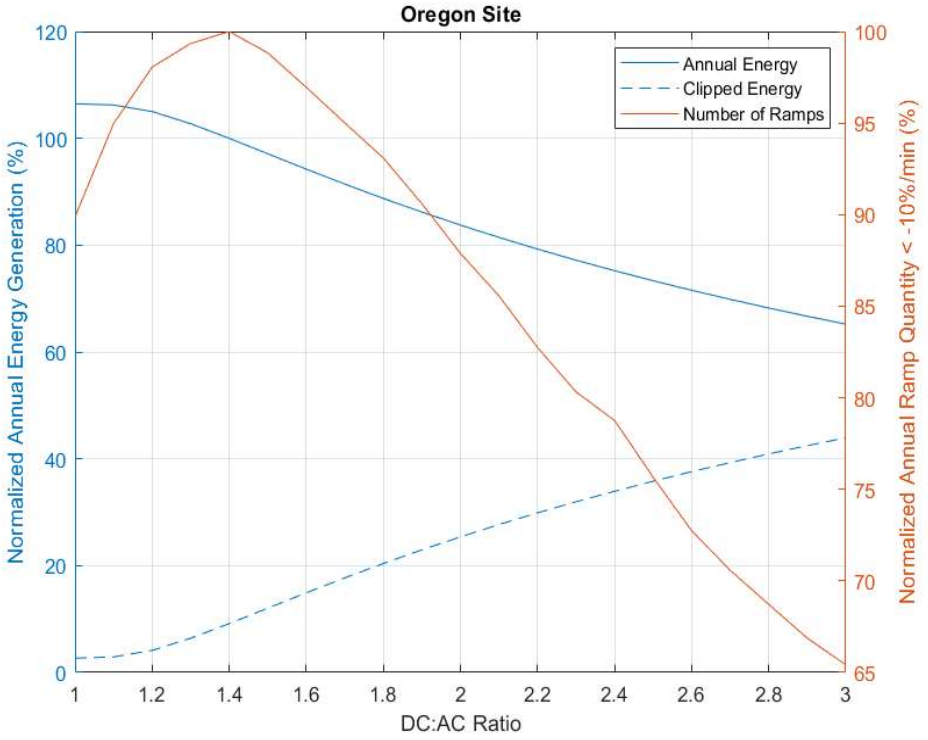

Figure 7: Annual energy generation and ramps as DC:AC ratio is varied with clipping loss captured.

Table 4: Summary of single parameter sweep.

	Annual Energy Generation Δ from Table 3	Ramps Δ from Table 3	CF_{DC} (%)	LCOE ($/kWh_{DC}$)
Tilt	-1.48%	-7.5%	15.7%	0.080
Azimuth	-19.2%	-30.6%	12.7%	0.100
DC:AC Ratio	-34.8%	-34.6%	10.2%	0.118

3.1.2.2 Multivariable Parameter Sensitivity

Multiple parameters were also varied to determine if a more optimal point for energy and RR value could be found from varying multiple parameters. The results show that varying two parameters away from their traditional optimal energy points can produce regions where energy and RR quantity are optimized. The changes in energy production and ramps from the optimal energy point to the ramp minimization are presented.

The tilt and azimuth angle were varied, with the DC:AC ratio held constant, to the same limits as the single variable sweeps were varied. The two variable results are shown in Figure 8 for the UO site and change in energy and RR are shown in Table 5. It can be seen from these combined views that for these combined parameters, the minimum number of ramps occurs in the corner case where tilt is at 60 degrees and azimuth is at 90 degrees. However, at the high tilt angle energy production is significantly reduced by the high tilt angle. Analytically this can be seen in Eq. (1) for the AOI. With all other variables being constant, the cosine terms will be close to zero when both azimuth and tilt are at high angles, which reduces energy production. Overall, the combination of suboptimal tilt and azimuth angle reduce RR quantity to a lesser extent than their single parameter variation, but the energy and LCOE is slightly higher when compared to the baseline configuration in Table 3. The optimal RR design point with a 10-degree tilt

angle and 90-degree azimuth is normalized against the baseline design with the results given in Table 5.

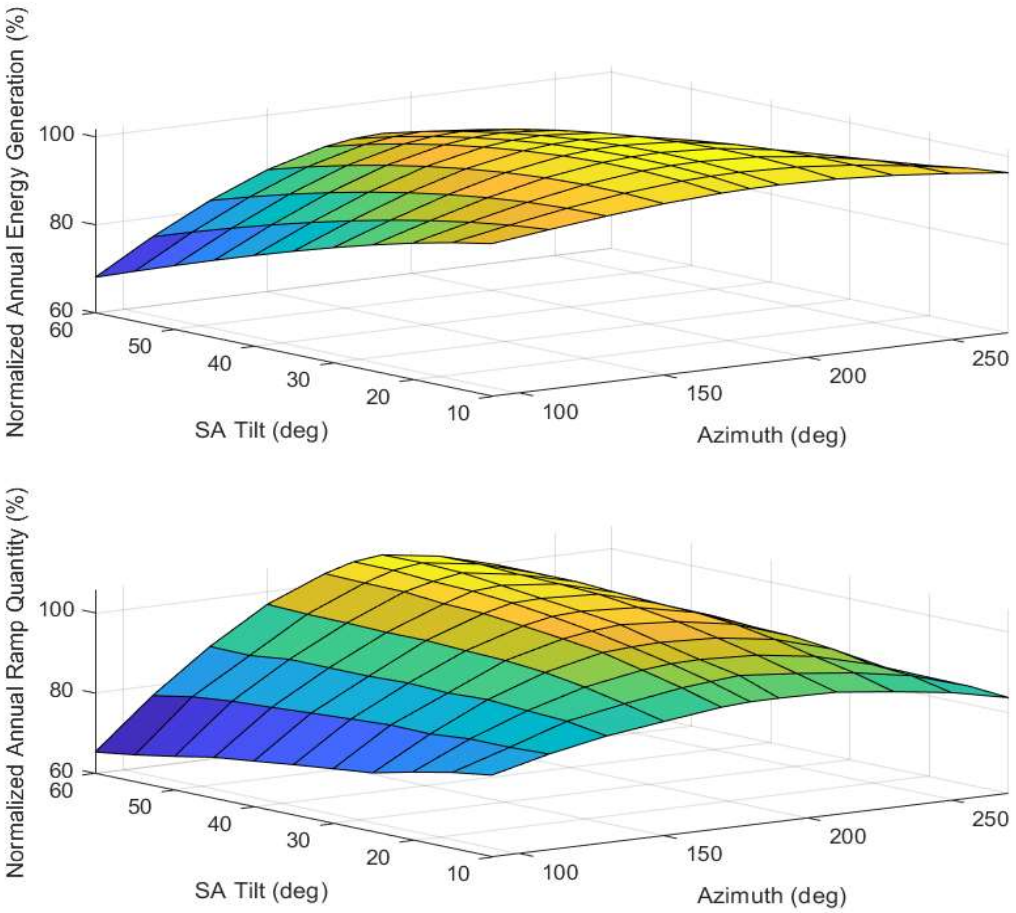

Figure 8: Annual energy generation and ramps as tilt and azimuth are varied.

The tilt angle and DC:AC ratio were varied across the same values as the single variable sweeps were performed, with the azimuth angle fixed. The two variable results are shown in Figure 9 for the UO site. With the AC size reduced as

the DC:AC ratio increases, the energy and RR quantity decrease proportionally. It can be seen in Figure 9 that the energy plane is relatively flat for ratios around 1.5 DC:AC ratio. The optimal RR design point for this two-parameter variation occurs with a 10-degree tilt angle and 3.0 DC:AC ratio. The LCOE is at a maximum for this case due to the reduced energy production from this case. The normalized comparison of this two-parameter variation against the baseline design is shown in Table 5.

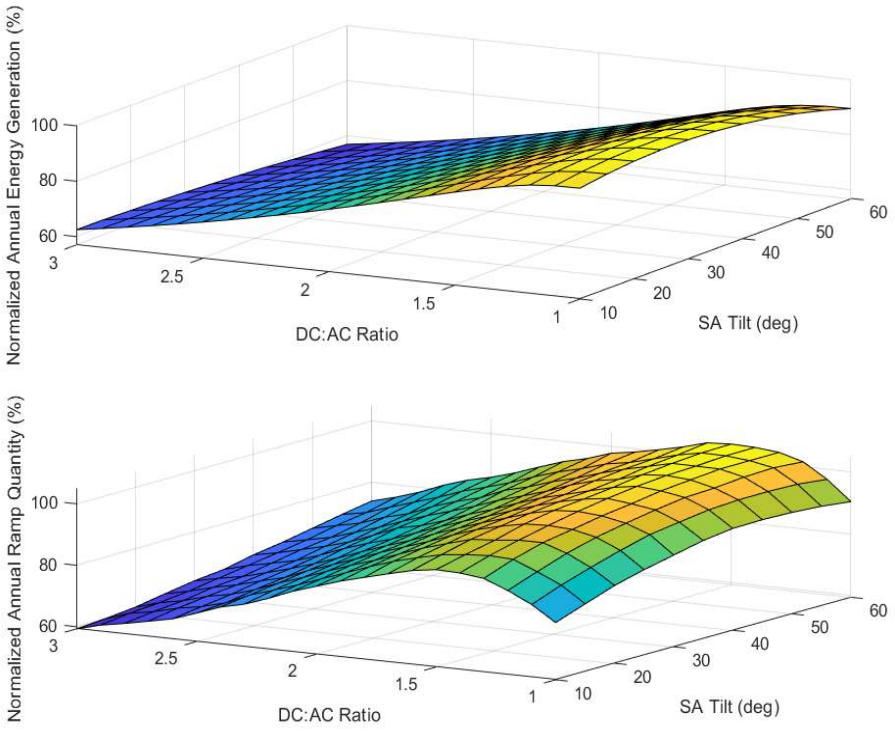

Figure 9: Annual energy generation and ramps as DC:AC ratio and tilt are varied.

The azimuth angle and DC:AC ratio varied between the same limits as the single variable sweeps were performed, with the tilt angle fixed. The two variable results for annual energy production and are shown in Figure 10. As with the single parameter sweeps, maximum energy occurs at a 180-degree azimuth and minimum RR quantity at 90 degrees. PV CF and RR quantity improve with higher DC:AC ratio. The optimal RR design point with a 90-degree azimuth angle and 3.0 DC:AC ratio is evaluated against the baseline, with results shown in Table 5.

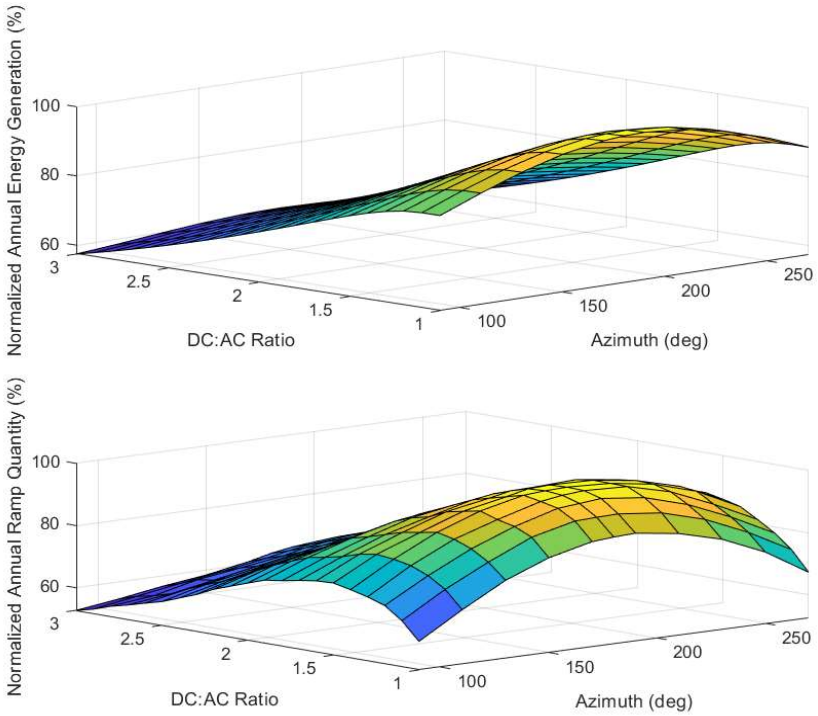

Figure 10: Annual energy generation and ramps as DC:AC ratio and azimuth are varied.

Finally, the evaluation of all three parameters was made at the minimum RR found from the two-parameter sweep results (e.g. Tilt of 10º, Azimuth of 90º, and DC:AC ratio of 3.0). The results are summarized in Table 5 and compared against the baseline configuration in Table 3. The variation of tilt with DC:AC ratio is the most balanced solution in terms of reducing RR while having a reduced increased in LCOE. Figure 11 shows the histogram result of the three-parameter variation. When compared to the initial optimal energy configuration shown in Table 3, RR is reduced along the entire spectrum of ramp rates with a 46% overall reduction in annual RR quantity with ramps worse than negative 70% per minute eliminated. The results show comparable benefit to varying all parameters as shown from varying DC:AC with azimuth or tilt.

Table 5: Summary of multiple parameter sweep.

	Annual Energy Generation Δ from Table 3	Ramps Δ from Table 3	CF_{DC} (%)	LCOE ($/kWh_{DC}$)
Tilt & Azimuth	-5.4%	-19.5%	15.1%	0.085
Tilt & DC:AC	-33.5%	-40.7%	10.6%	0.114
Azimuth & DC:AC	-38.8%	-47.3%	9.7%	0.124
Tilt & Azimuth & DC:AC	-34.8%	-46.4%	10.7%	0.117

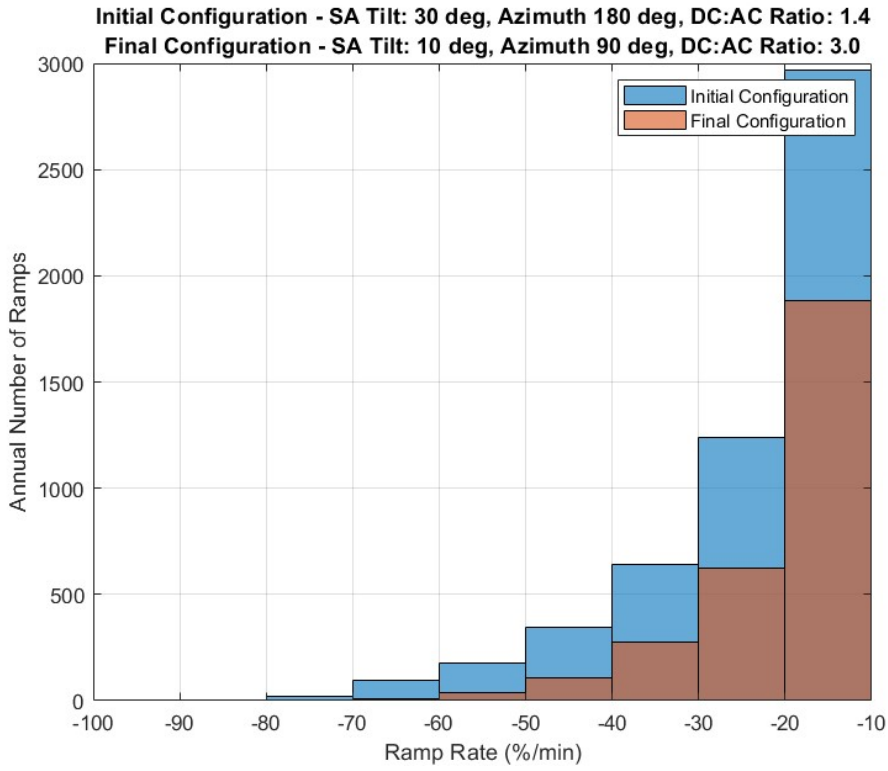

Figure 11: Annual ramp rate count with three parameter variation incorporated.

3.2 BESS Model

This section covers the development of the BESS model for the primary purpose of providing ramp rate control for the renewable sources. The use of BESS for ramp rate control is well understood. This section covers the incorporation of ramp rate control with aging effects of the battery to determine the minimum initial size to support a 10-year operational life.

3.2.1 Battery Cyclical Degradation and Rainflow Algorithm

To properly evaluate the coupling of renewable sources and BESS, the operational constraints of a BESS need to be properly bounded. A major contributor to battery life expectancy is cycle degradation, which is the incremental degradation of a battery as a function of its depth of discharge (DOD) per interval cycle. The cycle life curve is referenced from [49] and curve fitted with a two-parameter exponential curve to align with the degradation analysis performed later. The expression is shown in Eq. (10) with the full range curve fitted shown in Figure 12.

$$Cycle(t) = A(DOD)^B \tag{10}$$

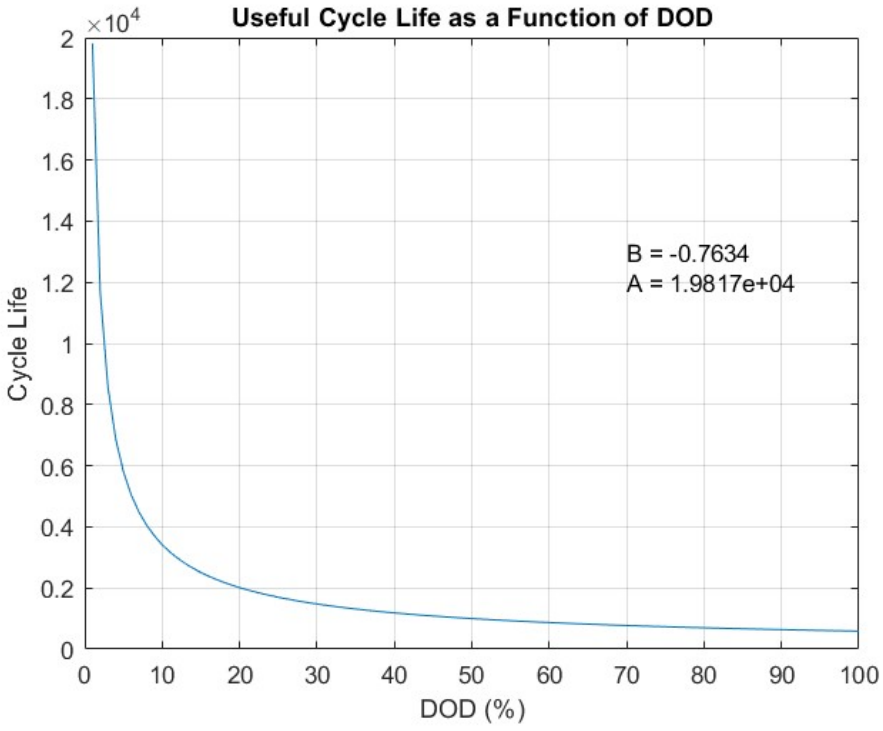

Figure 12: Battery cycle life as a function of DOD.

The cycles of a BESS with multiple use cases are not typically full 100% cycles. To account for sub-cycles and determine their equivalent effect on the BESS degradation, a rainflow algorithm is implemented. The rainflow algorithm is a step-by-step method of consolidating a list of time series data into a series of rising and falling slopes to determine where the changes in DOD slope occur and their magnitude. The full rainflow algorithm is discussed in depth in [31] and is summarized as follows:

- The full one-minute DOD dataset is reduced to a smaller dataset, DOD_r, to account for times when the DOD has peaks and valleys with a +/-0.5% dead band applied to account for trickle charge or discharge (which are counted as part of the calendar aging effects shown later).
- The first three points in the series are sorted into line segments as follows:

$$R_x(t_i) = |DOD_r(t_i) - DOD_r(t_i + 1)| \tag{11}$$

$$R_y(t_i) = |DOD_r(t_i + 1) - DOD_r(t_i + 2)| \tag{12}$$

- Rainflow cycles, RF, are determined to be either a half cycle (0.5) or a full (1.0) if the second line is larger and satisfies the following criteria:

$$RF(t_i) = \begin{cases} 0.5, if\ R_x(t_i) \le R_y(t_i)\ and\ t_i = 1 \\ 1.0,\ if\ R_x(t_i) \le R_y(t_i) \end{cases} \tag{13}$$

- The range (DOD in this case) is found from the difference between R_x and R_y.
- The sequence is repeated for the next three points until all rising and falling line segments are accounted for.

The cycle counts from this process are then summed against the DOD for each cycle interval to give the full degradation per cycle from the annual dataset. Combining Eq. (10) – (13), the full degradation expression for this is given by:

$$D_{cycle}(t_i) = \sum_{i=1}^{n} \frac{RF(t_i)}{Cycle(t_i)} \times 100. \quad (14)$$

3.2.2 Other Aging Factors

Another factor in the life of a battery cell is calendar degradation, sometimes referred to as aging losses. For days when the battery is not utilized to support, for example, PV generation (e.g. a rainy day with no RR events and minimal irradiance), the battery still experiences a slight degradation from being energized and held to an average 50% SOC. From [49], the calendar loss for a battery that is initially charged to 50% SOC is approximately 3% per year. The daily loss is then accounted for by dividing the annual loss to obtain the following:

$$D_{calendar}(t) = \frac{3\%/year}{365.25\ days/year} = 0.008\ \%\ loss/day \quad (15)$$

Additionally, lithium-ion batteries are also very sensitive to operating temperature. Temperatures too high or too low can negatively impact capacity and increase aging. The cell analyzed in this study has an optimal operating temperature of 35 degrees Celsius [49] and is the assumed operating temperature for this study. Thermal management is not considered further.

Finally, battery life is negatively impacted by high current rates. This is typically defined as C-rate, which is the ratio of maximum current to the amp-hour capacity. From [49], the cycle life testing performed was at a maximum 1C rate. This constraint is rolled into the model and the minimum battery is sized to always stay under 1C.

3.2.3 Minimum BESS Sizing

After the initial BESS sizing, the minimum size in terms of megawatt-hours, is determined by analyzing the annual degradation to determine if the battery exceeds the maximum of 3% per year. The annual degradation is the sum of the cycle and calendar losses:

$$D_{annual} = \sum D_{cycle} + \sum D_{calendar} \leq 3\%/year. \quad (16)$$

If the annual degradation exceeds this inequality, the BESS size is incrementally increased in a 5% per interval and the SOC and rainflow calculation is repeated. This process continues until the degradation criteria is satisfied. The full process flow of the model is shown in Figure 13.

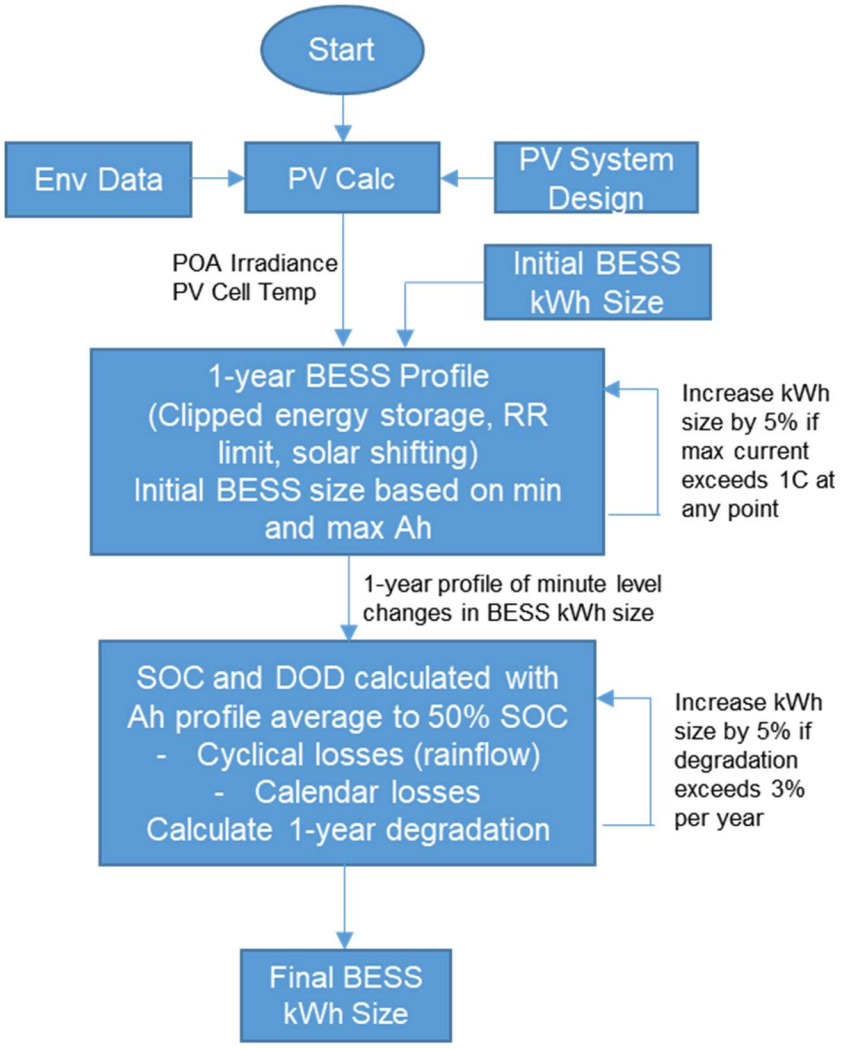

Figure 13: Flowchart of the process to determine the minimum BESS size from input parameters to final size.

3.2.4 BESS Model Results and Validation

Scenarios were analyzed with the 2022 UO dataset based on varying the RR between having no limit to having a 50% per minute limit along with the DC:AC ratio varying from 1.0 to 2.0 in 0.1 increments. In total, 77 unique cases were evaluated and summarized in Table 6. The relationship between DC:AC ratio and

RR requirements to the minimum BESS size are provided in Figure 14. The results show capturing the clipped losses from high DC:AC ratio is the primary driver of BESS sizing, and it is even more pronounced when considering a high DC:AC ratio and a small RR limit. There is also a slight shift in the BESS minimum size when considering systems with no RR limit and small DC:AC ratio versus other configurations. This is largely due to the differential between the positive RR (e.g. charging) and negative RR (e.g. discharging) throughout the year. There can be cases with larger positive ramps or larger negative ramps, which varies the minimum sizes for the various RR cases.

Table 6: Minimum BESS initial capacity (MWh) for 10-year operational life.

RR/DC:AC	1.0	1.2	1.4	1.6	1.8	2.0
+/- 5%/min	17.8	51.0	130.4	205.9	267.5	319.5
+/- 10%/min	13.7	50.6	135.7	216.2	284.8	337.4
+/- 15%/min	10.1	49.7	137.8	220.4	294.1	349.0
+/- 20%/min	7.6	48.3	137.5	227.5	301.1	357.9
+/- 25%/min	6.2	48.3	138.1	227.7	302.3	359.8
+/- 50%/min	3.9	51.4	143.9	235.1	309.8	364.6
No RR limit	4.6	53.5	145.3	235.1	310.7	365.5

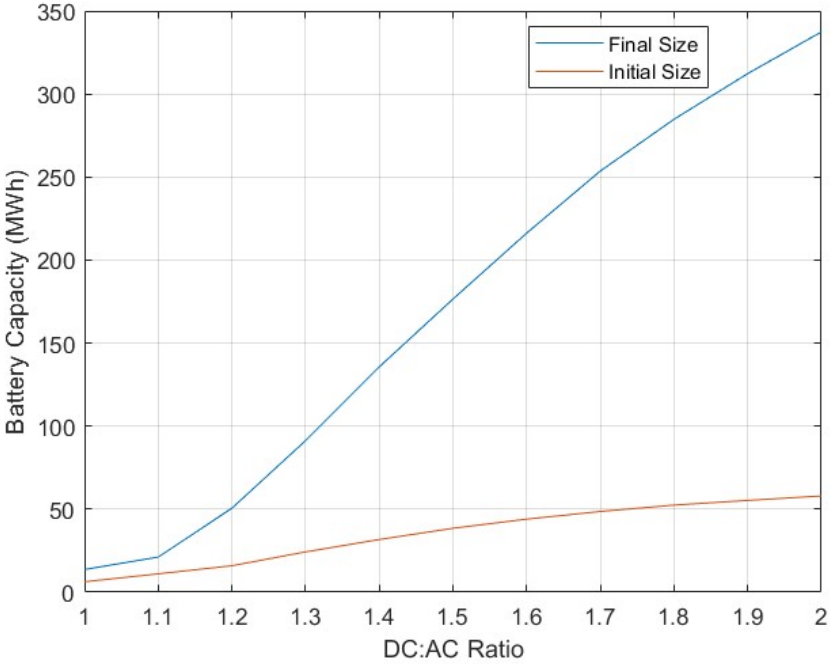

Figure 14: Minimum BESS growth as a function of DC:AC ratio with RR limited to +/- 10 per minute.

3.3 SMR Model

The SMR model is based on the design of the 45 MWe NuScale SMR that was approved by the U.S. Nuclear Regulatory Commission in 2020 [50]. This section covers two different methods of modeling the SMR. The first is the dynamic power model, which is based on literature and validating the model to the publicly available International Atomic Energy Agency (IAEA) simulator for this SMR. The result is an 8th order transfer function of the input power setpoint to net electrical power output. The second model is a linear interpolation of energy balance model based on the Rankine cycle of the referenced SMR. Both models are utilized as part of the study, and both are validated against the publicly available SMR simulator.

The dynamic model is used for transient analysis, while the interpolated model is used for minute level annual energy analysis.

3.3.1 Reactor Dynamics Model

The SMR model developed for this study is based on the Mann reactor core model [51] for a pressurized water reactor (PWR). The objective of the model is to represent the energy flow from the fuel rods in the reactor to the turbine-generator electrical power in terms of a high order time invariant transfer function. The model was further validated against the International Atomic Energy Agency (IAEA) model for NuScale SMR performance [52]. Figure 15 shows the notional reactor diagram with key parameters identified. The first part of the model is the derivation of the reactor core neutron flux, as described in [37] and [53]:

$$\frac{d\varphi_f}{dt} = \left(\frac{\rho}{\Lambda} - \frac{\beta}{\Lambda}\right)\varphi + \lambda C \tag{17}$$

$$\frac{dC}{dt} = \frac{\beta}{\Lambda}\varphi_f - \lambda C \tag{18}$$

The heat transfer model is derived from [54] with NuScale specific parameters incorporated from [37] with the temperature relationships defined as

$$\frac{dT_f}{dt} = \frac{\tau P_r \varphi + h_{fc} A_{fc} (T_{\theta 1} - T_f)}{m_f c_{pf}} \tag{19}$$

$$\frac{dT_{\theta 1}}{dt} = \frac{(1-\tau)P_r\varphi + h_{fc}A_{fc}(T_f - T_{\theta 1})}{m_c c_{pc}} + \frac{2\dot{m}_{cp}(T_{\theta 1} - T_{\theta 2})}{m_c} \tag{20}$$

$$\frac{dT_{\theta 2}}{dt} = \frac{(1-\tau)P_r\varphi + h_{fc}A_{fc}(T_f - T_{\theta 1})}{m_c c_{pc}} + \frac{2\dot{m}_{cp}(T_{CL} - T_{\theta 1})}{m_c} \tag{21}$$

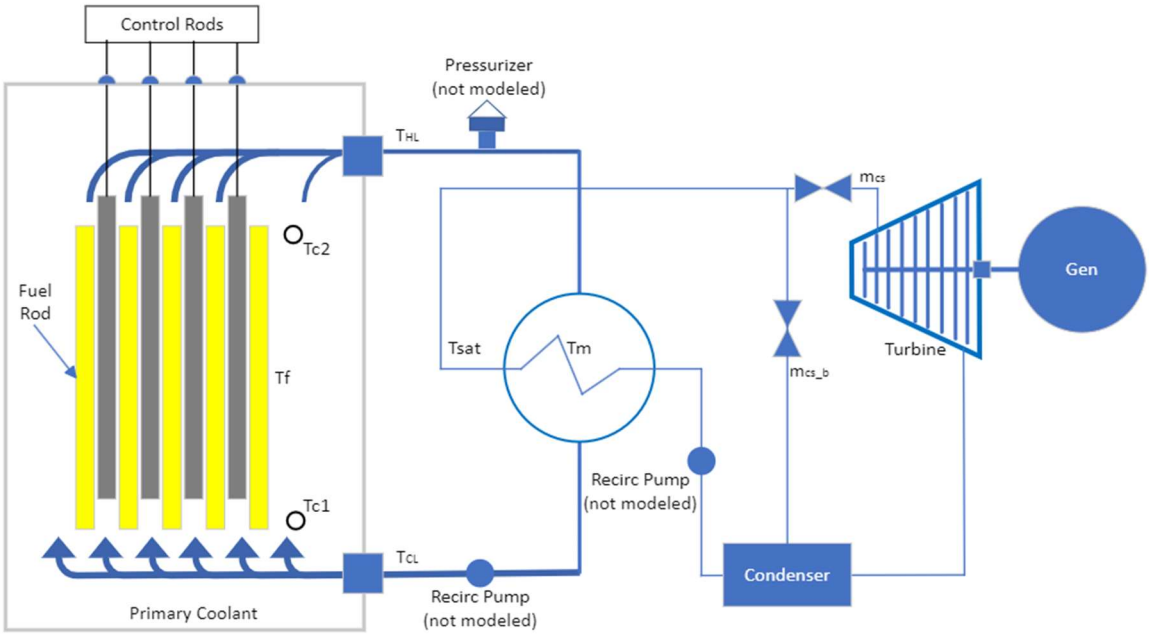

Figure 15: Simplified diagram of a pressurized water reactor.

The heat transfer from the primary coolant loop is estimated from the hot leg temperature and design parameters for the reactor. From there, the temperature in the heat exchanger, or metal lump, is defined as:

$$\frac{dT_p}{dt} = \frac{\dot{m}_{cp}(T_{HL} - T_p) + h_{pm}A_{pm}(T_m - T_p)/c_p}{m_p} \tag{22}$$

$$\frac{dT_m}{dt} = \frac{h_{pm}A_{pm}(T_p - T_m) + h_{ms}A_{ms}(T_{sat} - T_m)}{m_m c_m} \quad (23)$$

The change in saturation pressure in the secondary loop is determined by the mass flow, change in enthalpy, and based on multiple empirical points in the denominator estimated from literature [54]:

$$\frac{dP_{sat}}{dt} = \frac{h_{pm}A_{pm}(T_m - T_{sat}) + \dot{m}_{cs}(U_{const})}{m_{sw}\frac{dU_w}{dp} + m_{sv}\frac{dU_v}{dp} - \frac{U_{wv}dv_g}{v_{wv}\ dp}} \quad (24)$$

Finally, the net electrical power out of the turbine is determined as the product of the change in enthalpy and the steam mass flow through the turbine. Generator and turbine efficiency was estimated as a function of power level from literature [55] and shown as the following:

$$P_{SMR} = \eta_{elec}(P_{turb})\eta_{mech}\Delta h \cdot \dot{m}_{cs} \quad (25)$$

3.3.2 Steam Cycle Mass Flow and Energy Balance Model

The second modeling approach is a detailed mass and energy balance model of the Rankine cycle developed and validated against the IAEA simulator [52]. The advantages of this model over the dynamics model in Section 3.3.1 is coupling power to inlet water temperature and much faster simulation time with comparable results. Eq. (26) through (39) present the basic mass and energy relationships that

govern the operation of the SMR model. The model assumes a constant thermal load from the reactor module and is utilized to assess the impact of variation in the inlet cooling water temperature and condenser fouling on the power output of the SMR unit. As discussed in [56], these parameters influence the heat removal from the condenser, the operating pressure of the condenser, which influences the thermal efficiency of the steam power cycle within the SMR unit. Eq. (26) - (39) describe the fundamental relationships between the energy transferred through the condenser and the physical design of the condenser. This model is also utilized to assess the impact of power regulation on the performance of the SMR unit in the form of steam bypass for cases where hydrogen storage is not utilized. For cases with PEM storage, bypass is not considered. Constant and relational values are found from the International Atomic Energy Association (IAEA) simulator for the NuScale SMR [52]. Table 7 summarizes the key constant values from the simulator nominal operating point as well as design assumptions for the SMR model. Figure 16 presents a graphical depiction of the SMR model. The relationship for the energy balance model is the following:

$$m_1 = m_2 + m_3 \tag{26}$$

$$m_2 = m_4 + m_5 + m_6 + m_7 \tag{27}$$

$$Q_{boil} = m_1(h_1 - h_{13}) \tag{28}$$

$$W_{turb} = m_4(h_2 - h_4) + m_5(h_2 - h_5) + m_6(h_2 - h_6) + m_7(h_2 - h_7) \tag{29}$$

$$Q_{cond} = m_3(h_3 - h_8) + m_4(h_{14} - h_8) + m_5(h_{15} - h_8)$$

$$+m_6(h_{16} - h_8) + m_7(h_7 - h_8) \quad (30)$$

$$W_{pump,1} = m_1(h_9 - h_8) \quad (31)$$

$$W_{pump,2} = m_1(h_{12} - h_{11}) \quad (32)$$

$$m_4(h_4 - h_{14}) = m_1(h_{13} - h_{12}) \quad (33)$$

$$m_5(h_5 - h_{15}) = m_1(h_{11} - h_{10}) \quad (34)$$

$$m_6(h_6 - h_{16}) = m_1(h_{10} - h_9) \quad (35)$$

$$Q_{cond,1} = \dot{m}_{cs}(h_7 - h_8) \quad (36)$$

$$Q_{cond,2} = \frac{UAF_t(\dot{T_{co}} - T_{ci})}{ln\frac{(T_{shell} - T_{ci})}{(T_{shell} - T_{co})}} \quad (37)$$

$$Q_{cond,3} = \dot{m}_{cw}C_p(T_{co} - T_{ci}) \quad (38)$$

$$Q_{cond,1} = Q_{cond,2} = Q_{cond,3} \quad (39)$$

Table 7: Simulator values and design assumptions.

Parameter	Value	Parameter	Value
m_{cp}	586.9 kg/sec	T_1	219.9 ˚C
m_1	77.6 kg/sec	T_{10}	260 ˚C
p_1	2,730 kPa	T_{11}	260 ˚C
p_9	1,000 kPa	T_{13}	260 ˚C
p_{12}	3,970 kPa	P_{th}	164 MWt

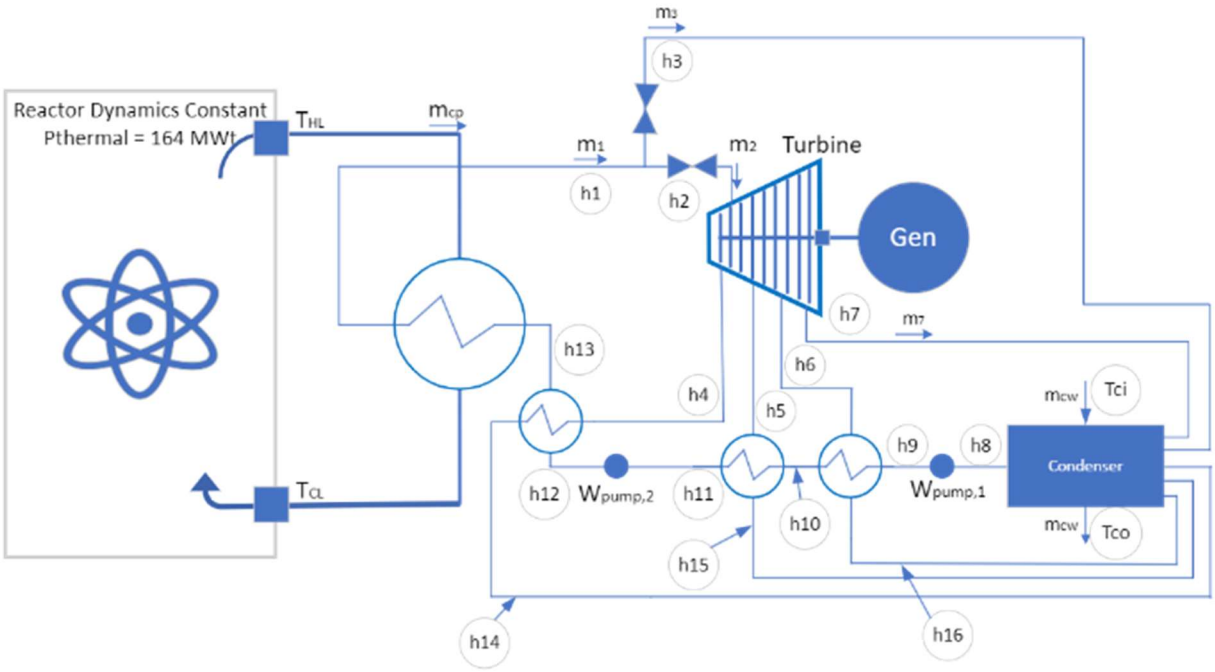

Figure 16: Simplified diagram of the SMR Rankine cycle.

Condenser area and cooling water flow parameters are designed to meet the rated 45 MWe at a 20-degree Celsius condenser inlet temperature per [52], using the given design parameters from the IAEA model.

The relationships in Eq. (26) to (39) are used with given parameter values from the IAEA simulator [52] in Table 7 to develop the overall steam power cycle mass and energy balance model. Utilizing the relationships given in Eq. (26) to (39), a relationship for turbine power as a function of inlet water temperature is found for typical steam bypass ratios that the SMR unit will experience. Figure 17 shows the relationship between cooling inlet water temperature and turbine power output

at different steam bypass levels. The impact of considering inlet water temperature on power production is shown in Table 8.

Table 8: SMR annual average power with variable inlet water considered.

Reference: 2022 Platte River Colorado [57]	Annual Average Power (MW)	% Change
Constant water inlet temperature (20 ˚C)	45.2	-
Annual river water data (15-minute interval)	46.8	+3.5%

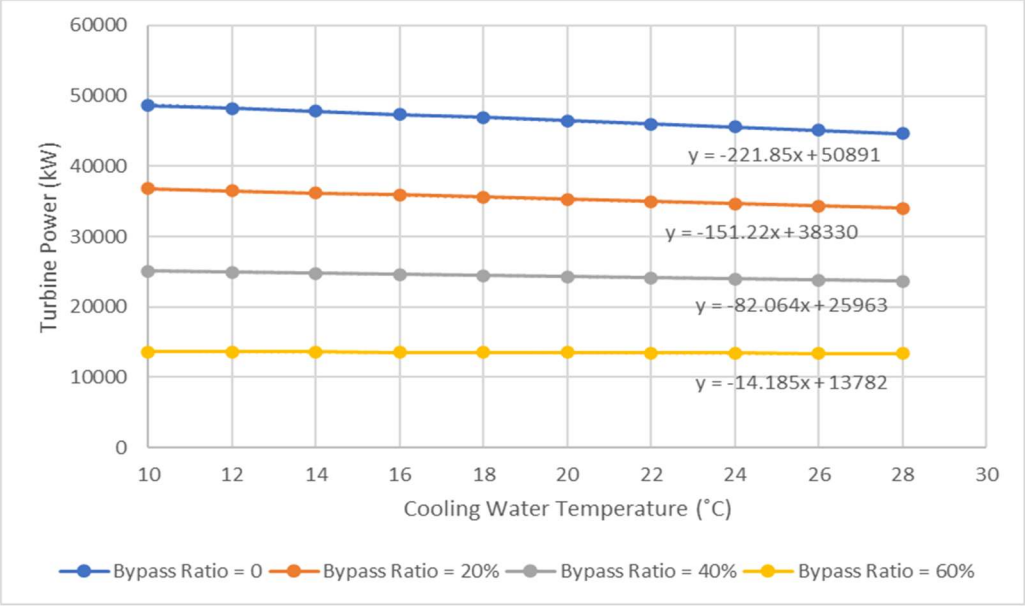

Figure 17: Relationship between turbine power and cooling temperature & steam bypass ratio.

The equations for turbine power as function of inlet water temperature and steam bypass are the following:

$$P_{turb}(T_{ci}, 0\ bypass) = -221.85(T_c) + 50891 \quad (40)$$

$$P_{turb}(T_{ci}, 20\%\ bypass) = -151.22(T_c) + 38330 \quad (41)$$

$$P_{turb}(T_{ci}, 40\%\ bypass) = -82.06(T_c) + 25693 \quad (42)$$

$$P_{turb}(T_{ci}, 60\%\ bypass) = -14.19(T_c) + 13782 \quad (43)$$

Finally, the net electrical power out of the synchronous generator is expressed as the following:

$$P_{SMR}(T_{ci}) = \eta_{elec}(P_{mech})P_{turb} \quad (44)$$

3.4 WTG Model with Wake Effects

The WTG model is developed empirically, based on the performance of the Enercon E-82 wind turbine [58]. This turbine was selected due to its attribute of being a Type IV wind turbine (e.g. fully converted output) with a gearless drive for high reliability and low O&M. The power from wind is based on the standard power equation and is given as

$$P_{WTG}(v) = 0.5\rho_{air}A_{WTG}v^3C_p(v) \quad (45)$$

The environmental data used for wind speed uses measurement data from 10 meters above the ground. The cut in speed of 2.5 meters per second and cutout speed of 25 meters per second. Given the non-linear nature of wind speed, an adjustment factor [59] is applied to determine the wind speed at the WTG hub height of 100 meters,

$$v = \left(\frac{heigh\ _{actual}}{height_{measured}}\right)^{a} v_{measured} \tag{46}$$

To accurately model the performance of the WTG, the coefficient of power (Cp) curve was modeled as a linear curve fit between the points in the E-82 profile, as shown in Figure 18. This was determined to be a more efficient approach, from an annual energy analysis, than modeling the WTG pitch control system.

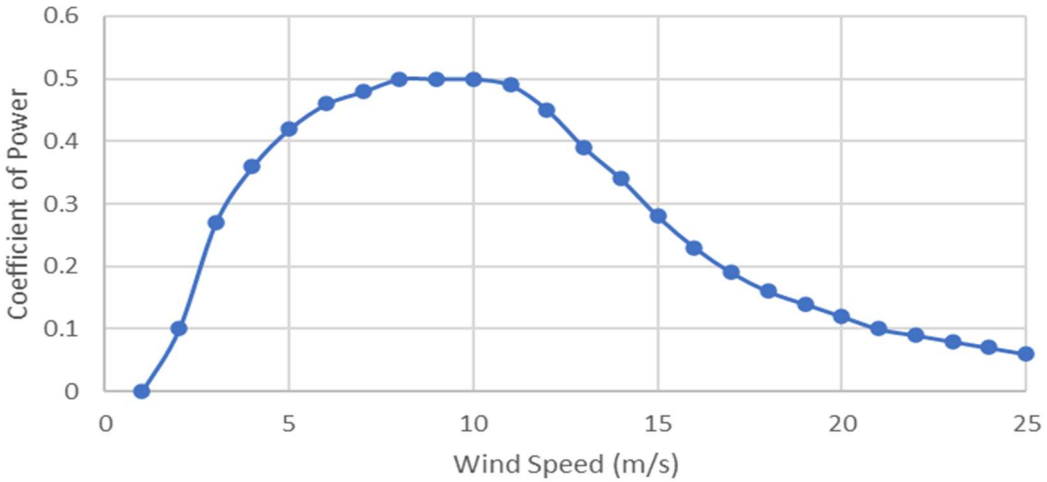

Figure 18: Power profile for the Enercon E-82 WTG.

C1. Wake Modeling

Wake is an important consideration for a multiturbine wind farm. It is caused by turbulent air flow from upstream WTG impacting performance of downstream units. For this study, the Park Wake Model is utilized [59]. The relationship for wake effect impacts on wind speed is the following,

$$\delta V = \left(1 - \sqrt{1 - C_T}\right)\left(\frac{D_0}{D_0 + 2kx_{01}}\right)^2 \frac{A_{overlap}}{A_1} \tag{47}$$

$$v_{adj} = v(1 - \delta V) \tag{48}$$

The wake model is calculated for each row of WTGs, accounting for the impact of the turbulence caused by the preceding rows. For simplicity, turbine rows in this study were assumed to be 10 turbines long, with successive rows assumed to have 10 rotor diameters of spacing. A representation of the assumed WTG row layout to minimize wake effects is shown in Figure 19. A maximum of five rows were assessed with the decreasing CF of each row shown in Table 9.

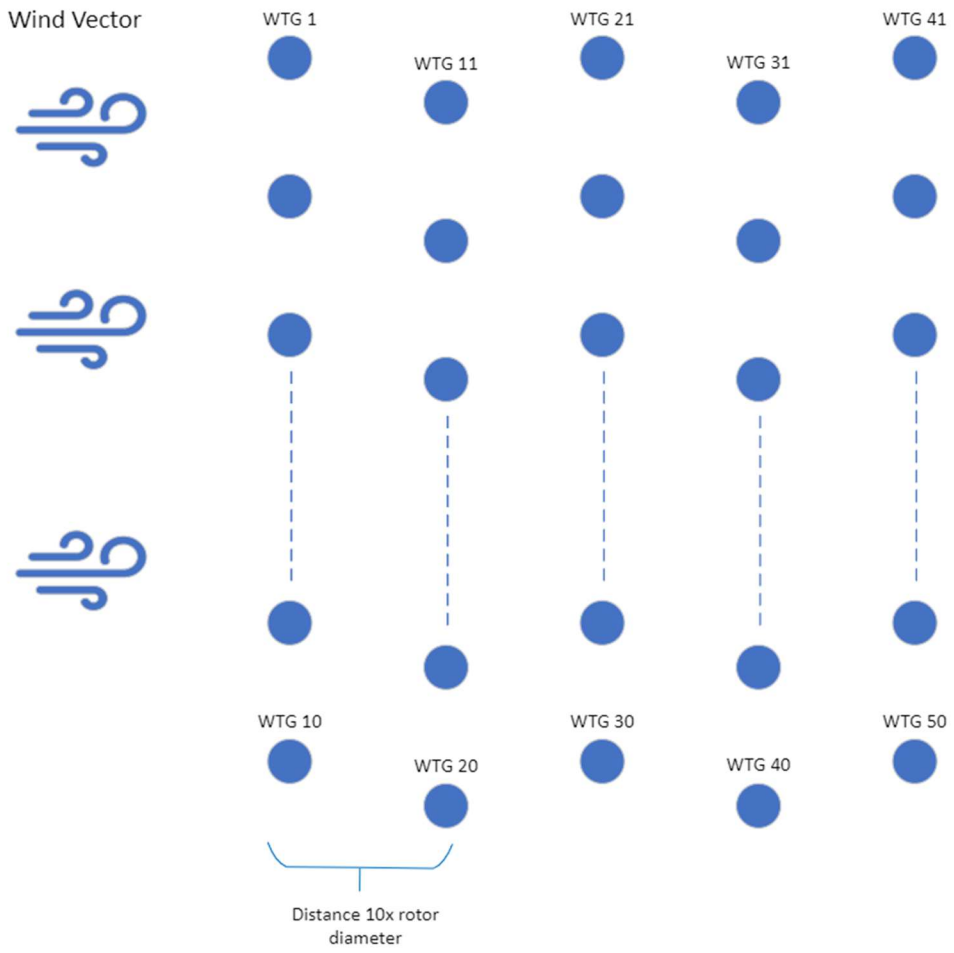

Figure 19: Layout of the proposed WTG to minimize wake effects.

Table 9: WTG wake effects impact on energy production.

NREL Region	Annual CF				
	Row 1	Row 2	Row 3	Row 4	Row 5
With Wake Effects	28.3%	27.1%	25.9%	24.7%	23.6%
Without Wake Effects	28.3%				

3.5 PEM Model

With HES load following generation, there are periods where excess power is available which can be either stored or curtailed. For long duration energy

storage, the most practical solution was determined to be hydrogen. Other storage options, such as flywheel or compressed air storage, are relatively immature for techno-economic evaluation. Large scale battery energy storage is currently non-viable from an economic standpoint. Hydrogen as a storage sink presents many opportunities beyond just electricity production. Hydrogen is used as clean rocket fuels, agriculture, home heating, and carbon free transportation. As such, the scope of this study only includes hydrogen production up to its storage and considers the value of hydrogen as improving the overall HES IRR. PEM was selected as a technically mature and commercially available hydrogen production method. The most common commercial PEM uses a membrane to separate the immersed anode and cathode terminals. As current passes through the water, hydrogen ions pass through the membrane and collect on the cathode [60]. The net chemical formula for these reactions is summarized as:

$$2H_2O + 2e^- \rightarrow 2H_2 + O_2 \tag{49}$$

The rate of hydrogen production in grams per second is given as a function of the voltage applied and several design parameters given in [60] and defined as:

$$H2_{rate} = \frac{2.01 n_f n_{elec\_f}}{V_{stack} F_{constant} z} I \tag{50}$$

The rate of H2 production can then be integrated over time to find the cumulative production over the one-year analysis period. Excess renewable and SMR generation are measured against the current reference demand power. The PEM is modeled as a load, subject to the relationship in Eq. (50). A minimum power of five megawatts is maintained through the PEM to keep current flowing to maintain operating temperatures. As shown in [60], keeping current flowing through the PEM is critical for maintaining efficient energy conversion as load demands change. The implementation with the SMR+WTG bus (e.g. AC bus) and PVdc bus is shown in Figure 20. The final step in hydrogen production is to compress the hydrogen into a liquid. Per [61], approximately 17 megajoules per kilogram is needed to store hydrogen as a liquid for use. This rate is multiplied by the real time hydrogen production rate in kilograms per second to determine instantaneous power consumption. For the HES model, the power for compression is assumed to come from the gross power production with net power output considered in the HES models' financial evaluation.

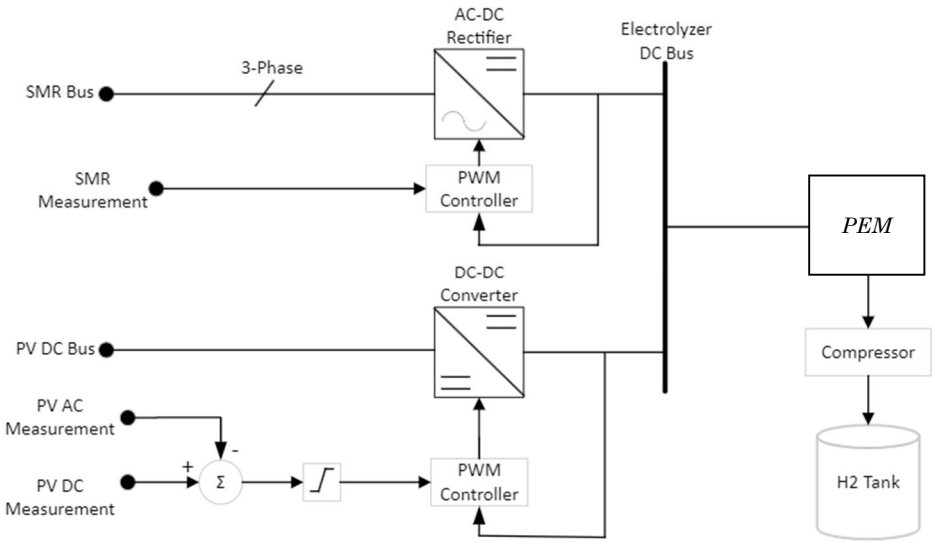

Figure 20: Power flow from excess sources to the PEM.

3.5.1 PEM Aging Effects

The PEM ages from an increase cell voltage over time. The rate of decay limits PEM useful life to approximately 96,000 hours, or about 10.9 years [62]. This is caused by the oxidation of the electrodes over time. For this study, 10-year life is considered, with the average voltage growth of 10 microvolts per hour [62]. The average decrease in efficiency is 1.33 percent per year and is incorporated into the 30-year financial analysis.

3.6 Models of Power Conversion Device Efficiencies

For energy conversion devices (e.g. power electronics, generators, motors, PEM) efficiency is applied as a function of power input. The respective maximum efficiencies are modeled based on literature-based test measurements. The power electronics curve is applied to all DC-DC converters, DC-AC inverters, and AC-DC

rectifiers. This curve is referenced from the SMA Sunny Central inverter [48] as power electronics follow the same profile. The generator efficiency is based on the efficiency measurements for synchronous generators used in a marine environment [55]. Two curves are utilized, one for unity (1.0) power factor and the other for 0.8 power factor (either leading or lagging). Finally, the PEM efficiency curve is based on a calculated value of efficiency as a function of current density for a development unit [63]. The load factor-efficiency relationship for all three conversion devices is shown in Figure 21 with two curves provided for the synchronous generator at different power factors. The efficiency representations of these units provide variable loss factors and, when coupled with their respective time constants, a practical representation of the power profile with the HES.

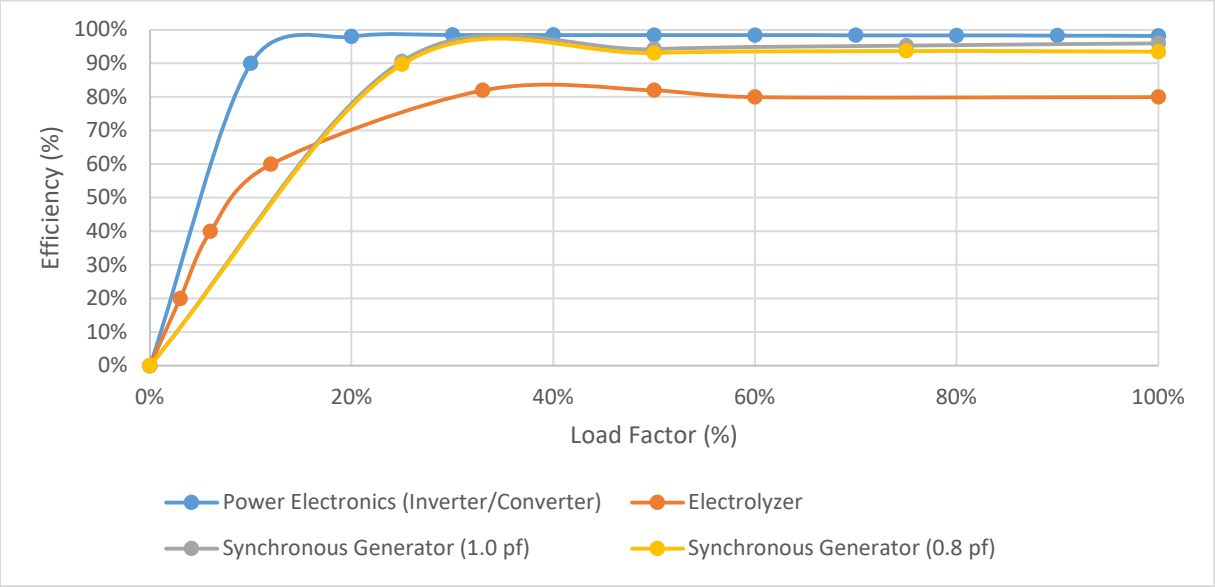

Figure 21: Efficiency as a function of load for each conversion source.

CHAPTER 4

INTEGRATED HES MODEL

Two integrated HES models were developed. The first is the annual energy model to determine deficits and surpluses in energy provided on a minute level time scale. The second, a transient model based on the IEEE 9 Bus model was developed to evaluate the viability of the HES to respond to frequency perturbations as part of a large contribution (40% in this case) of the system load. To evaluate all the sources operating together, a coordinated control model was developed and covered in Section 4.1. Additionally, in the case of the transient model, governor control, transformer phase shifting, and field excitation are also considered. This section is an expansion of the study published in [Publication C] – [Publication D].

4.1 HES Control Modes

Multiple methods were attempted for HES control. This section covers the three viable approaches determined, with only two included in the HES models. The first control option is SMR control rod actuation. In this option, the renewable sources output the maximum amount of available power and the control rods within the SMR reactor are raised or lowered to reduce the reactivity in the core. While this option is the most fuel efficient, as it reduces fuel consumption for periods of low power, the economic benefits are minimal and do not offset the operational wear and power performance impacts, as discussed in Section 4.1.1. As a result, the

methods selected are SMR steam bypass regulation, for cases without PEM storage, and PEM load regulation for cases considering this configuration.

4.1.1 HES Control via SMR Steam Bypass Regulation

SMR power output is flexible with two primary methods of regulating power output through a nuclear power plant: control rod actuation and steam turbine bypass. While control rod actuation is more energy efficient, for this study, only steam turbine bypass is considered. This is because a significant concern with control rod actuation, particularly when coupled with PV production, is the buildup of Xe-135 which can lead to xenon poisoning of the core [19]. This poisoning reduces the reactivity of the core and leads to reduced power production. Steam bypass resides on all steam plants as a means to rapidly shutdown a turbine in an emergency situation. It has also been used in [35] as a primary method of SMR power regulation with renewables. The advantages of this approach are faster response times to changing load conditions. The disadvantages are increased valve aging and reduced energy efficiency due to the steam bypassed around the turbine, which are not considered in this study. A proportional integral differential (PID) controller for steam bypass was developed and implemented as shown in Figure 22. The control loop was tuned to allow for the rated 22% per minute ramp rate specified in the IAEA simulator [52] and optimized for disturbance rejection (e.g. variable output from the PV subsystem). The closed loop PID is stable for all normal operational bounds.

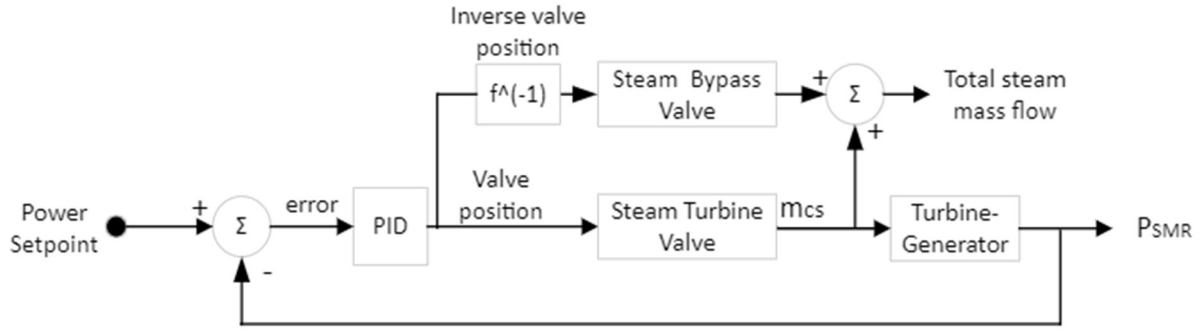

Figure 22: PID control loop for steam turbine bypass.

4.1.2 HES Control via PEM Regulation

For the HES, there are two control methods. The first one, for configurations without H2 storage, the steam bypass around the SMR regulates power output. Once it has reached its operational limits, power is further curtailed in the PV and then the WTG. The second method is for configurations with H2 storage, the PEM is the primary control loop and regulates electrolyzer current based on the load reference point. Each configuration utilizes a PID controller with a sub-minute time constant to properly adjust power output to respond to changing load requirements and resource variability. These control loops are shown in Figure 23 and Figure 24.

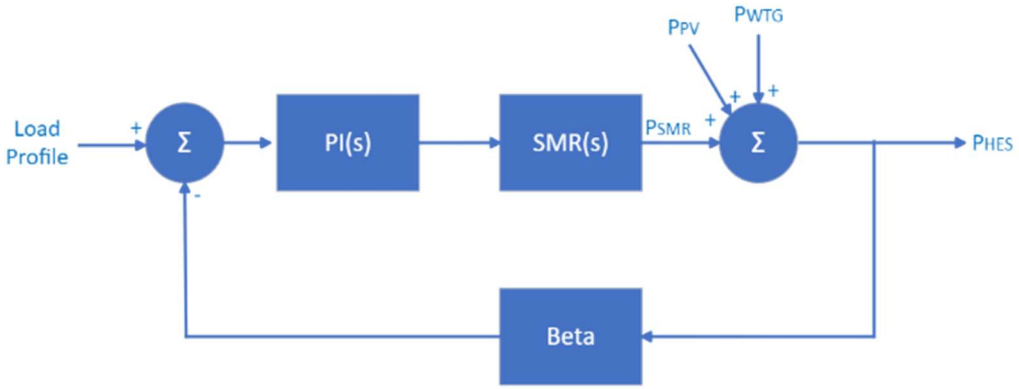

Figure 23: Closed loop control for fully curtailed energy cases.

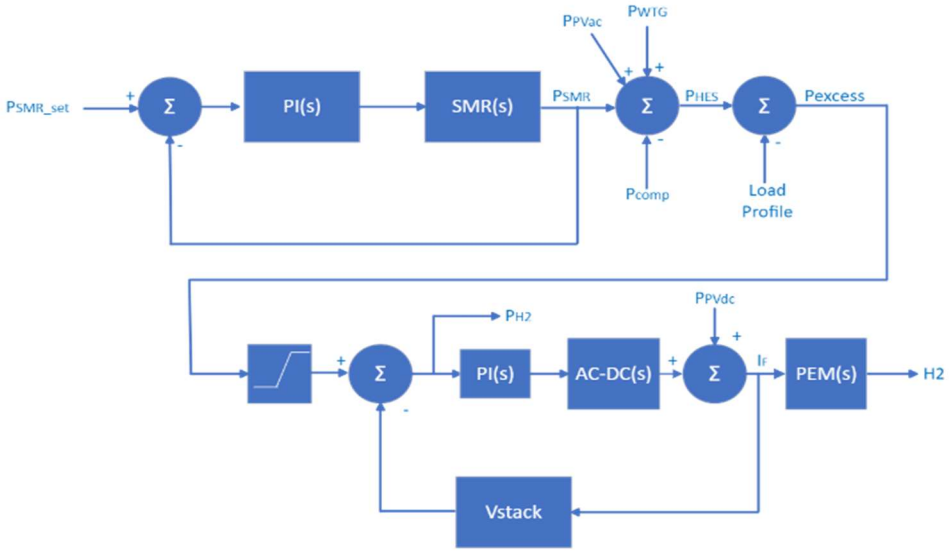

Figure 24: Closed loop PEM storage energy cases.

4.2 Integrated HES Energy Model

The full model was incorporated into Simulink. The model is set to sample at one second intervals to capture the controller response and reactor time constants. The weather and load data are inputs, interpolated to one second to align with the model sample rate. The following equation gives the full HES stack up as a function of all the variable environmental constraints, as well as time:

$$P_{HES}(AOI, T_c, POA_{IRR}, v, T_{ci}, t) = P_{PVac} + P_{WTG} + P_{SMR} \pm P_{BESS} - P_{H2} - P_{comp} \quad (51)$$

4.3 Ramp Rate Control

RR control is implemented by charging the BESS for positive ramps and discharging for negative ramps when the predefined limit is exceeded. This control loop is applied to the measured output of the combined HES and results in a response by the BESS. The definition of RR is written as:

$$RR = \frac{P_{PV}(t_0 - 1) - P_{PV}(t_0)}{1\ minute} \quad (52)$$

This limit looks at the change in power over a rolling one-minute measurement. The RR limit is imposed based on the AC power output when it exceeds its defined limit. The power limit is defined as:

$$P_{AC-Regulated} = P_{AC} * (1 + RR_{limit}) \quad (53)$$

Where RR_{limit} = The ramp rate limit in terms of percent power change per minute which is set to +/-10% per minute for this study. For this study, open loop control for ramp rates is implemented to prevent the unstable interaction with the overall plant controller. As such, the open loop controller was tuned to ensure

compliance to the ramp rate limit for all cases analyzed. A block diagram of the open loop ramp rate control is given in Figure 25.

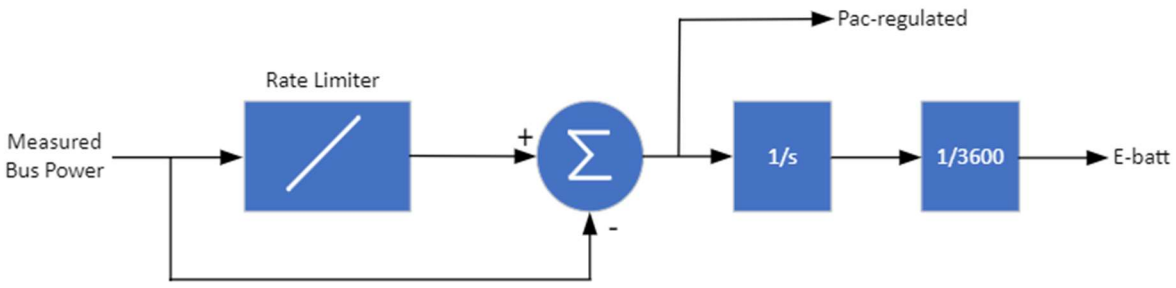

Figure 25: Open loop ramp rate control for BESS regulation.

4.4 Network Effects Model

The HES transient model was incorporated into the IEEE 9 bus model that is part of Simscape [64] within MATLAB/Simulink. This model was selected for giving a minimum amount of network details to assess a bounding transient response. This is done to ensure that the worst-case variability of the renewable resources will not negatively affect system bus voltage and frequency stability. Additionally, it ensures the HES control loop can respond to transient events. The key relationship between SMR generator terminal voltage and frequency/rotational speed is based on the d-q transformation for rotational frame reference relationships captured in this model and given as the following:

$$e_d = \frac{1}{\omega_{base}} \frac{d\psi_d}{dt} - \psi_q \omega_r - R_a i_d \tag{54}$$

$$e_q = \frac{1}{\omega_{base}} \frac{d\psi_q}{dt} - \psi_d \omega_r - R_a i_q \quad (55)$$

$$e_0 = \frac{1}{\omega_{base}} \frac{d\psi_0}{dt} - R_a i_0 \quad (56)$$

The model in [64] is modified such that the HES nameplate is approximately 40 percent of the nominal load. The SMR is modeled as a full turbine generator with steam turbine and field excitation controls with its rated +/-20% per minute ramp rate applied based on rated limitations [52]. The PEM storage is modeled as a variable load and the renewables sources as negative loads. Frequency response is embedded into every subsystem in the HES and functions as detailed in [14] for response to over and under frequency events. Full configuration details are provided in the Results section. The modified 9 bus test model is shown in Figure 26.

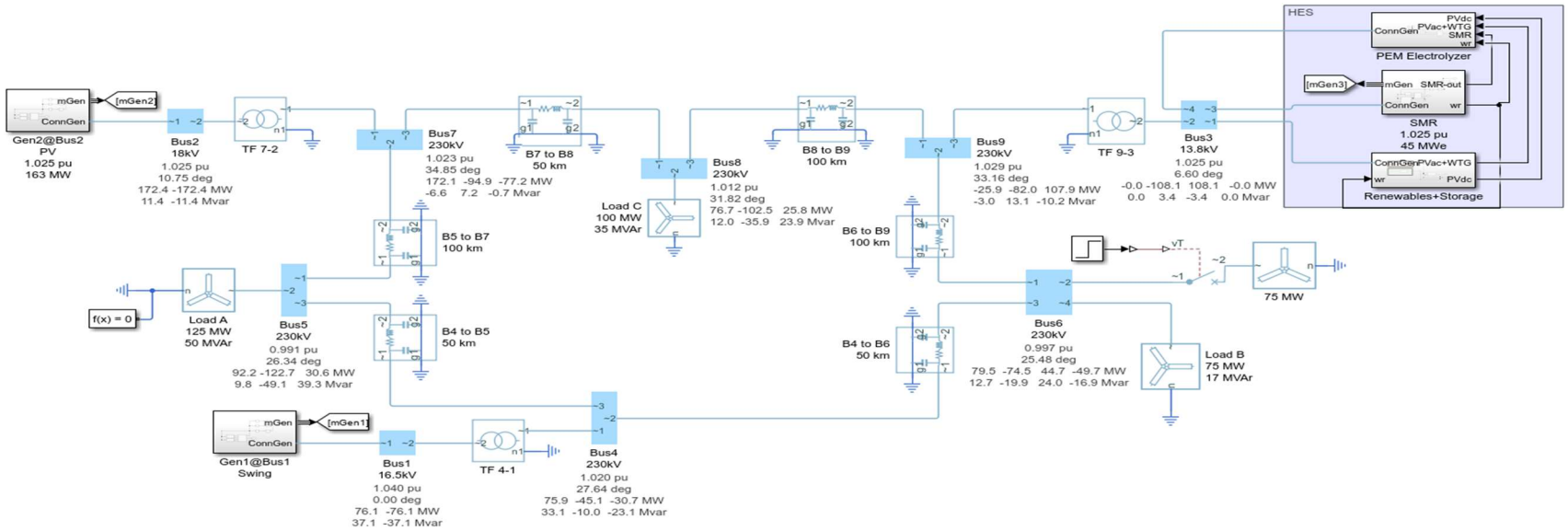

Figure 26: IEEE 9 test bus configuration [64], modified with proposed HES on Bus 3.

4.4.1 Frequency Response

One critical operation for power generating units is to respond autonomously to major frequency deviations in the power system. In North America, the nominal system frequency is 60 hertz with a deadband of +/-0.1 hertz applied for most generating units in the Western Electricity Coordinating Council (WECC) region [65]. Deviations above the deadband correspond to a surplus of generation on the system and a reduction in power is required. Frequency deviations below the deadband correspond to a deficit of power and an increase in power is required. With the proposed HES, this can also be achieved by varying load through changing the BESS operating point and ramping down power into the PEM (e.g. acting as reserve margin). Each resource is set to autonomously follow a specific frequency response depending on the severity and direction. The intent for each is to reduce generation and add load in the case of an over frequency event, with the inverse operation for an under-frequency event. For this study, each resource in the HES responds according to their own constraints to compensate for the frequency event. Table 10 summarizes the response of each source to varying degrees of frequency perturbations.

Table 10: FR autonomous action by each resource.

Frequency	PV	BESS	SMR	H2
f>60.2	Ramp to 0	Max Charge	Ramp to Min Power	Excess Storage
60.1<f≤60.2	Max PV	Max Charge	Max Power	Excess Storage
59.9≤f≤60.1 (nominal)	Max PV	RR Control	Max Power	Excess Storage
59.8≤f<59.9	Max PV	Max Discharge	Max Power	Excess Storage
59.8<f	Max PV	Max Discharge	Max Power	Min Power

To validate the frequency response, a test curve from National Grid in the UK was adopted and modified to the WECC limits [66] for 60 hertz operation and applying the appropriate thresholds. The frequency test profile was incorporated into the annual energy production simulation to ensure the HES remained stable and responded correctly as variations in load and solar production occurred over the sample period. The frequency response of the HES is shown in Figure 27. It can be seen from the results that each resource followed the steps defined in Table 10. In particular, the response of the PV system varies from ramping versus ramping up.

This is due to the lack of storage support, as the BESS is also ramping due to the frequency transient. As a result, the slower ramp up following frequency restoration is regulated by the inverter controls. All other sources respond as expected.

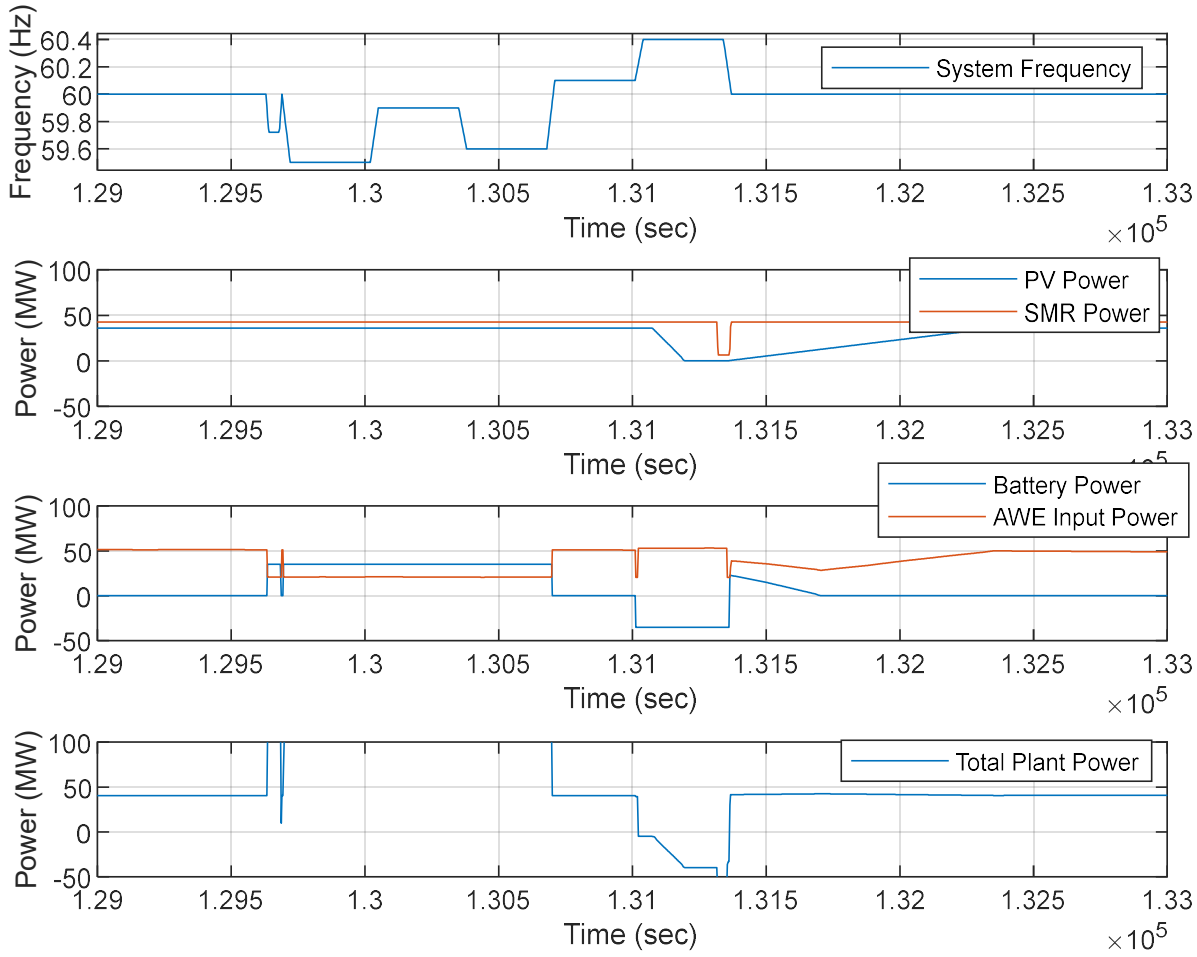

Figure 27: HES response to frequency events.

4.5 Model Validation

Given the novelty of the fully integrated model, full validation against an existing comparable model is not possible. However, individual pieces can be evaluated against referenced, or other publicly available tools. The SMR model is

validated against the IAEA simulator [52]. The PV model is validated against PVWatts [67]. The WTG model is evaluated against the rated performance datasheet [57]. Finally, the PEM nominal conversion efficiency is validated against the literature efficiency range 67 to 82%, with an average efficiency of 74.5% [62]. The results of the validation are shown in Table 11. The results show that the individual model results are within range of the reference sources. Reasons for variation are consistent with higher fidelity (e.g. cell temperature, wind speed, multiple irradiance vectors), in the case of the PV model versus the PVWatts estimate, and differences in input assumptions.

Table 11: Model validation results.

Subsystem	Comparison	HES Model	Reference	% Diff
PV	Annual Energy Production UO region in PVWatts	9.52 GWhac	9.15 GWhac	+4.02%
WTG	Rated WTG at 8 m/sec from datasheet	2.28 MWac	2.30 MWac	-0.89%
SMR	Rated SMR Output from IAEA simulator	45.20 MWe	45.09 MWe	+0.24%
PEM	Average electrolyzer efficiency	76%	74.5%	+2.01%

CHAPTER 5

FINANCIAL MODEL

To determine the best HES configuration, a financial model is developed to evaluate each configuration's financial merit. The objective of the financial assessment is to normalize the parameters of meeting energy production, deficit, curtailment and storage to a common resultant: profitability. For this study, IRR is assessed for each HES configuration to determine its viability. The target threshold for profitability is set at five percent IRR over the project life. For results below the target threshold, the HES is not a compelling investment. This chapter covers the development of the financial model and the normalization of results to IRR. This topic is an expansion of [Publication D], which covers the development of the financial model, with this chapter having a more comprehensive discussion.

5.1 Financial Assumptions

To construct a financial model for a novel technology, like an HES with an SMR, multiple assumptions need to be made. With the lack of empirical data for a completed and operational SMR, references come from literature for expected cost projections and targets. The financial information for PV, WTG, and BESS comes from NREL market surveys of recent installations. The SMR and PEM are more dependent on cost projections. For the combined HES, assumptions are made for the reuse of things like substation interconnection and not considered for all sources. Additionally, a timeline is constructed to account for initial construction period,

partial operation, full operation, refueling, and 10-year replacement cycles for the PEM and BESS with their operation ceasing after year 31. For replacement cycles, it is assumed that 40% of the PEM and BESS can be reused (e.g. non battery cell, electrode components). The assumptions for tax rate, inflation, and interest are based on a PV+BESS study in [68]. Table 12 has the full list of financial assumptions and inputs with the operational timeline given in Figure 28. Not considered in this evaluation is the residual value or salvage value of the HES.

Table 12: Financial input references and assumptions.

Parameter	Value	Parameter	Value
Base PPA	$60/MWh	Energy Deficit Penalty [69]	$98/MWh NREL $93/MWh UO
Base H2	$2/kg	SMR Life	4-year build 30-year operation
Finance Life	30 years	SMR Refueling	2-months every 22 months
Interest Rate [68]	5.0%	PV Life	1-year build 34-year operation
Annual Inflation	3%	WTG Life	2-year build 1 failed WTG per year after year 25 34-year operation
Down Payment	20.0%	BESS	1-year build 10-year operation

Parameter	Value	Parameter	Value
Tax Rate [68]	28%	H2 Life	1-year build 10-year operation
Battery Cell Recycling [70]	$0.32/kg	SMR O&M [72]	$750/kW-yr
Water Cost [71]	$7.5e-4/L	PV O&M [68]	$16/kW-yr
SMR CapEx [72]	$6025/kW	WTG O&M [73]	$40/kW-yr
PV CapEx [68]	$940/kW	BESS O&M [68]	$10/kW-yr
WTG CapEx [73]	$1501/kW	H2 O&M [70]	$14.5/kW-yr
BESS CapEx [68]	$845/kWh	BESS Re-use	40% of CapEx
H2 CapEx [70]	$1803/kW	PEM Re-use	40% of CapEx

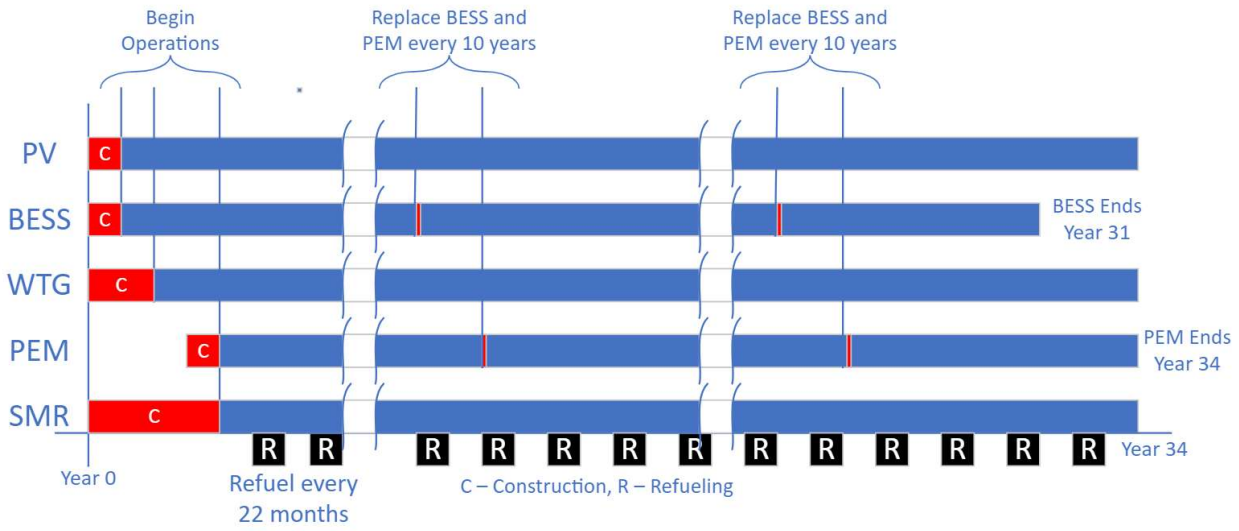

Figure 28: Operational profile over the finance lifetime of the HES.

5.1.1 Tax Credits

The cases considered are evaluated both with and without subsidies applied, in the form of tax credits. The tax credits applied are based on current federal law in the United States and codified by the 2022 Inflation Reduction Act (IRA). They are utilized in the financial model to assess the sensitivity of the various HES configurations to subsidies and how that changes the optimal configuration. They include the following incentives by source:

- 30% investment tax credit (ITC) for advanced nuclear reactors (e.g. SMR), wind power, and PV [74] applied to the CapEx for each source.
    - Investment tax credit (ITC) applied against the capital costs in Table 12 as a 0.7 multiplier.
- For non-carbon sources, $3 per kilogram production tax credit (PTC) for H2 production [74].

- Applied to the H2 rate in Table 12 as an effective $5 per kilogram.
- Applies to first 10 years of operation. Given the PEM is replaced every 10 years, it is assumed the credit will be renewed with each installation.
- PTC is valid through 2044. It is assumed that this credit will be renewed and valid throughout project life.

5.2 Net Present Value and Internal Rate of Return

IRR is used to determine which configuration is the best financial option. It is assumed that the minimum IRR for financial viability is at least 5% per year. The IRR is found from assessing the net present value (NPV) of each configuration considered. For this study, the NPV expression varies depending on the phase of the project. For the first year of construction, there is only incurred capital costs. For the second through fourth years the production and operating cost are considered as the PV and WTG come online and it is given as:

$$NPV(t_k) = \begin{cases} \frac{-Capital}{(1+i)^{t_k}}, for\ t_k = 1, for\ t_k = 1 \\ \frac{E_{PV_t} PPA - PV_{O\&M} - Capital}{(1+i)^{t_k}}, for\ t_k = 2 \\ \frac{(E_{PV_t} + E_{WTG_t}) PPA - PV_{O\&M} - WTG_{O\&M} - Capita}{(1+i)^{t_k}}, for\ t_k = 3,4 \\ \frac{E_{HES_t} PPA + H\ \ prod_t H2_{price} - HES_{O\&M} - Capital - 0.6 * CapEx_{BESS} - Recyc}{(1+i)^{t_k}}, \\ for\ t_k = 12,22 \\ \frac{E_{HES_t} PPA + H\ \ prod_t H2_{price} - HES_{O\&M} - Capital - 0.6 * CapEx_{H2}}{(1+i)^{t_k}}, \\ for\ t_k = 14,24 \\ \frac{E_{HES_t} PPA + H2_{prod_t} H2_{price} - O\&M - Capital}{(1+i)^{t_k}}, for\ all\ other\ cases \end{cases} \quad (57)$$

Additionally, for years when profitable operation has occurred, a 28% tax rate, as listed in Table 12, is applied and applied as the following:

$$NPV(t_k) = \begin{cases} \frac{E_{HES_t}PPA + H_{\ prod_t}H2_{price} - O\&M - Capita}{(1+i)^{t_k}}, & NPV(t_k) \leq 0 \\ \frac{E_{HES_t}PPA + H_{\ prod_t}H2_{price} - O\&M - Capital}{(1+i)^{t_k}}(1 - tax), & NPV(t_k) > 0 \end{cases} \quad (58)$$

To determine IRR, an explicit relationship is not possible. However, it can be found, with the numerical solver in MATLAB, using the following implicit relationship:

$$NPV = \sum_{t_k=1}^{T} \frac{E_{HES_t}PPA + H_{\ prod_t}H2_{price} - O\&M - Capital}{(1+IRR)^{t_k}} \quad (59)$$

5.3 Full Financial Model

Each HES configuration considered runs for 34 years total. The first four years are for the construction phase with each source providing power as they come online. After year four, full HES operation commences with load following as primary operating mode. Over the 30-year operation, aging and replacement periods are considered as listed in Table 12. The full flow chart of the financial assessment is shown in Figure 29.

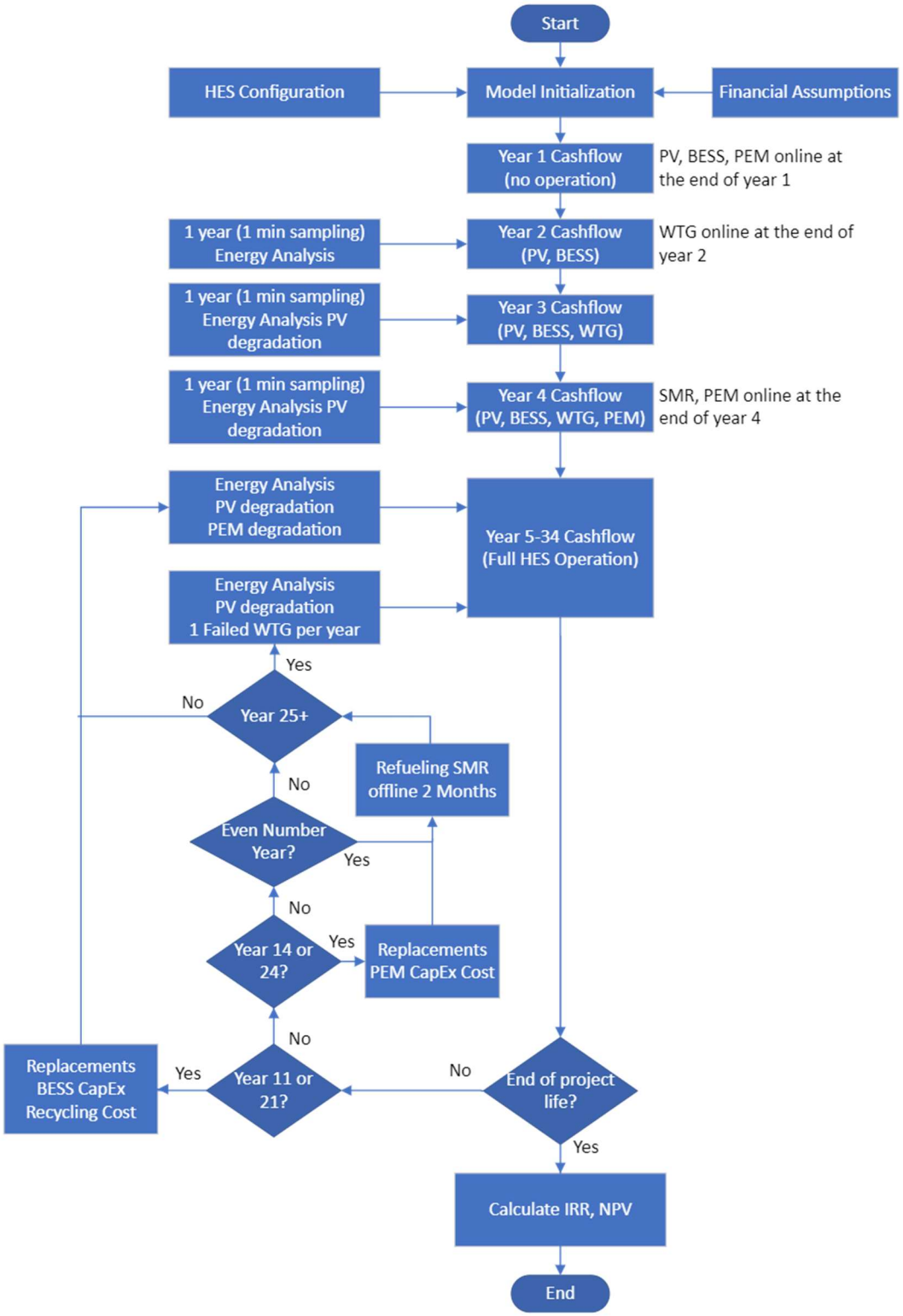

Figure 29: Flow chart for the 4-year build and 30-year operational power and financial assessment.

CHAPTER 6

SIMULATION AND FINANCIAL RESULTS

In this chapter, the simulation and optimization results of the full HES models are presented and discussed. This includes a summary of the cases evaluated, assumptions applied, and a financial assessment. This work culminated in [Publication D], however, due to the compressed nature of paper publications, expanded results are presented here. The expansion includes more details on the selection/rejection criteria for HES configurations evaluated. It also includes more details on transient results in Section 6.4.

6.1 Environmental Regions Evaluated

The solar and wind resource data is referenced from the NREL Measurement and Irradiance Data Center (MIDC) [75]. Minute level irradiance vectors, temperature, wind speed, and sun angles for calendar year 2022 to determine minute-level variations in power output. The two sites selected for evaluation were the NREL location in Golden, Colorado due to its relatively high solar irradiance and wind speeds, and the University of Oregon (UO) dataset in Eugene, Oregon for its comparatively lower resource levels. River water temperature data was referenced from the United States Geological Survey (USGS) for the Platte River in Colorado and Willamette River that are in the same county as the resource data locations [57] in 15-minute time intervals. The key environmental differences between the two regions are summarized in Table 13. It

can be seen for the UO site that the wind speed is minimal with the average wind speed at a 100-meter hub height is below the cut in wind speed of 2.5 meters per second for the WTG. As such, wind energy is not a viable option for the UO region.

Table 13: Average values for each region evaluated.

Region	Annual Average Values			
	GHI (W/m^2)	Wind Speed at 100 m (m/s)	Air Temp (˚C)	Water Temp (˚C)
NREL	209.4	7.7	10.2	13.7
UO	158.3	2.3	12.4	12.4

6.2 Load Profiles Evaluated

Two load profiles are used for this thesis. The first is from Portland Gas & Electric (PGE) and corresponds to the UO dataset [69]. The second is from the Western Area Power Administration – Rocky Mountain Region (WACM) from the Energy Information Administration (EIA) which corresponds to the NREL dataset [69]. Hourly load data for actual load demand for 2022 was used from both regions. The hourly load profile is used as an input into the model, interpolated into minute level data, to provide time varying input into the model. The 2022 load profile for each region is shown in Figure 30. The loads have been normalized to 1.0 for annual peak load with all other hours of the year a fraction of that output. The key difference between the two regions is that the WACM profile has greater extremes

with a minimum load of 30% of peak power, versus 40% of peak power from PGE. It is shown in the Results section that this variation does result in the UO region having comparatively higher IRR, while having a relatively lower renewable energy potential.

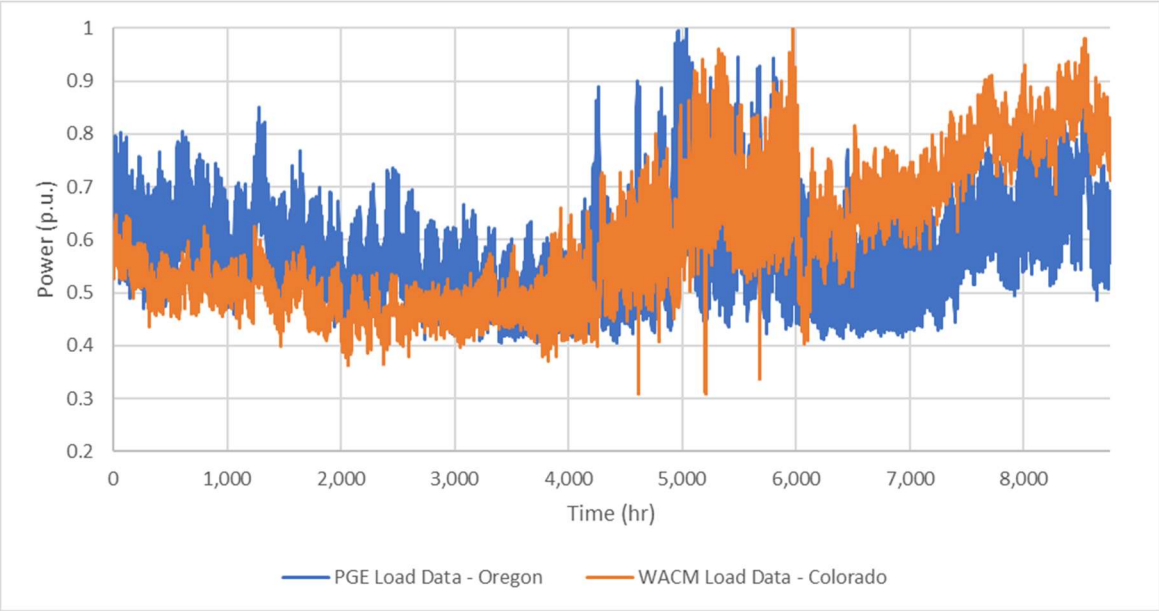

Figure 30: Annual normalized load profile for PGE and WACM for 2022.

For the load input, a ratio of peak power to SMR nameplate power is utilized. This is done because the SMR is the only controllable source of power, and the loads should be within the capabilities of the SMR. For a Load:SMR ratio of 1.0, the load profile is sized such that its maximum power is equal to the nameplate of the SMR. For a Load:SMR ratio of 2.0, or higher, the load is sized such that the minimum load is equivalent to the SMR nameplate. This relationship is illustrated in Figure 31. For periods of higher available HES power than demand, excess

energy is curtailed, or stored. For cases where the HES has less available power than demanded, a penalty payment is paid for each megawatt hour of energy demand not met.

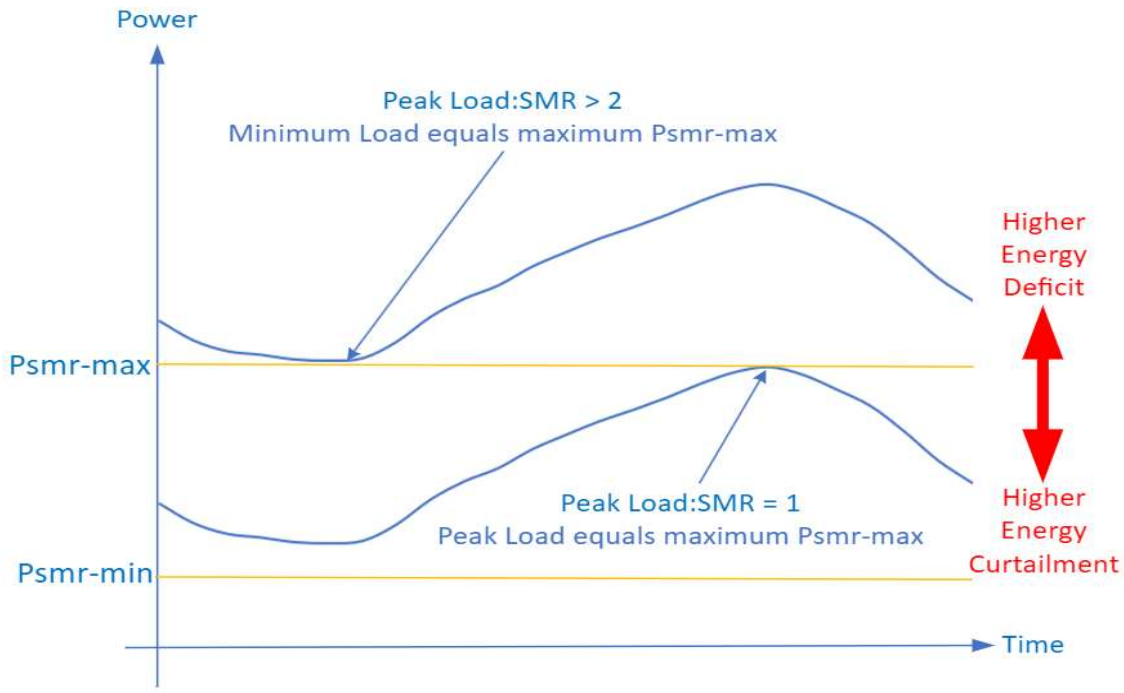

Figure 31: Example of SMR to energy demand profile.

6.3 Scenarios Evaluated and Optimization Loop

A wide range of configurations were evaluated to determine the sensitivity of each configuration to meeting requirements and giving the highest IRR over a 30-year project life. The optimization loop runs in two parts. The first part sweeps through each HES subsystem in 10% increments of its nominal value, using the steps shown in Table 14. Once the highest IRR case is found, a second sweep of +/- 5% resource sizes around the initial optimal point is performed to determine if a

higher IRR is adjacent to the result from the coarse sweep. The +/-5% variation corresponds to the smallest practical increment for the sources (e.g. 2.3-megawatt WTG size). Overall, almost 80,000 unique configurations can be evaluated. With each configuration taking between 1-3 minutes to run, this corresponds to up to 4,000 hours (~5.5 months of continuous operation) for the full set of results. Fortunately, most configurations can be rejected quickly due to IRRs that are negative and can be quickly determined from the aggregate configuration. Configuration rejection is shown in Figure 32 and based on any of following criterion being satisfied:

- If storage is not applied, configurations with Load:SMR ratios < 1.2.
    - Rationale: For no-storage configurations, low Load:SMR ratios mean that a significant amount of excess HES energy will be curtailed, which diminishes IRR.
- If storage is applied, but no tax credits, configurations with Load:SMR ratios > 1.6
    - Rationale: For cases without subsidies, higher Load:SMR ratios result in lower IRR due to higher capital cost and higher energy penalty payment.
- Low CF of < 10% for PV or WTG
    - Rationale: Low CFs are a nonstarter for obtaining an IRR that meets the threshold.
- PEM ratios greater than 0.5 are rejected.

- Rationale: As shown in the results, sizing the PEM to store the HES nameplates worth of rated power is not an optimal solution. The optimal configuration is lower and a saddle point between high storage cost vs lost revenue from curtailment.

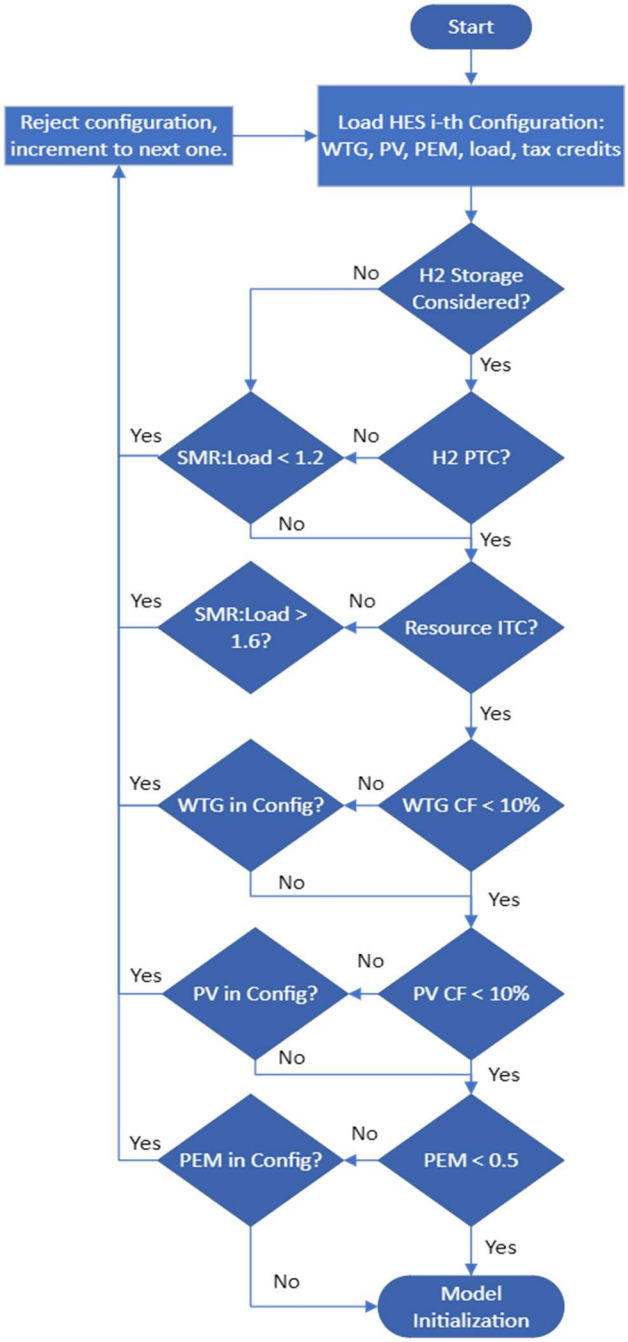

Figure 32: Rejection criteria for optimization loops based on configurations.

For the remaining valid cases, a sweep of all possible combinations is performed. The highest IRR from this subinterval sweep is the final configuration determined. The sequence is shown in Table 14.

Table 14: Financial assumptions and inputs.

Parameter	Initial	Final	Increment	Number of Steps
PV Nameplate	0.0 MWe	45 MWe	4.5 MWe	x11
WTG Nameplate	0.0 MWe	46 MWe	4.6 MWe	x11
PEM/HES Ratio	0.0	1.0	0.1	x11
Load:SMR Ratio	1.0	2.4	0.1	x15
Tax credits	Applied	Not Applied	1	x2
Regions	NREL	UO	1	x2
+/-5% Refinement	5% lower	5% higher	3 per source	+81
Total Number of Unique Possible Configurations				79,941

6.4 Transient Results and Findings

6.4.1 Annual Energy Results and Findings

Each configuration is evaluated over the 2022 empirical dataset for environmental and load data. Figure 33 shows an excerpt of one configuration for

the Colorado region for a configuration with all sources considered. The load command has periods of energy deficits where the HES cannot support requested load. It can also be seen that the PEM stores excess power throughout the profile, while maintaining a minimum five megawatts to keep the electrolyzer warm to support rapid changes in HES power levels. Overall, the energy model performs as expected with source and load variation balanced more storage.

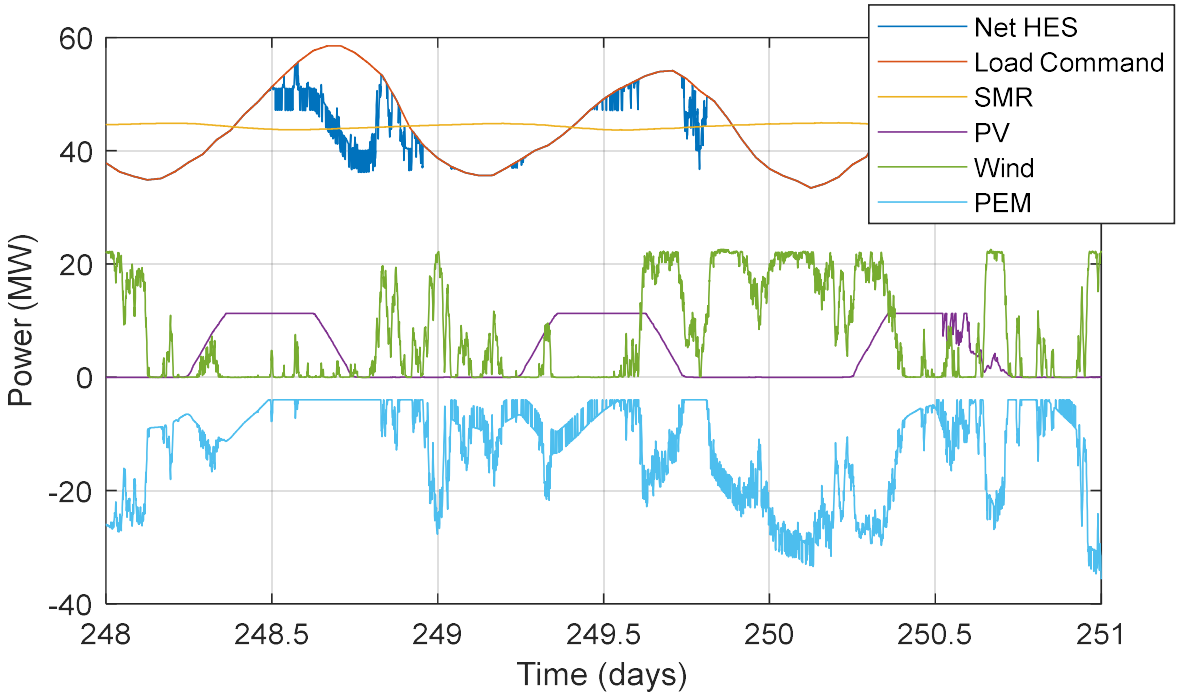

Figure 33: Three-day excerpt of the annual profile for an HES configuration.

The optimization model is run for six unique cases: two regions, with and without tax credits, with and without hydrogen storage. The best IRR results for each case are given in Table 15. It can be seen from the results that the optimal configuration can vary significantly depending on the region and tax credits being assumed. One of the clear correlations is that the maximum IRR is for an HES

configuration that balances stored energy against curtailed energy. It can be inferred from the results that either storing all excess energy or, alternatively, curtailing all excess energy is not the optimal financial solution. Sizing the HES to minimize, but not fully eliminate curtailed energy, with a minimal amount of storage corresponds to the highest IRR. Another result is that for cases with tax credits considered and PEM storage, the load ratio is around 1.0. This is due to the value of storage being high enough (e.g. $5 per kilogram) to make storing excess energy as hydrogen a profitable option. Finally, it can also be seen that the UO results have better overall IRR than the NREL region in some cases, despite having less renewable energy potential. This is due to the PGE load profile being more balanced and having less load variation. The higher the SMR CF against the load profile, the greater the profitability of the SMR contribution. The result is a relatively smoother load profile, which results in less deficit energy, higher SMR CF, and more profitable operating points. The best and worst results for Case 3 and Case 6 (e.g. highest IRR results) are provided in Section 6.4.2. Full results for the subsidized cases can be found in Appendix B.

Table 15: Optimal HES configuration per scenario.

Case 1: NREL dataset, WACM load profile, no storage, full IRA tax credit							
Load Ratio	PV (MW)	SMR (MW)	WTG (MW)	PEM Ratio	Energy Deficit (GWh, %)	Curtailed Energy (GWh, %)	IRR (%)

1.5	0	45.0	0	N/A	17.4, 5.1	59.6, 15.1	-0.3
Case 2: NREL dataset, WACM load profile, PEM storage, no IRA tax credit							
Load Ratio	PV (MW)	SMR (MW)	WTG (MW)	PEM Ratio	Energy Deficit (GWh, %)	Curtailed Energy (GWh, %)	IRR (%)
1.4	4.5	45.0	0	0.2	17.1, 3.1	10.1, 4.2	-6.8
Case 3: NREL dataset, WACM load profile, PEM storage, full IRA tax credit							
Load Ratio	PV (MW)	SMR (MW)	WTG (MW)	PEM Ratio	Energy Deficit (GWh, %)	Curtailed Energy (GWh, %)	IRR (%)
1.0	11.25	45.0	46.0	0.3	0.02, 0.01	49.4, 9.2	8.2
Case 4: UO dataset, PGE load profile, no storage, full IRA tax credit							
Load Ratio	PV (MW)	SMR (MW)	WTG (MW)	PEM Ratio	Energy Deficit (GWh, %)	Curtailed Energy (GWh, %)	IRR (%)
1.6	0	45.0	0	N/A	12.3, 3.4	42.6, 10.8	1.6
Case 5: UO dataset, PGE load profile, PEM storage, no IRA tax credit							
Load Ratio	PV (MW)	SMR (MW)	WTG (MW)	PEM Ratio	Energy Deficit (GWh, %)	Curtailed Energy (GWh, %)	IRR (%)
1.45	0	45.0	0	0.2	5.6, 1.7	16.2, 4.1	-5.4
Case 6: UO dataset, PGE load profile, PEM storage, full IRA tax credit							

Load Ratio	PV (MW)	SMR (MW)	WTG (MW)	PEM Ratio	Energy Deficit (GWh, %)	Curtailed Energy (GWh, %)	IRR (%)
1.0	18.0	45.0	0	0.3	0.02, 0.01	22.0, 5.1	7.4

6.4.2 Best and Worst Configurations

The five best and worst results for the NREL Case 3 are shown in Table 16 with the optimal configuration for each case highlighted. Additionally, the five best and worst results for the UO Case 6 are shown in Table 17, again, with the optimal configuration for each case highlighted. The results show that the worst results have energy curtailment between three to six times higher than the highest IRR results.

Table 16: Case 3 (NREL dataset, WACM load profile, no storage, full IRA tax credits) best and worst results.

Scenario	Peak Load:SMR Ratio	WTG Number	PV Nameplate (kW)	PEM Ratio	PV CF (%)	Wind CF (%)	SMR CF (%)	HES CF (%)	BESS Size (kWh)
43	1	4	0	0.1	0.00	28.88	59.72	48.1	685.4
85	1	8	0	0.1	0.00	28.88	59.72	41.2	1257.5
92	1	8	4500	0.1	31.24	28.88	59.73	38.7	4111.7
127	1	12	0	0.1	0.00	28.67	59.72	36.0	1653.5
169	1	16	0	0.1	0.00	28.42	59.72	31.9	1937.1
185	1	16	9000	0.3	31.24	28.42	59.72	30.5	7927.7
671	1	16	9000	0.3	31.24	28.42	59.72	28.9	7927.7
674	1	16	11250	0.3	31.24	28.42	59.72	27.6	9764.1
680	1	17	9000	0.3	31.24	28.37	59.72	26.3	7854.3
683	1	17	11250	0.3	31.24	28.37	59.72	25.2	9750.0

Scenario	Curtailed Energy (kWh)	Load Energy (kWh)	H2 Production (kg)	Energy Deficit (kWh)	NPV ($)	Irr (%)
43	133,461,474.2	230176989.7	931108.9	9,804.9	(118,829,626.9)	-2.51%
85	147,677,091.9	230176989.7	1086514.3	9,764.9	(125,820,082.2)	-2.81%
92	134,903,900.8	230176989.7	1227404.7	2,604.0	(124,222,328.8)	-2.41%
127	161,461,967.0	230176989.7	1241920.1	9,924.2	(131,281,980.9)	-2.67%
169	174,824,368.9	230176989.7	1397326.2	10,218.5	(137,213,117.7)	-2.61%
185	41,413,750.7	230176989.7	5801599.1	29,977.2	99,629,721.9	8.13%
671	41,413,750.7	230176989.7	5801599.1	29,977.2	99,629,721.9	8.13%
674	40,429,285.3	230176989.7	5942264.9	26,636.9	100,731,193.2	8.12%
680	43,384,676.9	230176989.7	5930445.3	31,031.1	103,211,235.0	8.20%
683	42,289,038.5	230176989.7	6055861.0	27,863.2	103,047,702.6	8.15%

Table 17: Case 6 (UO dataset, PGE load profile, PEM storage, full IRA tax credits) best and worst results.

Scenario	Peak Load:SMR Ratio	WTG Number	PV Nameplate (kW)	PEM Ratio	PV CF (%)	Wind CF (%)	SMR CF (%)	HES CF (%)	BESS Size (kWh)
1	1	0	0	0.1	0.00	0.00	57.02	56.5	0.00
8	1	0	4500	0.1	24.14	0.00	57.02	51.8	3475.63
15	1	0	9000	0.1	24.14	0.00	57.02	47.5	6968.93
22	1	0	13500	0.1	24.14	0.00	57.02	43.9	10394.21
29	1	0	18000	0.1	24.14	0.00	57.02	40.7	13811.57
38	1	0	22500	0.3	24.14	0.00	57.01	38.0	17236.02
59	1.1	0	9000	0.3	24.14	0.00	62.67	52.2	6968.93
157	1	0	18000	0.3	24.14	0.00	57.01	40.7	13811.56
164	1	0	22500	0.3	24.14	0.00	57.01	38.0	17236.02
185	1.1	0	9000	0.3	24.14	0.00	62.67	52.2	6968.93

Scenario	Curtailed Energy (kWh)	Load Energy (kWh)	H2 Production (kg)	Energy Deficit (kWh)	NPV ($)	Irr (%)
1	133,031,078.3	224762581.8	793430.0	654.6	(111435489.7)	-1.72%
8	112,263,483.1	224762581.8	937911.2	-	(110,876,030.08)	-1.48%
15	87,657,732.6	224762581.8	1100618.7	1.47E-11	(109,807,325.03)	-1.20%
22	68,141,159.1	224762581.8	1265103.4	3.38E-10	(108,644,716.57)	-0.93%
29	60,895,846.5	224762581.8	1430984.2	9.66E-10	(107,478,573.41)	-0.68%
38	25,959,393.5	224762581.8	4760298.4	30,937.48	64,025,289.70	7.21%
59	10,613,074.8	247238840.0	3685319.4	204,117.31	58,312,383.61	7.22%
157	22,063,361.2	224762581.8	4556575.7	28,256.14	67,756,939.35	7.41%
164	25,959,393.5	224762581.8	4760298.4	30,937.48	64,025,289.70	7.21%
185	10,613,074.8	247238840.0	3685319.4	204,117.31	58,312,383.61	7.22%

6.4.3 Network Transients

The optimal Case 3 configuration from Table 15 is integrated into the IEEE 9 Bus model shown in Figure 26. A test case is run, using empirical data from March 10, 2022. Starting at 11:55 am, where PV power doubles from 5.5 to 11 megawatt over one minute. At the same time, the load on the network at Bus 6 instantaneously drops by 75 megawatts (50% of load at the bus, 20% of the overall network load). After five minutes, the load at Bus 6 is restored. The combination of these two events results in an over-generation event followed by an under-generation. The response of the HES is shown in Figure 34. The HES bus voltage swings up to 2.3 percent before the SMR voltage regulator returns it to nominal operation in four seconds. Likewise, the system frequency goes up to 60.47 hertz, before returning below 60.1 hertz in approximately 82 seconds. A similar swing is observed for the underfrequency event (e.g. 59.5 Hz recovering in <80 seconds). A comparison to the WECC frequency limits is given in Table 18 in correspondence to a 1% allowable change in frequency. It is important to note that regional balancing authorities and/or local interconnecting utilities might have tighter frequency restrictions, but the WECC limits are used for this assessment. The frequency response is slower than the voltage response, driven by the ramp rate limitation of the SMR. Per the generator limits in the North American Electric Reliability Council (NERC) PRC-024-1, these excursions do not result in mandatory trips to generating units and adhere to nominal operation [76]. For a 33% drop in load with a corresponding step change in PV generation does not result in a mandatory trip of

generating sources with a recovery in under 82 seconds. The response of the storage units to this event are shown in Figure 35 and are consistent with the FR response defined in 4.4.1 with load being added for over frequency and generation added for underfrequency.

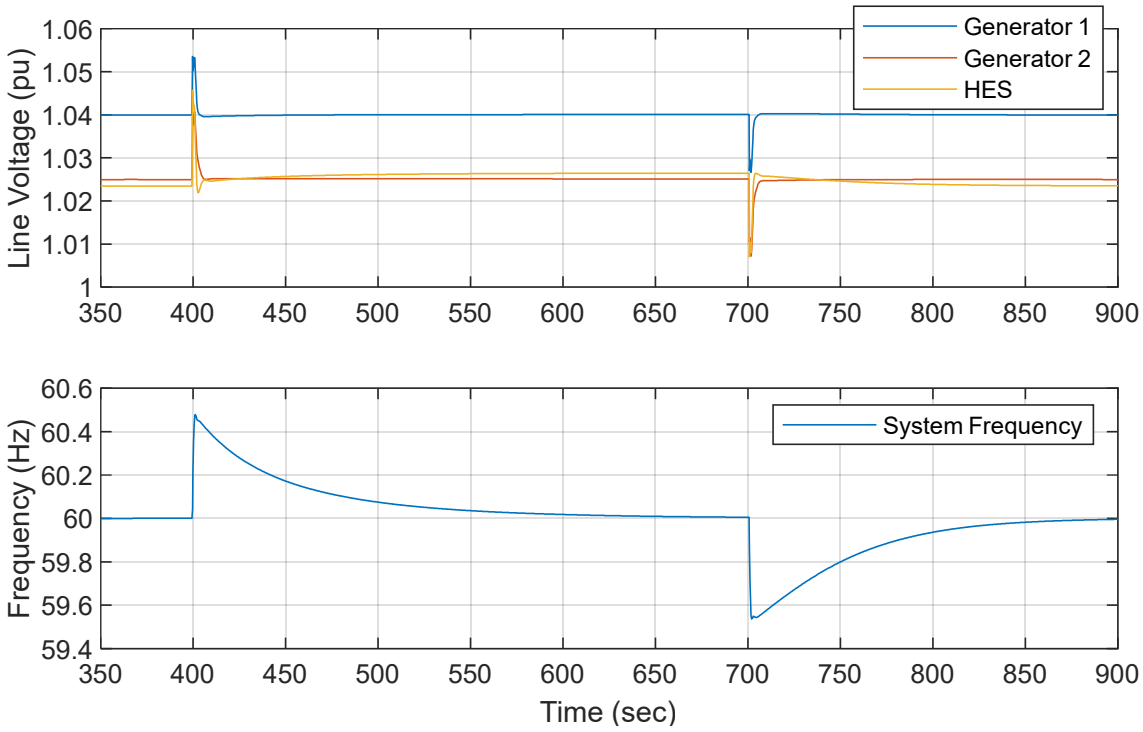

Figure 34: Transient results from a 20% loss of load occurring when PV power increases 100% and subsequent load recovery.

Table 18: Comparison of observed frequency perturbation versus the WECC operational limits.

	Measured	WECC Limit for Continuous Operation
Maximum Frequency Excursion	60.47 Hz	60.6 Hz
Minimum Frequency Excursion	59.5 Hz	59.4 Hz

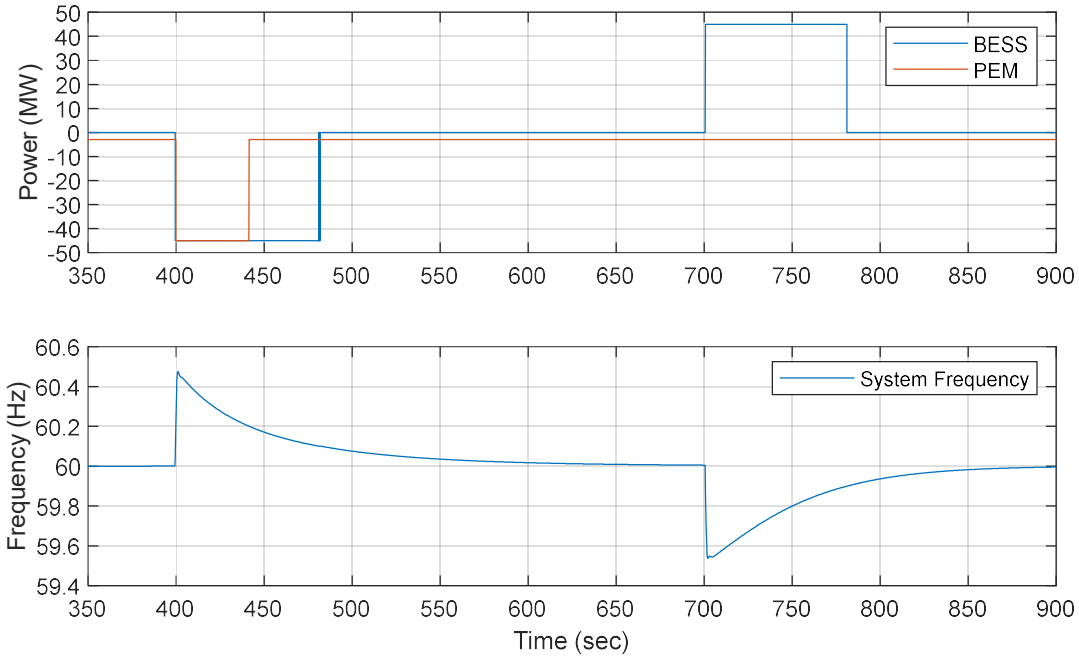

Figure 35: Transient results from scenario with corresponding HES storage response.

6.5 Financial Findings

From the project life assessment, multiple relationships were determined. The relationships found between IRR and storage, tax subsidies, and capital cost are summarized in this section.

6.5.1 No PEM Financial Sensitivity

For cases with no PEM storage, the results show an optimal point between balancing the amount of energy curtailed against the deficit energy penalty paid. When factoring in the cost penalty, the optimal solution is when the SMR:load ratio is around 1.5~1.6. This results in the highest IRR at a minimum level of energy deficit, approximately 5% of the energy demanded. This relationship can be seen in Figure 36 with the IRR result given. Conversely, the consideration of subsidies does not change the optimal solution, only the magnitude of the IRR value.

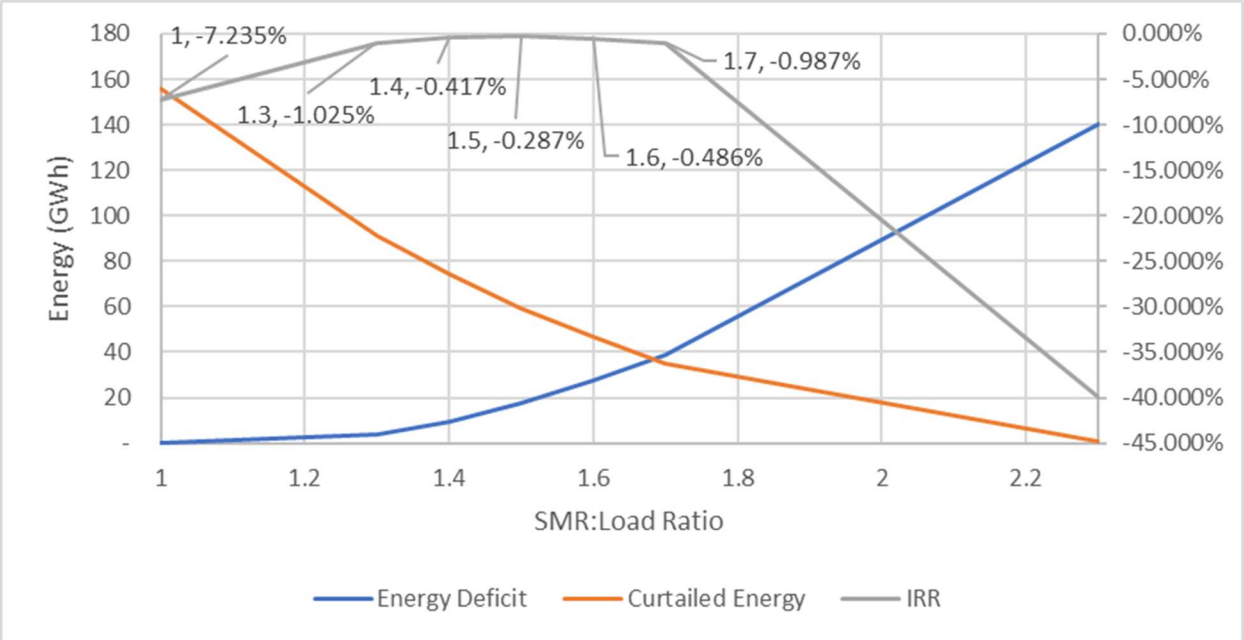

Figure 36: Relationship between curtailed and deficit energy for Case 1 where no PEM storage is considered.

6.5.2 PEM Financial Sensitivity

For cases where hydrogen storage is considered, the ratio of energy stored versus curtailed is also the key consideration. The results show that the most economical point is approximately between a PEM:HES ratio of 0.2 to 0.3. As such, the optimal solution results in some energy still being curtailed. This is due to the diminishing returns of storing excess energy against the increasing CapEx to the PEM. Figure 37, shows the configuration for Case 3 with the PEM ratio swept. It can be seen that value of the energy curtailed reduces as the ratio increases, but settles at a PEM:HES ratio of 0.3. Above 0.3 the cost of adding more PEM capacity outweighs the value of the stored hydrogen.

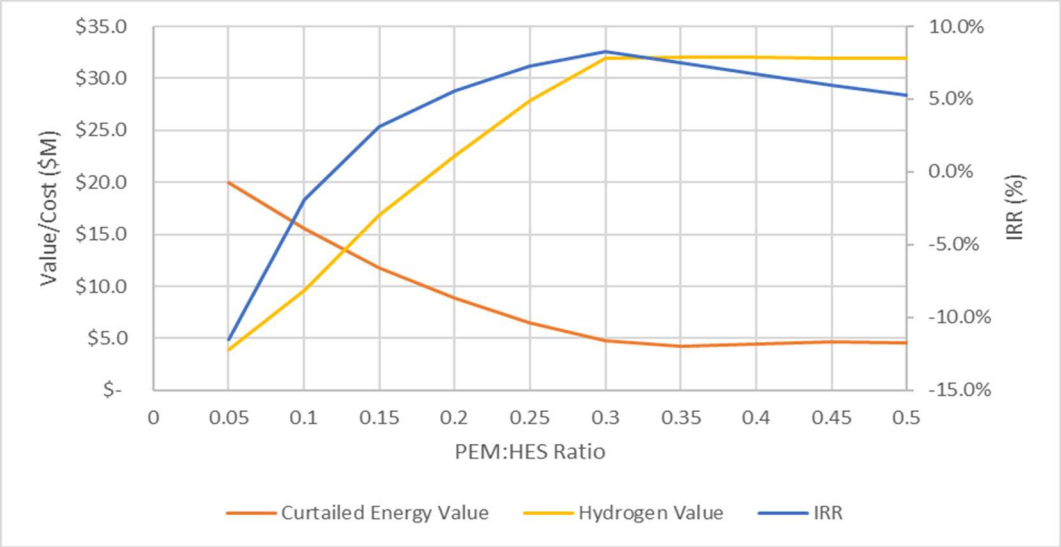

Figure 37: Relationship between stored versus curtailed energy and its impact on IRR.

6.5.3 Subsidy Cost Sensitivity

It can be seen in Table 15 that IRA tax subsidies are critical to having a positive IRR. To determine which subsidy is the most impactful, Cases 3 and 6 from Table 15 are evaluated with only the PTC applied, and then another run with only the ITC. The results of these different subsidy considerations are summarized in Table 19. As can be seen from the table, the greatest impact on IRR is the PTC. For Case 3, considering the PTC changes the IRR from -15.4% to +1.9% (17.3% increase), whereas the ITC changes the IRR from -15.4% to -2.1% (13.3% increase). Similar results are found for Case 6. This indicates that one of the key drivers to financial viability for an HES is the value of the energy stored.

Table 19: Tax credit subsides impact on IRR.

Configuration	IRR			
	No Subsidies	ITC Only	PTC Only	All Subsidies
Case 3	-15.4%	-2.1%	+1.9%	+8.2%
Case 6	-11.3%	-2.1%	+2.1%	+7.4%

6.5.4 SMR Cost Sensitivity

For the unsubsidized cases, IRR is negative for all HES configurations. In addition to the value of stored energy, another contributor to the low IRR is the CapEx for the SMR, which is referenced to be $6025 per kilowatt, as stated in Table

12. Given the novelty of SMRs, the early and long-term CapEx estimates vary significantly. To account for this uncertainty, a sensitivity analysis is performed by sweeping the SMR CapEx to find the minimum value necessary for an unsubsidized IRR greater than five percent. The configuration from Case 2 in Table 15 is used. The value of CapEx is swept from $6025 to less than $100 per kilowatt. The results are shown in Figure 38. It can be seen that SMR CapEx needs to drop below $3,000 per kilowatt before an acceptable unsubsidized IRR can be achieved.

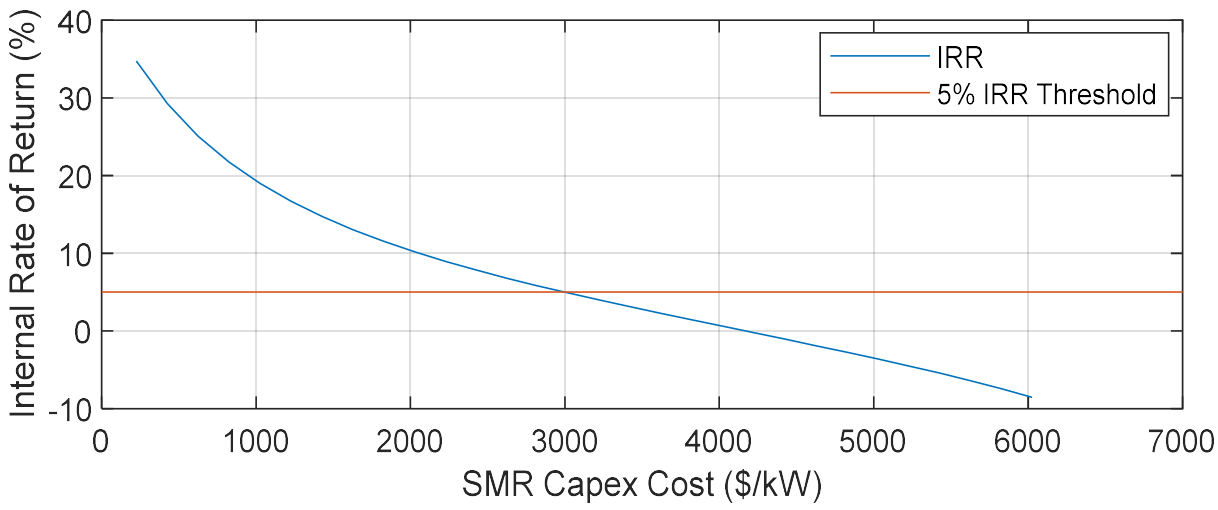

Figure 38: Sensitivity of the SMR CapEx to the overall HES IRR.

6.5.5 PPA and Hydrogen Rate Cost Sensitivity

The baseline production rate prices were also evaluated to determine the range of profitability as each initial rate value was varied. As shown in Table 19, the impact of subsidies is required for projects to be profitable with contemporary financial assumptions applied. In addition to subsidy and capital cost sensitivity,

the production rate prices strongly couple to profitability as well. To determine the sensitivity, the unprofitable Case 5 in Table 15 is considered and the initial rate of the PPA and H2 production were swept to determine the region where profitability lies. The PPA rate was swept from $0 to $180 per megawatt-hour (up to three times higher than the baseline) and H2 swept from $0 to $18 per kilogram (up to nine times higher than baseline). The results are shown as a region plot in Figure 39. From the results, it can be seen that profitability lies in a region where PPA price is greater than $120 per megawatt-hour without hydrogen, to as low as $30 per megawatt-hour for the case where hydrogen is at $18 per kilogram. The key finding from these results is that the current market rates would have to be multiple times higher in order for the unsubsidized Case 5 result to offer an IRR greater than five percent.

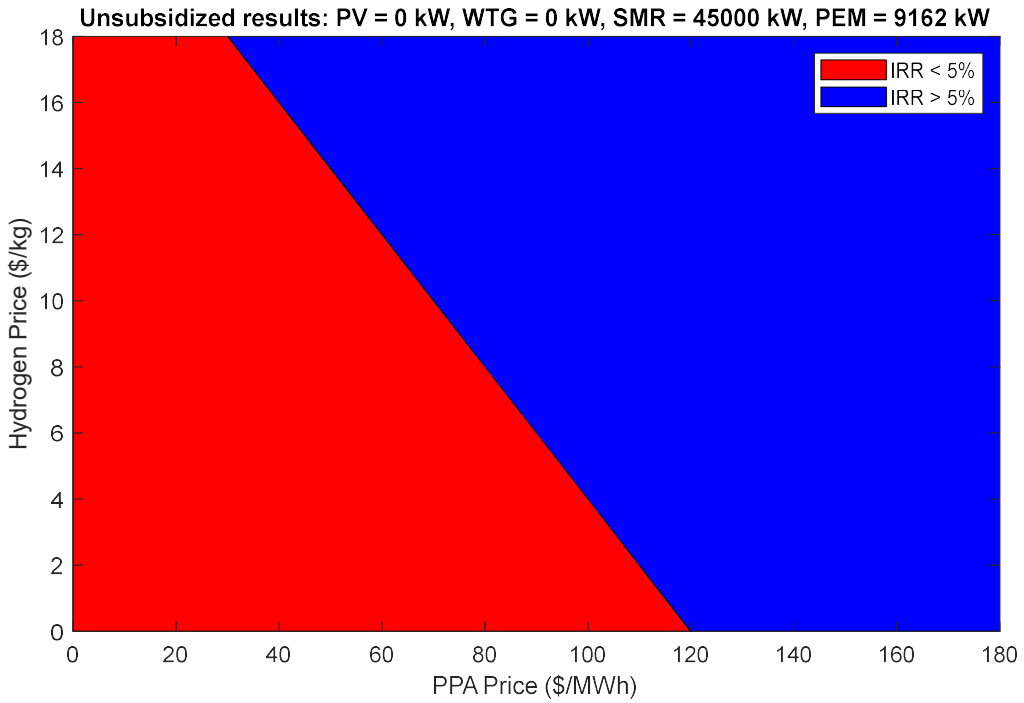

Figure 39: Sensitivity of PPA and H2 rate to the overall HES IRR.

CHAPTER 7

CONCLUSIONS AND FUTURE WORK

In the final chapter, a summary of the thesis is provided. The work from the previous chapters is summarized and the limitation of the current research is covered in Section 7.1. Additionally, future research topics are suggested in Section 7.2.

7.1 Conclusions and Key Findings

This thesis covered the development of an HES model based on new and previously developed models. The models were developed to assess the annual energy power profile on a minute scale and transient responses on a sub-second scale. A financial assessment was performed considering network and resource constraints of a clean HES optimized for highest IRR and considering resource constraints. The key findings are summarized as the following:

- HES solutions that meet network frequency response and ramp rate limits are possible with a proportional utilization of SMR, renewables and storage.
- Clean HES are capable of profitably meeting flexible energy demands when considering subsidies from the 2022 IRA.
- For unsubsidized results, profitable HES solutions can be found if either the price of hydrogen increases and/or the SMR CapEx decreases. To achieve profitable results without subsidies, the CapEx of the SMR would need to be below $3000 per kilowatt. Alternatively, the cost of hydrogen would need to

go over $5 per kilogram to be profitable with assumptions applied in this study.

- It was also discovered that for a clean energy HES, a small amount of energy curtailment is necessary for the highest economic value. The results show storing nominally 30% of HES nameplate capacity as hydrogen is the most cost-effective solution, when considering subsidies.
- Ramp rate control through BESS can effectively mitigate ramps from a PV and WTG system. The cost impacts are minimal for sizing a BESS with a 10-year life to support ramp rate control.
- The network results show that an HES with a SMR as the primary energy source can integrate into a contemporary power system, and support power system stability. Particularly, when coupled with BESS to provide fast, sub-second, transient response.

7.1.1 Limits of the Results

Several limitations were identified as part of this study and are summarized in this section.

- **Limitation 1: Comprehensive Financial Model.** This study provided a financial evaluation for a comparative evaluation of HES configurations to determine the best option and the key drivers for financial viability. It did not intend to be a comprehensive financial evaluation considering the full scope of financial considerations (to name a few: investment alternatives, market factors, salvage value). With most of the results from this study

resulting in non-compelling IRR, there is much work to be done to make a clean HES a more desirable option in a free energy market.

- **Limitation 2: Transient Modeling.** From the initial results presented in this study it is determined that the HES can support a stable power system. The combination of turbine-generator rotating inertia and steam bypass controls allows for the optimal operation of the HES with renewable sources providing energy as available. However, this was not intended to be a comprehensive study of all possible transient cases. The outline of the model is provided in Appendix A.2 to support future studies.

7.2 Future Work

There are multiple tangential areas of study that can be built off the research topic presented in this thesis. Primarily, the transient work can be expanded to consider further transient cases. With storage being the critical piece to the viability of clean hybrid systems, continuing to evaluate the practicality of emerging technologies is needed. Finally, given the significant number of solutions that exist, more robust sizing algorithms should be developed for this topic.

7.2.1 Black Start Assessment

The HES transient model was developed to address operational transients from frequency perturbations. Another area that would be of interest for research into HES is black start capability, that is, helping to start up a portion of an electrical network following a widespread outage. One of the well-known challenges

with stand-alone renewable energy sources today is their lack of black start capability due to their inverter-based generation typically being load following [77]. In this configuration, the inverters can only connect to an existing grid, and not generate the reference voltage to establish the grid network on its own. One of the inherent advantages of coupling renewable energy sources with conventional synchronous generator-based generation is the ability of the synchronous generator to provide the grid reference, such that, existing grid following inverters can be utilized. This would also need to consider ancillary power sources, like backup diesel generators to support the internal power consumption of the SMR to start its operation. The topic of black start using HES is a natural progression from the results presented in this study.

7.2.2 Alternative Storage Options

This study utilized lithium-ion battery storage for short transients and hydrogen via PEM for bulk energy storage. While discussed in this thesis that these represent practical, contemporary storage options, this field is experiencing rapid development. Future work could consider more novel technologies assessed as part of a hybrid system. For example, solid state batteries [78] could offer much higher cycle life over contemporary lithium-ion batteries, which makes the presented battery sizing algorithm inapplicable.

Additionally, there is more research ongoing in the field of regenerative fuel cells, which can support closed loop storage and generation of excess energy.

Current research into the topic is relatively in its early stages with a focus on application for space habitats [79]. Due to the high cost and relatively low round trip efficiency, the technology is not at commercial development yet, but could be a valuable source to evaluate as part of future studies.

7.2.3 Optimization Algorithm

The model presented in this study used a parameter sweep of resource interval step sizes. With the boundaries of profitability determined in this study, the next logical step would be to expand the evaluation to include an algorithm that can track along the relationships determined in this study to find an optimal solution with less processing time. With the parabolic shape of most parameter sweeps, this leads to the practicality of convex programming to find the optimal point for a particular number of constraints applied.

7.2.4 Extraterrestrial HES for Lunar Habitats

Another potential application for HES is for extraterrestrial applications. The near-term interest in this topic can be found in NASA's Artemis program which is working to return Astronauts to the moon this decade and eventually leading to a permanent presence on there [80]. One of the key challenges is a diverse power supply that can provide power through long Lunar eclipses. The combination of nuclear and PV technology is a natural hybrid combination for this environment with the two sources providing energy security for a permanent habitat. Research

into this topic could also include the utilization of regenerative fuel cells to augment these sources [81].

BIBLIOGRAPHY

[1] "Sources of Greenhouse Gas Emissions," [Online]. Available: https://www.epa.gov/ghgemissions/sources-greenhouse-gas-emissions.

[2] IEEE Xplore Search Results. [Online]. https://ieeexplore.ieee.org/search/searchresult.jsp?newsearch=true&queryText=hybrid%20wind%20solar. Accessed: March 1, 2024

[3] IEEE Xplore Search Results. [Online]. https://ieeexplore.ieee.org/search/searchresult.jsp?newsearch=true&queryText=Hybrid%20Renewables%20Storage. Accessed: March 1, 2024

[4] IEEE Xplore Search Results. [Online]. https://ieeexplore.ieee.org/search/searchresult.jsp?newsearch=true&queryText=Hybrid%20Renewables%20Hydrogen. Accessed: March 1, 2024.

[5] IEEE Xplore Results. [Online]. https://ieeexplore.ieee.org/search/searchresult.jsp?newsearch=true&queryText=Hybrid%20Nuclear%20Renewables. Accessed: March 1, 2024.

[6] IEEE Xplore Results. [Online]. https://ieeexplore.ieee.org/search/searchresult.jsp?newsearch=true&queryText=Hybrid%20Solar%20Nuclear%20Wind. Accessed: March 1, 2024.

[7] IEEE Xplore Results. [Online]. https://ieeexplore.ieee.org/search/searchresult.jsp?newsearch=true&queryText=Hybrid%20Nuclear%20Hydrogen. Accessed: March 1, 2024.

[8] Integrated Energy – Idaho National Laboratory. https://inl.gov/integrated-energy/. Accessed: March 1, 2024.

[9] D.J. Arent, S.M. Bragg-Sitton, D.C. Miller, T.J. Tarka, J.A. Engel-Cox, R.D. Boardman, P.C. Balash, M.F. Ruth, J. Cox, D.J. Garfield, 2021. “Multi-input, multi-output hybrid energy systems.” Joule, 5(1), pp.47-58.

[10] K. Frick, S. Bragg-Sitton, S. Cristian, R. Cristian. “Modeling the Idaho National Laboratory Thermal-Energy Distribution System (TEDS) in the Modelica Ecosystem.” 2020. Energies. 13. 6353. 10.3390/en13236353.

[11] C. Forsberg, S.M. Bragg-Sitton, “Maximizing clean energy use: Integrating nuclear and renewable technologies to support variable electricity, heat, and hydrogen demands.” (2020). Bridge. 50. 24-31.

[12] V. V. V. S. N. Murty and A. Kumar, "Optimal Energy Management and Techno-economic Analysis in Microgrid with Hybrid Renewable Energy Sources," in Journal of Modern Power Systems and Clean Energy, vol. 8, no. 5, pp. 929-940, September 2020, doi: 10.35833/MPCE.2020.000273.

[13] E. Naderi, B. K. C., M. Ansari and A. Asrari, "Experimental Validation of a Hybrid Storage Framework to Cope With Fluctuating Power of Hybrid Renewable Energy-Based Systems," in *IEEE Transactions on Energy Conversion*, vol. 36, no. 3, pp. 1991-2001, Sept. 2021, doi: 10.1109/TEC.2021.3058550.

[14] M. H. Nehrir *et al.*, "A Review of Hybrid Renewable/Alternative Energy Systems for Electric Power Generation: Configurations, Control, and

Applications," in *IEEE Transactions on Sustainable Energy*, vol. 2, no. 4, pp. 392-403, Oct. 2011, doi: 10.1109/TSTE.2011.2157540.

[15] C. Lowe, J. Stanley, F. Alosaimi, M. Yousf, J. Bordelon and H. B. Karayaka, "Load Following Capability for Hybrid Nuclear and Solar Photovoltaic Power Plants with an Energy Storage System," *2020 52nd North American Power Symposium (NAPS)*, Tempe, AZ, USA, 2021, pp. 1-6, doi: 10.1109/NAPS50074.2021.9449816.

[16] K. Joshi, B. Poudel, R. Gokaraju, "Investigating Small Modular Reactor's Design Limits for its Flexible Operation with Photovoltaic Generation in Micro-Communities". ASME. ASME J of Nuclear Rad Sci. July 2021; 7(3): 031303. https://doi.org/10.1115/1.4048896

[17] K. Dykes, J. King, N. DiOrio, R. King, V. Gevorgian, D. Corbus, N. Blair, K. Anderson, G. Stark, C. Turchi, P. Moriarty, "Opportunities for Research and Development of Hybrid Power Plants." United States: N. p., 2020. Web. doi:10.2172/1659803.

[18] K. Joshi, B. Poudel, R. Gokaraju, "Exploring Synergy Among NEW Generation Technologies: Small Modular Rector, Energy Storage and Distributed Generation – a Strong CASE FOR Remote Communities." (2019). Journal of Nuclear Engineering and Radiation Science. 6. 10.1115/1.4045122.

[19] G. Locatelli, S. Boarin, F. Pellegrino, M.E. Ricotti,. "Load-following with small modular reactors (SMR): A real options analysis." Energy 2015;80(2015):41–54.

[20] D. T. Ingersoll, C. Colbert, Z. Houghton, R. Snuggerud, J. W. Gaston, and M. Empey, "Can nuclear power and renewables be friends?" in Proc. ICAPP, Nice, France, May 2015, pp. 1–9.

[21] A. Baker, "Three Trends for Optimizing Utility-Scale Solar Ramp Rate Controls in 2018," https://www.affinityenergy.com/optimizing-utility-scale-solar-ramp-rate-controls-2018/

[22] J. Kleissl, C. Chow, M. Lave, P. Mathiesen, A. Nottrott, B. Urquhart, "Solar Variability and Forecasting" Presentation. https://www.bnl.gov/energy/files/nserc/UCSan_Diego_Solar_Variability_and_Forecasting.pdf

[23] X. Chen, D. Yang, "Forecasting Based Power Ramp-Rate Control For PV Systems Without Energy Storage." 2017 IEEE 3rd International Future Energy Electronics Conference and ECCE Asia, 2017.

[24] National Solar Radiation Database. https://nsrdb.nrel.gov/data-viewer. Accessed: March 1, 2024.

[25] M. Lave, J. Kleissl, "Solar variability of four sites across the state of Colorado," Renewable Energy, vol. 35, no. 12, 2867-2873, 2010.

[26] M. Hossain, M. Ali, "Statistical Analysis of the Ramp Rates of Solar Photovoltaic System Connected to Grid." 2014 IEEE Energy Conversion Congress and Exposition (ECCE), 14-18 Sept. 2014

[27] B. Parsons, M. Hummon, J. Cochran, B. Stoltenberg, P. Batra, B. Mehta, D. Patel, "Variability of Power from Large- Scale Solar Photovoltaic Scenarios in

the State of Gujarat," National Renewable Energy Laboratory, Golden, CO, Tech. Rep., NREL/CP-7A40-61555, Apr. 2014.

[28] S. S. Giri, A. Ahmad, V. Katiyar, "Avoiding Power Clipping Losses by Inverter having High DC-to-AC Loading Ratio in Grid Connected Solar PV Plant Using Battery Energy Storage System," 2019 2nd International Conference on Power Energy, Environment and Intelligent Control (PEEIC)

[29] J. Warmuz and R. W. De Doncker, "PV- and Battery-Ratio for very large Modular PV Parks with DC Coupled Battery Converters," 2019 IEEE 10th International Symposium on Power Electronics for Distributed Generation Systems (PEDG), Xi'an, 2019, pp. 444-450, doi: 10.1109/PEDG.2019.8807771.

[30] A. Colthorpe, "Finding Li-Ion Battery Degradation Sweet Spots can be an Economic Trade-off". Sep. 2018. https://www.energy-storage.news/news/finding-li-ion-battery-degradation-sweet-spots-can-be-an-economic-trade-off

[31] M. J. E. Alam and T. K. Saha, "Cycle-life degradation assessment of Battery Energy Storage Systems caused by solar PV variability," 2016 IEEE Power and Energy Society General Meeting (PESGM), Boston, MA, 2016, pp. 1-5, doi: 10.1109/PESGM.2016.7741532.

[32] V. Muenzel, J. de Hoog, M. Brazil, A. Vishwanath and S. Kalyanaraman, "A multi-factor battery cycle life prediction methodology for optimal battery management", Proc. ACM 6th Int. Conf. Future Energy Syst., pp. 57-66, 2015.

[33] G.F. Frate, P. Pena Carro, L. Ferrari, U. Desider, "Techno-economic sizing of a battery energy storage coupled to a wind farm: an Italian case study", 73rd Conference of the Italian Thermal Machines Engineering Association (ATI 2018), 12–14 September 2018, Pisa, Italy

[34] IAEA TECDOC SERIES. "Nuclear–Renewable Hybrid Energy Systems for Decarbonized Energy Production and Cogeneration" Proceedings. IAEA-TECDOC-1885.

[35] D. T. Ingersoll, C. Colbert, Z. Houghton, R. Snuggerud, J. W. Gaston, and M. Empey, "Can nuclear power and renewables be friends?" in Proc. ICAPP, Nice, France, May 2015, pp. 1–9.

[36] H. Niaz and J. Liu, "Dynamic Model For Solar Hydrogen Via Alkaline Water Electrolyzer: A Real-Time Techno-economic Perspective With And Without Energy Storage System," 2020 20th International Conference on Control, Automation and Systems (ICCAS), 2020, pp. 814-819, doi: 10.23919/ICCAS50221.2020.9268396.

[37] B. Poudel, K. Joshi and R. Gokaraju, "A Dynamic Model of Small Modular Reactor Based Nuclear Plant for Power System Studies," in *IEEE Transactions on Energy Conversion*, vol. 35, no. 2, pp. 977-985, June 2020, doi: 10.1109/TEC.2019.2956707.

[38] Chia-Jeng Tseng and D. P. Siewiorek, "The Modeling and Synthesis of Bus Systems," *18th Design Automation Conference*, Nashville, TN, USA, 1981, pp. 471-478, doi: 10.1109/DAC.1981.1585398.

[39] M. T. K. Niazi, Arshad, M. Ali and A. Hussain, "Influence of Fault and Wind Turbine Type on Voltage Stability of IEEE 14 Bus System," 2018 IEEE 21st International Multi-Topic Conference (INMIC), Karachi, Pakistan, 2018, pp. 206-212, doi: 10.1109/INMIC.2018.8595498.

[40] K. Loji, N. Loji and M. Kabeya, "Flexibility Assessment of a Solar PV Penetrated IEEE 9-Bus System Using Dynamic Transient Stability Evaluation," 2022 IEEE PES/IAS PowerAfrica, Kigali, Rwanda, 2022, pp. 1-5, doi: 10.1109/PowerAfrica53997.2022.9905395.

[41] Q. Shi, D. Liu, H. Luo and Y. Gao, "Study on the faults of nuclear power plant and effects on transient stability of power system," 2012 China International Conference on Electricity Distribution, Shanghai, China, 2012, pp. 1-5, doi: 10.1109/CICED.2012.6508682.

[42] M. A. Ullah, A. Qaiser, Q. Saeed, A. R. Abbasi, I. Ahmed and A. Q. Soomro, "Power flow & voltage stability analyses and remedies for a 340 MW nuclear power plant using ETAP," 2017 International Conference on Electrical Engineering (ICEE), Lahore, Pakistan, 2017, pp. 1-6, doi: 10.1109/ICEE.2017.7893436.

[43] IEEE 9-Bus System, Mathworks, https://www.mathworks.com/help/sps/ug/ieee-9-bus.html, Accessed. Sep 15, 2023.

[44] Sandia PVPerformance Model Collaboration, https://pvpmc.sandia.gov/modeling-steps/, Accessed Aug. 1, 2019.

[45] Armstrong, S., Hurley, W.G., “A Thermal Model for Photovoltaic Panels Under Varying Atmospheric Conditions.” Applied Thermal Engineering 2010. Volume 30. pages: 1488-95

[46] G. Tina and R. Abate, “Experimental verification of thermal behaviour of photovoltaic modules”, in Proc. 14th IEEE Mediterranean 2008, pp. 579– 584

[47] Canadian Solar MAXPOWER CS6U-325|330|335P, https://www.canadiansolar.com/upload/2e46a5e4e1c8ba14/9da8c57eb4c725d5.pdf, Accessed. Aug 1, 2019

[48] SUNNY CENTRAL 1000CP XT, https://files.sma.de/dl/25585/SC1000CP-DEN1751-V23web.pdf. Accessed. Aug 1, 2019.

[49] M. Ecker, N. Nieto, S. Kabitz, J. Schmalstieg, H. Blanke, A. Warnecke, and ¨ D. U. Sauer, “Calendar and cycle life study of Li(NiMnCo)O2-based 18650 lithiumion batteries,” J. Power Sources, 248, 839 (2014).

[50] “U.S. Nuclear Regulatory Commission Accepts NuScale Power’s Standard Design Approval Application”, https://www.nuscalepower.com/en/news/press-releases/2023/us-nuclear-regulatory-commission-accepts-nuscale-powers-standard-design-approval-application, Accessed. Sep 15, 2023.

[51] J. Kapernick, “Dynamic Modeling of a Small Modular Reactor for Control and Monitoring,” MS Thesis, Dept. of Nuclear Engineering, UT-K, Knoxville, TN, 2015.

[52] C. Batra. Integral Pressurized Water Reactor Simulator Manual. International Atomic Energy Agency, Vienna, Austria, 2018, vol. 1.

[53] S. E. Arda, “Nonlinear dynamic modeling and simulation of a passively cooled small modular reactor,” Doctoral Dissertation, Dept. Elect. Eng., Arizona State Univ., Tempe, AZ, USA, 2016.
[54] T. W. Kerlin, E. Katz, J. G. Thakkar, and J. E. Strange, “Theoretical and experimental dynamic analysis of the H. B. robinson nuclear plant,” Nucl. Technol., vol. 30, no. 3, pp. 299–316, 1976
[55] H. Kifune, M. K. Zadhe and H. Sasaki, "Efficiency Estimation of Synchronous Generators for Marine Applications and Verification With Shop Trial Data and Real Ship Operation Data," in IEEE Access, vol. 8, pp. 195541-195550, 2020, doi: 10.1109/ACCESS.2020.3033404.
[56] M. Walker, R. Theregowda, I. Safari, J. Abbasian, H. Arastoopour, D. Dzombak, M.K. Hsieh, D. Miller, “Utilization of municipal wastewater for cooling in thermoelectric power plants: Evaluation of the combined cost of makeup water treatment and increased condenser fouling,” Energy, Volume 60, 2013, Pages 139-147, ISSN 0360-5442, https://doi.org/10.1016/j.energy.2013.07.066.
[57] USGS Water Data for the Nation, https://waterdata.usgs.gov/nwis, Accessed. Mar 1, 2024.
[58] Enercon Product Portfolio, https://www.enercon.de/en/wind-turbines/product-portfolio, Accessed. Mar 1, 2023.
[59] J. Freeman, J. Jorgenson, P. Gilman, T. Ferguson, “Reference Manual for the System Advisor Model’s Wind Power Performance Model”, Technical Report NREL/TP-6A20-60570 August 2014
[60] R. Pinsky, P. Sabharwall, J. Hartvigsen, J. O’Brien, ”Comparative review of hydrogen production technologies for nuclear hybrid energy systems,”. United Kingdom: N. p., 2020. Web. doi:10.1016/j.pnucene.2020.103317.
[61] U. Bossel, B. Eliasson, “Energy and the Hydrogen Economy,” https://afdc.energy.gov/files/pdfs/hyd_economy_bossel_eliasson.pdf
[62] Ho. Zhang and T. Yuan, “Optimization and economic evaluation of a PEM electrolysis system considering its degradation in variable-power operations,” Applied Energy, Volume 324, 2022, 119760, ISSN 0306-2619, https://doi.org/10.1016/j.apenergy.2022.119760.
[63] Ho. Zhang, G. Lin, J. Chen, "Evaluation and calculation on the efficiency of a water electrolysis system for hydrogen production", International Journal of Hydrogen Energy, Volume 35, Issue 20, 2010, Pages 10851-10858, ISSN 0360-3199, https://doi.org/10.1016/j.ijhydene.2010.07.088.
[64] IEEE 9-Bus System, Mathworks, https://www.mathworks.com/help/sps/ug/ieee-9-bus.html, Accessed. Sep 15, 2023.
[65] Standard PRC-024-1 — Generator Frequency and Voltage Protective Relay Settings https://www.nerc.com/pa/Stand/Reliability%20Standards/PRC-024-1.pdf, Accessed. Dec 20,2023
[66] K. Smethurst, H. Hynes, O. Rook-Grignon, V. Walsh. “TESTING GUIDANCE FOR PROVIDERS OF FIRM FREQUENCY RESPONSE BALANCING

SERVICE," National Grid. November 2017. https://www.nationalgrid.com/sites/default/files/documents/FFR%20Testing%20Guidance%20verD11%20Final.pdf

[67] PVWatts Calculator, https://pvwatts.nrel.gov/pvwatts.php, Accessed. Mar 1, 2024.

[68] D. Feldman, V. Ramasamy, R. Fu, A. Ramdas, J. Desai, R. Margolis, "U.S. Solar Photovoltaic System and Energy Storage Cost Benchmark: Q1 2020" United States. https://doi.org/10.2172/1765601

[69] Real-time Operating Grid - U.S. Energy Information Administration (EIA), https://www.eia.gov/electricity/gridmonitor/dashboard/electric_overview/US48/US48, Accessed. Mar. 1, 2024.

[70] K. Mongird, V. Viswanathan, J. Alam, C. Vartanian, V. Sprenkle, R. Baxter, "2020 Grid Energy Storage Technology Cost and Performance Assessment." Technical Report Publication No. DOE/PA-0204 December 2020

[71] 2023 Business Water Rates, https://www.denverwater.org/business/billing-and-rates/2023-rates, Accessed. May. 1, 2023.

[72] C. Vlahoplus, S. Lawrie, "Small Modular Reactors – A Viable Option for a Clean Energy Future?" https://www.kenan-flagler.unc.edu/wp-content/uploads/2021/08/SMRs-A-Viable-Option-for-Clean-Energy-Future_2021.07.19_Final.pdf

[73] T. Stehly, P. Duffy, "2021 Cost of Wind Energy Review." United States: N. p., 2023. Web. doi:10.2172/1907623.

[74] A. Loomis, A. Kobos, J. Kwok, R. Reigner, M. Emmert, "Navigating the Inflation Reduction Act of 2022: A Practical Guide", Troutman, https://www.troutman.com/insights/navigating-the-inflation-reduction-act-of-2022-a-practical-guide.html, Accessed. Sep 1, 2023.

[75] Measurement and Instrumentation Database Center, https://midcdmz.nrel.gov/, Accessed. Mar 1, 2024.

[76] Standard PRC-024-1 — Generator Frequency and Voltage Protective Relay Settings https://www.nerc.com/pa/Stand/Reliability%20Standards/PRC-024-1.pdf, Accessed. Mar 1, 2024.

[77] E. Fix, A. Banerjee, U. Muenz and G. -S. Seo, "Investigating Multi-Microgrid Black Start Methods Using Grid-Forming Inverters," *2023 IEEE Power & Energy Society Innovative Smart Grid Technologies Conference (ISGT)*, Washington, DC, USA, 2023, pp. 1-5, doi: 10.1109/ISGT51731.2023.10066412.

[78] What is a Solid-state Battery? https://www.samsungsdi.com/column/technology/detail/56462.html?listType=gallery#:~:text=A%20solid%2Dstate%20battery%20has,safety%2C%20thus%20saving%20more%20space. Accessed. Mar 1, 2024.

[79] Z. Pu, G. Zhang, A. Hassanpour, D. Zheng, S. Wang, S. Liao, Z. Chen, S. Sun, "Regenerative fuel cells: Recent progress, challenges, perspectives and their applications for space energy system," Applied Energy, Volume 283, 2021, 116376, ISSN 0306-2619, https://doi.org/10.1016/j.apenergy.2020.116376.

[80] NASA's Lunar Exploration Program Overview https://www.nasa.gov/wp-content/uploads/2020/12/artemis_plan-20200921.pdf. September 2020. Accessed. Mar 1, 2024.

[81] L. Muccione *et al.*, "Regenerative Fuel Cell for Lunar Night Survival," *2023 13th European Space Power Conference (ESPC)*, Elche, Spain, 2023, pp. 1-16, doi: 10.1109/ESPC59009.2023.10298186.

APPENDIX A

A.1 Annual Energy Model in Simulink

The annual energy model was developed in MATLAB/Simulink with the following excerpts provided in this appendix. The information is provided for future expansion on this topic as part of follow on research. This information is intended to augment the details in Chapter 3. The figures included, show the following, in chronological order:

- Figure 40: Top level HES model.
- Figure 41: SMR 2-D curve fit model. Eq. (40) to (43) captured in the 2-D block.
- Figure 42: WTG model with row level wake effects.
- Figure 43: BESS model.
- Figure 44: PEM model.
- Figure 45: PV inverter and DC-AC ratio model.

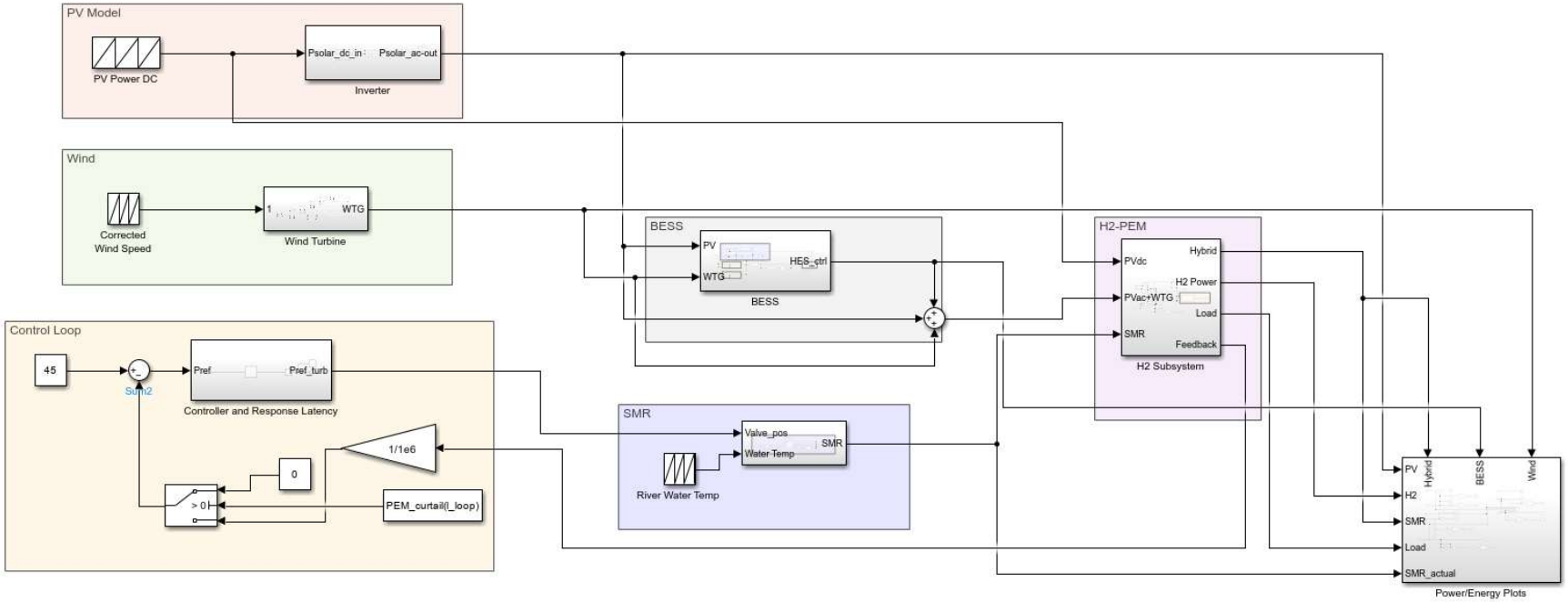

Figure 40: Top level HES model.

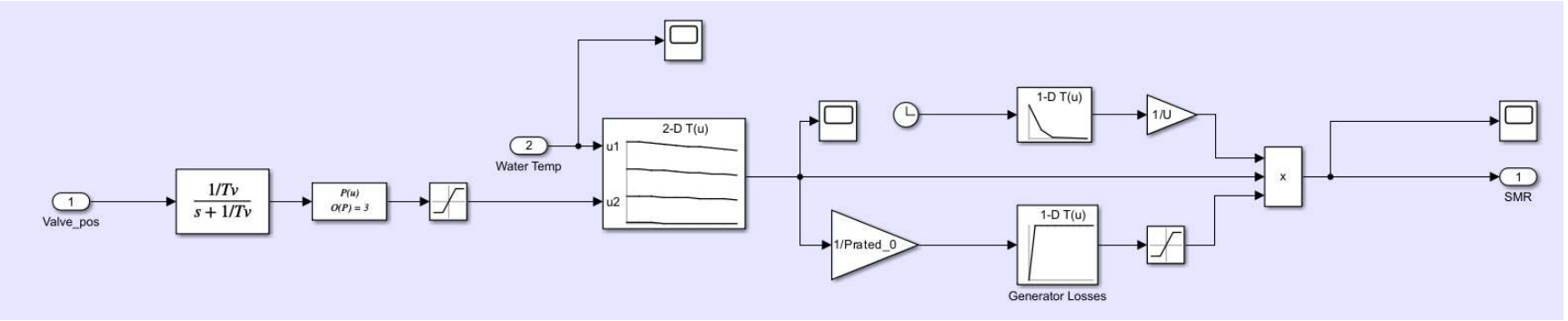

Figure 41: SMR 2-D curve fit model.

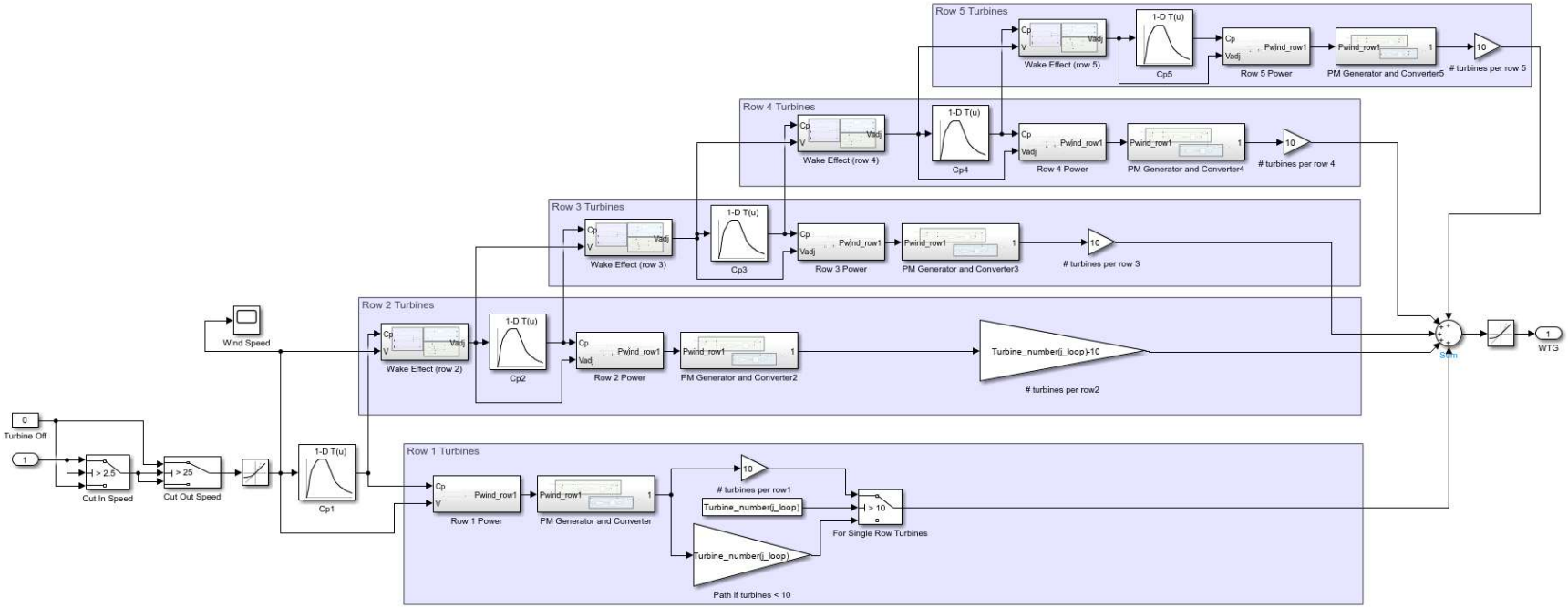

Figure 42: WTG model with row level wake effects.

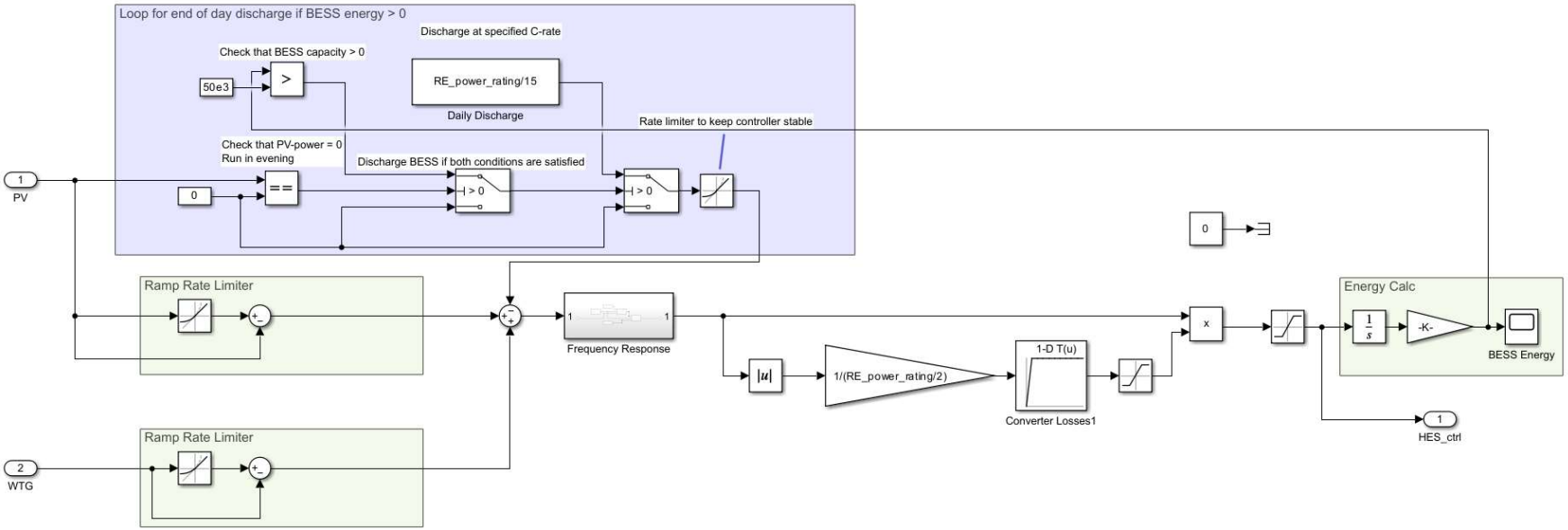

Figure 43: BESS model.

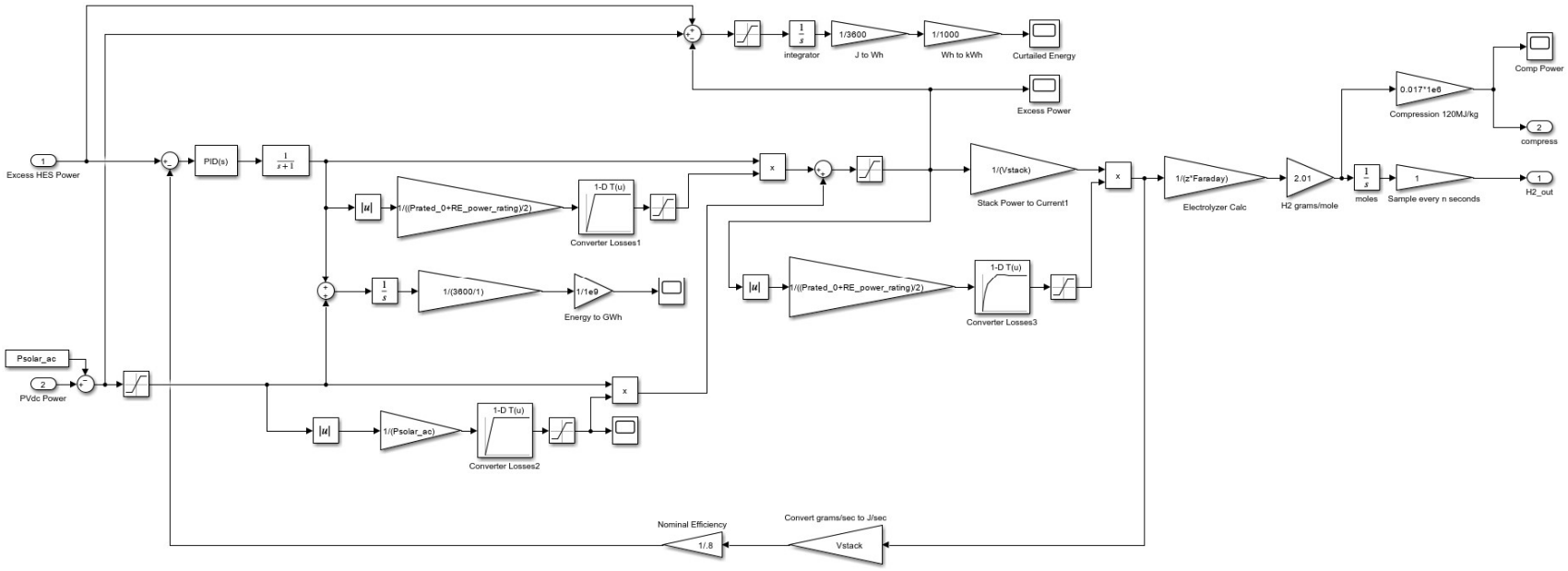

Figure 44: PEM model.

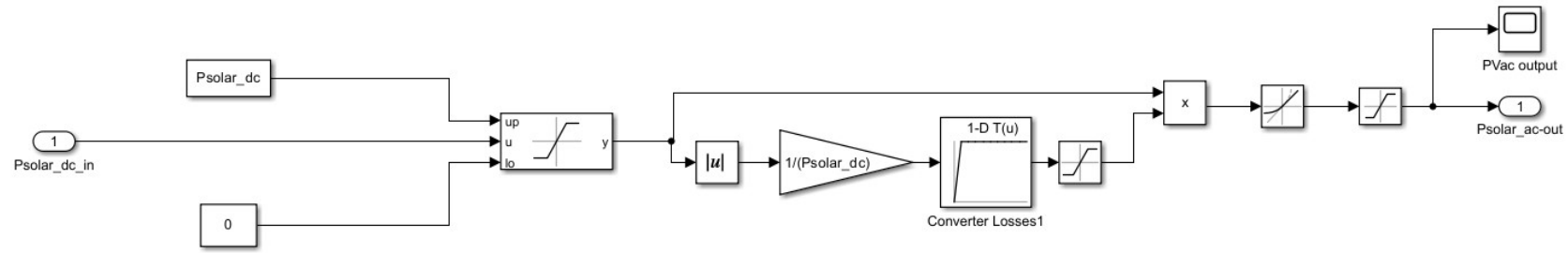

Figure 45: PV inverter and DC-AC ratio model.

A.2 Transient Model in Simulink

The transient model was developed in MATLAB/Simulink and building off the IEEE 9 Bus model as discussed in Section 4.4 with the following excerpts provided in this appendix. The information is provided for future expansion on this topic as part of follow on research. This information is intended to augment the details in Chapter 3. The figures included, show the following, in chronological order:

- Figure 40: Top level HES model.
- Figure 47: SMR turbine-generator transient model.
- Figure 48: SMR 2-D curve fit representation of mechanical power.
- Figure 49: PEM load represented as a variable load.
- Figure 50: PV+WTG+BESS represented as variable negative loa

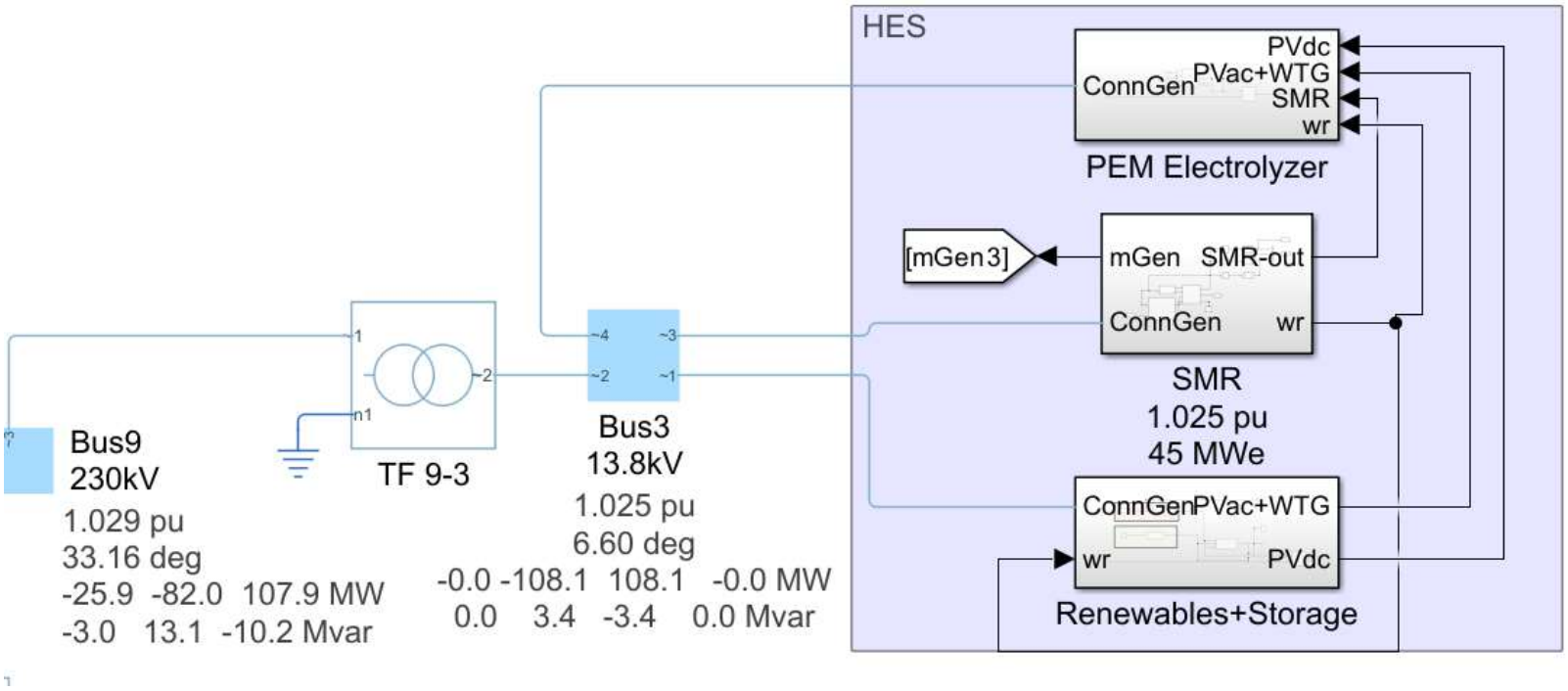

Figure 46: HES model within the HES model shown in Section 4.4.

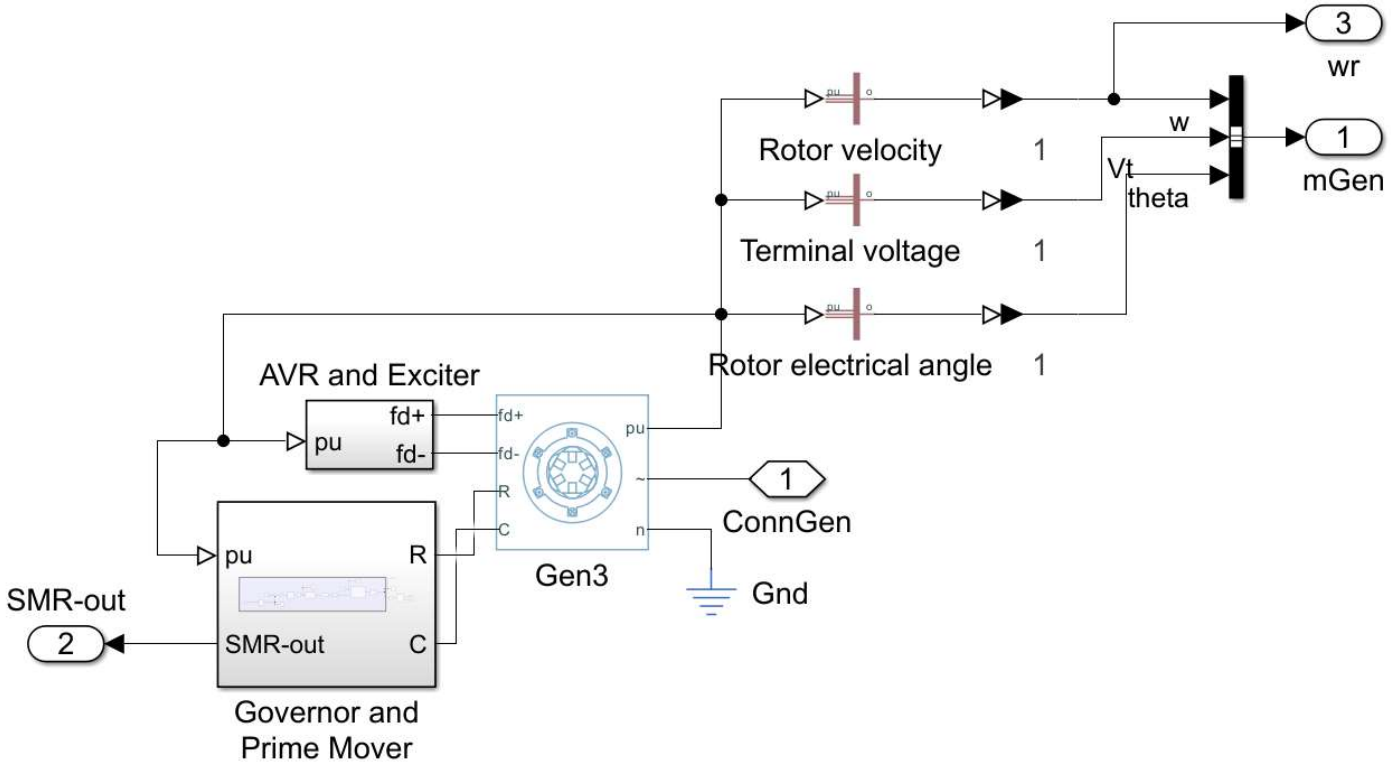

Figure 47: SMR turbine-generator transient model.

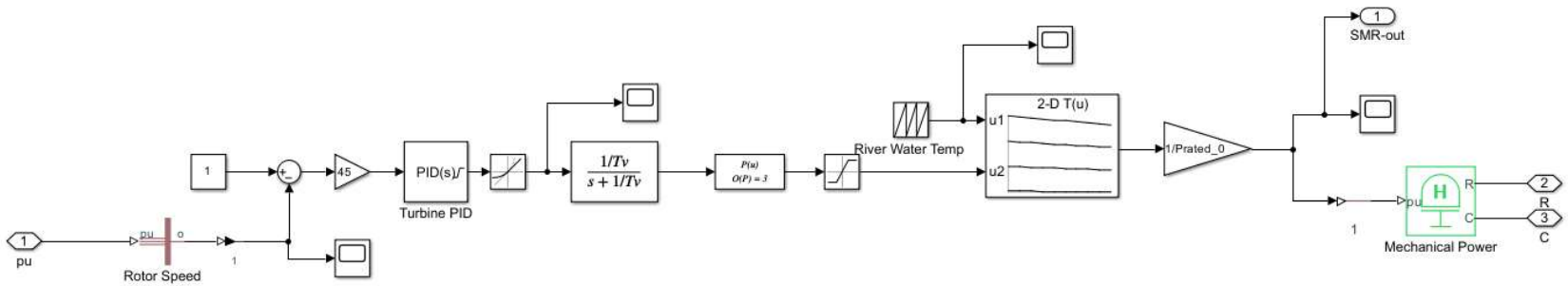

Figure 48: SMR 2-D curve fit representation of mechanical power.

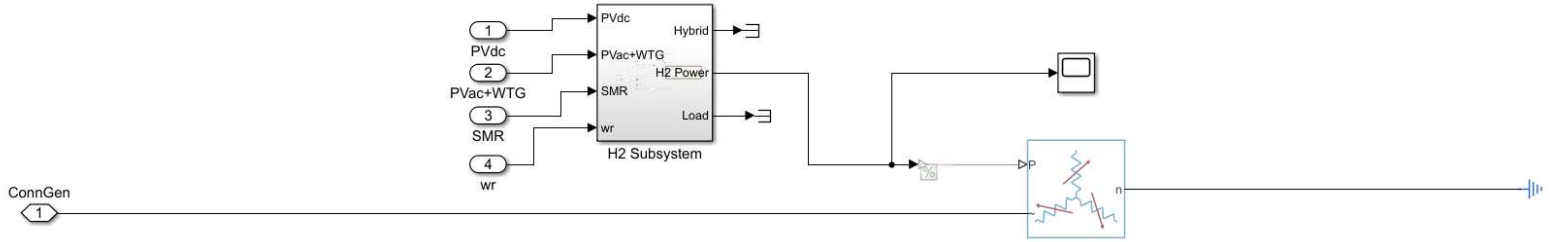

Figure 49: PEM load represented as a variable load.

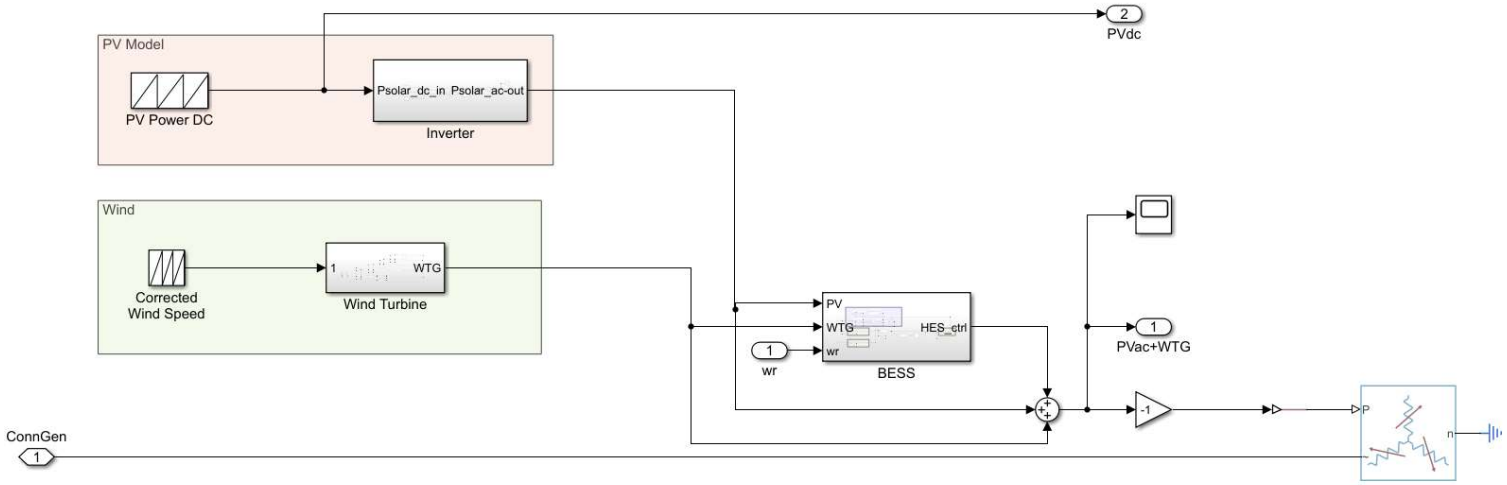

Figure 50: PV+WTG+BESS represented as variable negative load.

APPENDIX B

B.1 Optimization Loop Results

The full case results are provided here. Full results are only provided for the subsidized results, and after considering the rejection criteria, as discussed in Section 6.3 to limit page count. The full NREL subsidized results are provided in Table 20 and the full UO results are given in Table 21. From going through the full set of results, the most apparent relationship is found between the level of energy storage and the resulting IRR. For the subsidized cases, the higher IRR is typically found between PEM ratios of 0.3 to 0.4 relative to the HES power rating.

Table 20: Full results from NREL subsidized case.

Scenario	Peak Load:SMR	WTG Number	PV Nameplate (kW)	PEM Ratio	HES CF (%)	H2 Production (kg)	NPV ($)	Irr (%)
1	1	0	0	0.1	57.8	775,704.2	(107,745,582.1)	-1.43%
2	1	0	0	0.2	57.8	1,855,889.5	(39,242,825.1)	3.08%
3	1	0	0	0.3	57.8	2,715,935.9	6,416,009.2	5.28%
4	1	0	0	0.4	57.7	3,458,392.7	42,300,590.0	6.68%
5	1	0	0	0.5	57.7	3,462,062.1	22,092,952.0	5.86%
6	1	0	0	0.6	57.7	3,461,013.1	993,713.0	5.04%
7	1	0	0	0.7	57.6	3,467,091.1	(19,796,687.5)	4.25%
8	1	0	4500	0.1	53.1	916,957.6	(107,643,458.6)	-1.25%
9	1	0	4500	0.2	53.1	2,151,227.6	(30,393,287.6)	3.58%
10	1	0	4500	0.3	53.1	3,148,137.9	22,096,753.6	5.91%
11	1	0	4500	0.4	53.1	3,705,794.6	40,696,595.4	6.56%
12	1	0	4500	0.5	53.1	3,714,438.5	17,503,563.8	5.66%
13	1	0	4500	0.6	53.0	3,706,540.0	(7,214,206.7)	4.73%
14	1	0	4500	0.7	53.0	3,710,432.2	(31,204,031.6)	3.86%
15	1	0	9000	0.1	48.7	1,076,030.2	(107,053,793.0)	-1.02%
16	1	0	9000	0.2	48.7	2,479,380.9	(20,733,058.5)	4.07%
17	1	0	9000	0.3	48.6	3,628,362.3	39,525,863.4	6.54%

18	1	0	9000	0.4	48.7	3,956,224.9	37,095,486.0	6.38%
19	1	0	9000	0.5	48.6	3,964,262.2	10,075,110.7	5.37%
20	1	0	9000	0.6	48.6	3,956,200.6	(18,252,364.0)	4.35%
21	1	0	9000	0.7	48.6	3,958,894.1	(45,897,316.3)	3.39%
22	1	0	13500	0.1	44.9	1,236,840.1	(106,339,593.7)	-0.80%
23	1	0	13500	0.2	44.9	2,807,534.3	(11,210,830.5)	4.52%
24	1	0	13500	0.3	44.9	4,108,586.7	56,977,100.6	7.12%
25	1	0	13500	0.4	44.9	4,214,544.7	33,951,486.9	6.22%
26	1	0	13500	0.5	44.9	4,210,339.0	2,360,109.9	5.08%
27	1	0	13500	0.6	44.9	4,206,237.0	(29,296,673.5)	3.99%
28	1	0	13500	0.7	44.9	4,208,770.0	(60,585,126.2)	2.95%
29	1	0	18000	0.1	41.7	1,399,015.1	(105,641,760.4)	-0.60%
30	1	0	18000	0.2	41.7	3,135,687.6	(1,827,713.2)	4.92%
31	1	0	18000	0.3	41.7	4,454,649.9	64,082,346.5	7.30%
32	1	0	18000	0.4	41.7	4,466,540.2	30,207,398.5	6.05%
33	1	0	18000	0.5	41.7	4,462,605.7	(4,990,215.2)	4.83%
34	1	0	18000	0.6	41.7	4,456,452.2	(40,445,244.2)	3.65%
35	1	0	18000	0.7	41.7	4,457,926.9	(75,530,892.0)	2.54%
36	1	0	22500	0.1	38.9	1,562,282.1	(105,492,336.7)	-0.43%
37	1	0	22500	0.2	38.9	3,458,208.7	6,536,436.2	5.26%
38	1	0	22500	0.3	38.9	4,704,948.7	63,264,989.4	7.20%
39	1	0	22500	0.4	38.9	4,711,026.6	25,332,837.1	5.86%
40	1	0	22500	0.5	38.9	4,715,080.0	(12,917,537.5)	4.57%
41	1	0	22500	0.6	38.9	4,706,352.7	(52,224,579.0)	3.32%
42	1	0	22500	0.7	38.9	4,709,524.6	(90,725,138.8)	2.15%
43	1	4	0	0.1	48.1	931,108.9	(118,829,626.9)	-2.51%
44	1	4	0	0.2	48.1	2,228,606.9	(36,878,404.4)	3.23%
45	1	4	0	0.3	48.1	3,261,376.0	17,446,889.2	5.73%
46	1	4	0	0.4	48.0	3,930,734.0	43,672,093.8	6.67%
47	1	4	0	0.5	48.1	3,941,976.7	19,931,711.1	5.75%
48	1	4	0	0.6	48.0	3,934,024.8	(5,622,730.2)	4.79%
49	1	4	0	0.7	48.0	3,932,485.7	(30,831,970.9)	3.87%
50	1	4	4500	0.1	44.8	1,072,152.4	(117,690,323.1)	-2.15%
51	1	4	4500	0.2	44.8	2,523,944.9	(27,376,590.0)	3.74%
52	1	4	4500	0.3	44.8	3,693,578.0	34,022,467.1	6.34%
53	1	4	4500	0.4	44.8	4,178,691.5	43,094,258.4	6.60%
54	1	4	4500	0.5	44.8	4,190,259.1	15,934,636.7	5.58%
55	1	4	4500	0.6	44.7	4,177,877.6	(13,144,405.8)	4.53%
56	1	4	4500	0.7	44.7	4,178,386.8	(41,296,000.9)	3.55%
57	1	4	9000	0.1	41.6	1,230,714.0	(116,965,987.2)	-1.82%
58	1	4	9000	0.2	41.6	2,852,098.3	(17,684,162.5)	4.23%
59	1	4	9000	0.3	41.6	4,173,802.4	51,652,378.2	6.94%
60	1	4	9000	0.4	41.6	4,433,089.0	39,813,302.7	6.43%

61	1	4	9000	0.5	41.6	4,438,934.5	8,551,459.0	5.30%
62	1	4	9000	0.6	41.6	4,427,157.8	(24,086,070.8)	4.17%
63	1	4	9000	0.7	41.6	4,427,958.3	(55,834,010.1)	3.11%
64	1	4	13500	0.1	38.8	1,390,844.9	(116,457,894.6)	-1.54%
65	1	4	13500	0.2	38.8	3,180,251.7	(8,277,431.9)	4.65%
66	1	4	13500	0.3	38.8	4,653,587.0	69,010,278.0	7.46%
67	1	4	13500	0.4	38.8	4,689,728.5	36,465,832.7	6.27%
68	1	4	13500	0.5	38.8	4,687,896.9	977,768.0	5.03%
69	1	4	13500	0.6	38.8	4,677,229.4	(35,229,658.8)	3.83%
70	1	4	13500	0.7	38.8	4,675,605.0	(70,812,733.3)	2.69%
71	1	4	18000	0.1	36.4	1,552,251.5	(115,844,733.6)	-1.28%
72	1	4	18000	0.2	36.4	3,508,405.0	1,124,066.7	5.05%
73	1	4	18000	0.3	36.4	4,927,173.4	70,600,462.2	7.44%
74	1	4	18000	0.4	36.4	4,937,749.7	32,459,725.2	6.09%
75	1	4	18000	0.5	36.4	4,937,730.8	(6,535,583.9)	4.79%
76	1	4	18000	0.6	36.4	4,927,791.3	(46,318,725.3)	3.51%
77	1	4	18000	0.7	36.4	4,927,900.6	(85,380,898.9)	2.32%
78	1	4	22500	0.1	34.3	1,714,709.3	(115,252,898.6)	-1.04%
79	1	4	22500	0.2	34.3	3,836,558.4	10,431,642.0	5.40%
80	1	4	22500	0.3	34.3	5,178,825.8	70,409,906.7	7.37%
81	1	4	22500	0.4	34.3	5,189,331.4	28,618,934.1	5.93%
82	1	4	22500	0.5	34.3	5,185,005.3	(14,349,705.2)	4.54%
83	1	4	22500	0.6	34.2	5,176,467.8	(57,689,156.2)	3.21%
84	1	4	22500	0.7	34.2	5,177,729.0	(100,316,800.7)	1.96%
85	1	8	0	0.1	41.2	1,086,514.3	(125,820,082.2)	-2.81%
86	1	8	0	0.2	41.1	2,601,324.3	(30,818,831.0)	3.60%
87	1	8	0	0.3	41.1	3,806,816.1	32,527,412.7	6.27%
88	1	8	0	0.4	41.1	4,404,554.3	49,206,105.8	6.78%
89	1	8	0	0.5	41.1	4,412,418.4	20,909,933.9	5.74%
90	1	8	0	0.6	41.1	4,412,797.4	(8,120,212.3)	4.72%
91	1	8	0	0.7	41.1	4,405,393.1	(37,873,604.5)	3.70%
92	1	8	4500	0.1	38.7	1,227,404.7	(124,222,328.8)	-2.41%
93	1	8	4500	0.2	38.7	2,896,662.3	(20,887,808.1)	4.09%
94	1	8	4500	0.3	38.7	4,239,018.1	49,526,137.7	6.84%
95	1	8	4500	0.4	38.7	4,656,018.7	49,249,735.0	6.73%
96	1	8	4500	0.5	38.7	4,662,562.4	17,542,026.0	5.60%
97	1	8	4500	0.6	38.7	4,656,504.5	(15,210,137.8)	4.49%
98	1	8	4500	0.7	38.7	4,651,009.6	(47,909,670.5)	3.41%
99	1	8	9000	0.1	36.3	1,385,581.7	(123,579,056.5)	-2.07%
100	1	8	9000	0.2	36.3	3,224,815.7	(11,263,061.8)	4.53%
101	1	8	9000	0.3	36.3	4,718,639.6	67,097,736.8	7.37%
102	1	8	9000	0.4	36.3	4,910,021.5	45,909,281.7	6.56%
103	1	8	9000	0.5	36.3	4,913,815.4	10,347,313.3	5.34%

104	1	8	9000	0.6	36.3	4,903,928.6	(26,318,665.6)	4.14%
105	1	8	9000	0.7	36.3	4,897,959.3	(62,870,151.6)	2.99%
106	1	8	13500	0.1	34.2	1,545,185.1	(123,124,213.6)	-1.78%
107	1	8	13500	0.2	34.2	3,552,969.1	(1,884,633.8)	4.92%
108	1	8	13500	0.3	34.2	5,150,469.8	80,763,317.5	7.74%
109	1	8	13500	0.4	34.2	5,161,480.8	42,148,555.0	6.39%
110	1	8	13500	0.5	34.2	4,059,696.9	(81,826,047.0)	2.10%
111	1	8	13500	0.6	34.2	5,149,598.8	(37,771,665.5)	3.81%
112	1	8	13500	0.7	34.2	5,150,027.2	(77,318,292.5)	2.62%
113	1	8	18000	0.1	32.3	1,705,978.5	(122,784,637.6)	-1.52%
114	1	8	18000	0.2	32.3	3,881,122.4	7,316,711.5	5.28%
115	1	8	18000	0.3	32.3	5,401,463.1	80,414,790.6	7.65%
116	1	8	18000	0.4	32.3	5,413,570.6	38,243,908.2	6.22%
117	1	8	18000	0.5	32.3	5,413,700.4	(4,505,387.0)	4.86%
118	1	8	18000	0.6	32.3	5,400,177.7	(49,074,902.5)	3.51%
119	1	8	18000	0.7	32.3	5,399,505.9	(92,334,194.9)	2.25%
120	1	8	22500	0.1	30.6	1,867,774.7	(122,040,665.0)	-1.27%
121	1	8	22500	0.2	30.6	4,209,275.8	16,942,719.0	5.63%
122	1	8	22500	0.3	30.6	5,652,544.0	80,496,864.0	7.58%
123	1	8	22500	0.4	30.6	5,664,710.4	34,693,175.3	6.08%
124	1	8	22500	0.5	30.6	5,655,300.3	(12,807,807.9)	4.61%
125	1	8	22500	0.6	30.6	5,649,397.8	(60,078,964.6)	3.23%
126	1	8	22500	0.7	30.6	5,646,779.9	(107,257,834.5)	1.91%
127	1	12	0	0.1	36.0	1,241,920.1	(131,281,980.9)	-2.67%
128	1	12	0	0.2	36.0	2,974,041.7	(23,073,577.2)	4.02%
129	1	12	0	0.3	36.0	4,352,076.9	49,165,383.7	6.78%
130	1	12	0	0.4	36.0	4,865,583.0	55,359,644.4	6.88%
131	1	12	0	0.5	35.9	4,875,680.3	22,957,726.9	5.76%
132	1	12	0	0.6	35.9	4,874,390.5	(10,253,691.2)	4.67%
133	1	12	0	0.7	35.9	4,868,344.5	(44,105,688.4)	3.59%
134	1	12	4500	0.1	34.1	1,382,693.9	(129,324,335.2)	-2.30%
135	1	12	4500	0.2	34.1	3,269,379.7	(12,966,749.2)	4.47%
136	1	12	4500	0.3	34.1	4,783,681.6	66,446,059.0	7.31%
137	1	12	4500	0.4	34.1	5,118,461.9	55,656,688.5	6.84%
138	1	12	4500	0.5	34.1	5,124,988.6	19,794,425.7	5.64%
139	1	12	4500	0.6	34.1	5,120,084.1	(17,044,635.3)	4.46%
140	1	12	4500	0.7	34.1	5,114,158.9	(53,904,520.4)	3.33%
141	1	12	9000	0.1	32.2	1,540,571.0	(128,885,150.4)	-2.01%
142	1	12	9000	0.2	32.2	3,597,533.1	(3,454,479.7)	4.86%
143	1	12	9000	0.3	32.2	5,262,878.9	83,641,167.2	7.78%
144	1	12	9000	0.4	32.2	5,370,810.5	51,942,962.9	6.67%
145	1	12	9000	0.5	32.2	5,372,655.1	12,097,063.9	5.38%
146	1	12	9000	0.6	32.2	5,370,236.0	(28,068,351.0)	4.14%

147	1	12	9000	0.7	32.2	5,363,739.6	(68,637,150.2)	2.94%
148	1	12	13500	0.1	30.5	1,699,753.4	(128,675,716.3)	-1.76%
149	1	12	13500	0.2	30.5	3,925,686.4	5,693,660.1	5.22%
150	1	12	13500	0.3	30.5	5,613,954.9	91,135,258.4	7.93%
151	1	12	13500	0.4	30.5	5,625,376.7	48,408,150.6	6.51%
152	1	12	13500	0.5	30.5	5,624,185.3	4,693,064.5	5.14%
153	1	12	13500	0.6	30.5	5,616,582.6	(39,565,500.5)	3.83%
154	1	12	13500	0.7	30.5	5,611,329.8	(83,722,379.0)	2.57%
155	1	12	18000	0.1	29.0	1,860,046.8	(128,199,454.2)	-1.52%
156	1	12	18000	0.2	29.0	4,253,839.8	15,041,180.1	5.55%
157	1	12	18000	0.3	29.0	5,864,670.5	90,911,415.8	7.85%
158	1	12	18000	0.4	29.0	5,876,637.5	44,589,597.2	6.35%
159	1	12	18000	0.5	29.0	5,870,181.1	(3,179,134.7)	4.91%
160	1	12	18000	0.6	29.0	5,865,938.9	(50,773,878.7)	3.54%
161	1	12	18000	0.7	29.0	5,862,967.4	(98,333,383.0)	2.24%
162	1	12	22500	0.1	27.6	2,021,293.3	(127,526,174.3)	-1.29%
163	1	12	22500	0.2	27.6	4,581,993.2	24,512,098.7	5.86%
164	1	12	22500	0.3	27.6	6,115,817.8	90,843,649.4	7.77%
165	1	12	22500	0.4	27.6	6,123,632.3	40,553,759.9	6.20%
166	1	12	22500	0.5	27.6	6,117,745.8	(10,802,302.9)	4.69%
167	1	12	22500	0.6	27.6	6,113,639.6	(62,149,246.4)	3.27%
168	1	12	22500	0.7	27.6	6,111,815.9	(113,171,688.0)	1.92%
169	1	16	0	0.1	31.9	1,397,326.2	(137,213,117.7)	-2.61%
170	1	16	0	0.2	31.9	3,346,759.1	(15,919,084.9)	4.36%
171	1	16	0	0.3	31.9	4,896,452.1	65,124,365.9	7.21%
172	1	16	0	0.4	31.9	5,318,308.5	60,338,763.2	6.94%
173	1	16	0	0.5	31.9	5,324,828.6	23,458,335.7	5.74%
174	1	16	0	0.6	31.9	5,319,579.2	(14,219,843.6)	4.56%
175	1	16	0	0.7	31.9	5,323,249.6	(51,275,051.2)	3.46%
176	1	16	4500	0.1	30.4	1,538,008.3	(135,056,096.4)	-2.26%
177	1	16	4500	0.2	30.4	3,642,097.1	(5,620,026.5)	4.78%
178	1	16	4500	0.3	30.4	5,327,919.9	82,757,488.8	7.71%
179	1	16	4500	0.4	30.4	5,569,345.4	60,771,561.7	6.90%
180	1	16	4500	0.5	30.4	5,572,092.4	20,466,438.8	5.62%
181	1	16	4500	0.6	30.4	5,570,116.8	(20,185,391.0)	4.40%
182	1	16	4500	0.7	30.4	5,567,594.9	(60,892,417.1)	3.22%
183	1	16	9000	0.1	28.9	1,695,645.0	(134,742,738.2)	-2.00%
184	1	16	9000	0.2	28.9	3,970,250.5	3,756,731.4	5.14%
185	1	16	9000	0.3	28.9	5,801,599.1	99,629,721.9	8.13%
186	1	16	9000	0.4	28.9	5,822,015.2	57,111,613.0	6.74%
187	1	16	9000	0.5	28.9	5,823,274.9	13,069,371.4	5.39%
188	1	16	9000	0.6	28.9	5,820,468.3	(31,310,506.8)	4.09%
189	1	16	9000	0.7	28.9	5,817,612.9	(75,789,410.3)	2.86%

190	1	16	13500	0.1	27.6	1,854,483.7	(134,468,410.6)	-1.77%
191	1	16	13500	0.2	27.6	4,298,403.8	13,035,347.9	5.47%
192	1	16	13500	0.3	27.6	6,067,900.4	100,539,844.2	8.07%
193	1	16	13500	0.4	27.6	6,076,681.1	53,466,448.3	6.58%
194	1	16	13500	0.5	27.6	6,070,560.4	5,223,384.2	5.15%
195	1	16	13500	0.6	27.6	6,074,216.4	(42,268,100.0)	3.81%
196	1	16	13500	0.7	27.6	6,062,922.8	(91,068,783.0)	2.50%
197	1	16	18000	0.1	26.3	2,014,361.9	(134,008,207.5)	-1.54%
198	1	16	18000	0.2	26.3	4,626,557.2	22,402,520.2	5.78%
199	1	16	18000	0.3	26.3	6,318,550.1	100,331,206.7	7.99%
200	1	16	18000	0.4	26.3	6,324,485.7	49,392,226.4	6.43%
201	1	16	18000	0.5	26.3	6,317,476.5	(2,619,050.4)	4.93%
202	1	16	18000	0.6	26.3	6,321,265.7	(53,720,570.1)	3.54%
203	1	16	18000	0.7	26.3	6,313,743.3	(105,869,122.4)	2.18%
204	1	16	22500	0.1	25.2	2,175,145.0	(133,947,125.0)	-1.35%
205	1	16	22500	0.2	25.2	4,954,470.8	31,308,931.7	6.05%
206	1	16	22500	0.3	25.2	6,569,775.9	99,720,514.8	7.91%
207	1	16	22500	0.4	25.2	6,572,952.8	44,922,197.9	6.26%
208	1	16	22500	0.5	25.2	6,567,577.4	(10,618,530.9)	4.71%
209	1	16	22500	0.6	25.2	6,565,181.5	(65,875,746.0)	3.26%
210	1	16	22500	0.7	25.2	6,563,796.3	(121,410,834.4)	1.87%
211	1.05	15	6750	0.25	32.0	4,605,137.3	54,683,058.3	6.90%
212	1.05	15	6750	0.3	32.0	5,339,951.9	90,222,849.0	7.93%
213	1.05	15	6750	0.35	32.0	5,340,383.1	69,659,838.6	7.23%
214	1.05	15	9000	0.25	31.2	4,797,212.6	60,603,039.5	7.06%
215	1.05	15	9000	0.3	31.2	5,464,983.5	90,102,573.5	7.88%
216	1.05	15	9000	0.35	31.2	5,466,453.3	68,749,952.7	7.17%
217	1.05	15	11250	0.25	30.4	4,988,984.4	66,548,730.3	7.22%
218	1.05	15	11250	0.3	30.4	5,590,292.3	89,848,929.5	7.84%
219	1.05	15	11250	0.35	30.4	5,593,207.8	67,871,723.8	7.11%
220	1.05	16	6750	0.25	31.1	4,721,403.4	57,812,836.7	6.98%
221	1.05	16	6750	0.3	31.1	5,453,318.4	92,565,928.4	7.96%
222	1.05	16	6750	0.35	31.1	5,454,500.1	71,559,376.2	7.26%
223	1.05	16	9000	0.25	30.4	4,913,531.5	63,588,249.9	7.14%
224	1.05	16	9000	0.3	30.4	5,578,845.6	92,362,734.2	7.92%
225	1.05	16	9000	0.35	30.4	5,579,930.3	70,451,552.4	7.19%
226	1.05	16	11250	0.25	29.6	5,105,310.1	69,505,708.1	7.29%
227	1.05	16	11250	0.3	29.6	5,703,833.0	92,269,355.5	7.88%
228	1.05	16	11250	0.35	29.6	5,705,408.5	69,484,166.3	7.14%
229	1.05	17	6750	0.25	30.4	4,837,629.4	60,790,487.1	7.05%
230	1.05	17	6750	0.3	30.4	5,566,853.9	94,829,408.2	8.00%
231	1.05	17	6750	0.35	30.4	5,567,125.7	73,234,544.6	7.28%
232	1.05	17	9000	0.25	29.6	5,029,872.5	66,746,017.3	7.21%

233	1.05	17	9000	0.3	29.6	5,692,056.4	94,755,931.2	7.96%
234	1.05	17	9000	0.35	29.6	5,693,453.7	72,362,928.2	7.22%
235	1.05	17	11250	0.25	28.9	5,221,731.3	72,584,401.8	7.36%
236	1.05	17	11250	0.3	28.9	5,817,027.1	94,565,373.7	7.92%
237	1.05	17	11250	0.35	28.9	5,818,949.2	71,283,227.4	7.16%
238	1.1	0	0	0.1	63.5	775,704.2	(86,579,110.5)	0.09%
239	1.1	0	0	0.2	63.5	1,855,889.5	(20,557,443.7)	4.03%
240	1.1	0	0	0.3	63.3	2,715,935.9	23,830,524.7	6.01%
241	1.1	0	0	0.4	63.3	2,998,187.0	24,616,938.3	6.00%
242	1.1	0	0	0.5	63.2	3,011,214.9	4,454,033.2	5.18%
243	1.1	0	0	0.6	63.0	3,017,823.6	(17,236,974.3)	4.32%
244	1.1	0	0	0.7	62.8	3,039,304.4	(38,457,704.8)	3.50%
245	1.1	0	4500	0.1	58.4	916,957.6	(85,958,718.0)	0.26%
246	1.1	0	4500	0.2	58.3	2,151,227.6	(11,313,379.6)	4.49%
247	1.1	0	4500	0.3	58.2	3,148,137.9	40,302,995.7	6.62%
248	1.1	0	4500	0.4	58.3	3,236,016.7	23,384,503.6	5.92%
249	1.1	0	4500	0.5	58.2	3,243,330.1	(740,461.3)	4.97%
250	1.1	0	4500	0.6	58.1	3,253,045.6	(25,066,606.2)	4.05%
251	1.1	0	4500	0.7	57.9	3,268,508.1	(49,444,046.0)	3.15%
252	1.1	0	9000	0.1	53.5	1,076,030.2	(85,317,396.8)	0.42%
253	1.1	0	9000	0.2	53.5	2,479,380.9	(1,610,071.2)	4.93%
254	1.1	0	9000	0.3	53.4	3,482,963.6	47,140,412.4	6.83%
255	1.1	0	9000	0.4	53.4	3,492,386.6	20,334,135.7	5.77%
256	1.1	0	9000	0.5	53.4	3,490,242.6	(8,023,608.2)	4.70%
257	1.1	0	9000	0.6	53.3	3,497,796.9	(36,021,951.4)	3.68%
258	1.1	0	9000	0.7	53.1	3,511,805.1	(63,991,129.5)	2.70%
259	1.1	0	13500	0.1	49.4	1,236,840.1	(84,625,642.2)	0.58%
260	1.1	0	13500	0.2	49.4	2,807,534.3	7,911,551.5	5.33%
261	1.1	0	13500	0.3	49.3	3,733,393.1	47,130,184.5	6.77%
262	1.1	0	13500	0.4	49.3	3,743,601.6	16,770,515.8	5.61%
263	1.1	0	13500	0.5	49.3	3,740,495.0	(15,261,218.2)	4.45%
264	1.1	0	13500	0.6	49.2	3,746,392.6	(46,932,046.5)	3.35%
265	1.1	0	13500	0.7	49.1	3,759,101.0	(78,639,528.2)	2.28%
266	1.1	0	18000	0.1	45.9	1,399,015.1	(83,944,714.0)	0.73%
267	1.1	0	18000	0.2	45.8	3,135,687.6	17,307,025.3	5.70%
268	1.1	0	18000	0.3	45.8	3,981,757.0	46,867,991.9	6.71%
269	1.1	0	18000	0.4	45.8	3,991,202.3	12,725,575.7	5.45%
270	1.1	0	18000	0.5	45.8	3,990,692.2	(22,736,234.6)	4.21%
271	1.1	0	18000	0.6	45.7	3,995,823.8	(58,133,238.7)	3.02%
272	1.1	0	18000	0.7	45.6	4,008,418.2	(93,480,195.5)	1.89%
273	1.1	0	22500	0.1	42.8	1,562,282.1	(83,819,570.6)	0.85%
274	1.1	0	22500	0.2	42.8	3,458,208.7	25,663,905.1	6.00%
275	1.1	0	22500	0.3	42.8	4,230,249.9	46,203,304.4	6.64%

276	1.1	0	22500	0.4	42.8	4,241,682.3	8,361,661.3	5.29%
277	1.1	0	22500	0.5	42.7	4,239,973.4	(30,829,121.7)	3.97%
278	1.1	0	22500	0.6	42.6	4,245,968.6	(69,771,660.4)	2.71%
279	1.1	0	22500	0.7	42.5	4,257,589.6	(109,118,269.2)	1.50%
280	1.1	4	0	0.1	52.9	931,108.9	(97,430,731.8)	-0.79%
281	1.1	4	0	0.2	52.8	2,228,606.9	(18,208,165.8)	4.15%
282	1.1	4	0	0.3	52.8	3,261,376.0	35,376,030.3	6.44%
283	1.1	4	0	0.4	52.8	3,458,371.9	26,043,383.6	6.02%
284	1.1	4	0	0.5	52.7	3,473,842.0	1,859,595.1	5.07%
285	1.1	4	0	0.6	52.6	3,471,989.6	(24,010,223.3)	4.09%
286	1.1	4	0	0.7	52.5	3,484,058.8	(49,219,206.7)	3.15%
287	1.1	4	4500	0.1	49.2	1,072,152.4	(96,080,028.3)	-0.52%
288	1.1	4	4500	0.2	49.2	2,523,944.9	(8,337,451.5)	4.63%
289	1.1	4	4500	0.3	49.2	3,693,578.0	52,666,257.7	7.04%
290	1.1	4	4500	0.4	49.2	3,707,031.7	25,836,052.5	5.98%
291	1.1	4	4500	0.5	49.2	3,713,067.5	(2,166,715.7)	4.92%
292	1.1	4	4500	0.6	49.1	3,711,431.7	(30,955,599.6)	3.86%
293	1.1	4	4500	0.7	49.0	3,720,729.2	(59,296,564.6)	2.86%
294	1.1	4	9000	0.1	45.7	1,230,714.0	(95,362,669.5)	-0.28%
295	1.1	4	9000	0.2	45.7	2,852,098.3	1,436,014.7	5.06%
296	1.1	4	9000	0.3	45.7	3,950,723.4	53,557,639.9	7.01%
297	1.1	4	9000	0.4	45.7	3,961,129.0	22,688,796.5	5.83%
298	1.1	4	9000	0.5	45.7	3,961,591.2	(9,281,593.6)	4.67%
299	1.1	4	9000	0.6	45.6	3,957,732.2	(41,833,831.1)	3.52%
300	1.1	4	9000	0.7	45.6	3,966,050.6	(73,702,822.5)	2.44%
301	1.1	4	13500	0.1	42.7	1,390,844.9	(94,844,934.0)	-0.08%
302	1.1	4	13500	0.2	42.7	3,180,251.7	10,897,319.4	5.45%
303	1.1	4	13500	0.3	42.7	4,201,721.8	53,489,439.3	6.94%
304	1.1	4	13500	0.4	42.7	4,209,470.6	18,764,794.0	5.66%
305	1.1	4	13500	0.5	42.6	4,210,642.8	(16,852,683.0)	4.42%
306	1.1	4	13500	0.6	42.6	4,207,585.4	(52,853,592.5)	3.20%
307	1.1	4	13500	0.7	42.5	4,213,458.8	(88,761,927.1)	2.04%
308	1.1	4	18000	0.1	40.0	1,552,251.5	(94,235,264.8)	0.12%
309	1.1	4	18000	0.2	40.0	3,508,405.0	20,336,770.2	5.80%
310	1.1	4	18000	0.3	40.0	4,451,824.4	53,404,399.3	6.88%
311	1.1	4	18000	0.4	40.0	4,461,495.7	15,130,369.0	5.52%
312	1.1	4	18000	0.5	40.0	4,459,365.6	(24,335,435.7)	4.18%
313	1.1	4	18000	0.6	39.9	4,456,680.1	(64,025,406.5)	2.90%
314	1.1	4	18000	0.7	39.9	4,463,084.9	(103,526,556.2)	1.67%
315	1.1	4	22500	0.1	37.7	1,714,709.3	(93,655,591.9)	0.29%
316	1.1	4	22500	0.2	37.7	3,836,558.4	29,665,490.8	6.12%
317	1.1	4	22500	0.3	37.7	4,700,708.0	53,134,667.6	6.82%
318	1.1	4	22500	0.4	37.7	4,711,951.3	11,263,718.6	5.37%

319	1.1	4	22500	0.5	37.6	4,707,525.3	(31,976,716.0)	3.96%
320	1.1	4	22500	0.6	37.6	4,706,809.5	(75,252,902.6)	2.62%
321	1.1	4	22500	0.7	37.5	4,711,516.7	(118,636,554.3)	1.32%
322	1.1	8	0	0.1	45.2	1,086,514.3	(104,174,228.2)	-1.07%
323	1.1	8	0	0.2	45.2	2,601,324.3	(11,968,306.5)	4.47%
324	1.1	8	0	0.3	45.2	3,806,744.4	50,738,137.2	6.94%
325	1.1	8	0	0.4	45.2	3,933,739.9	31,745,220.1	6.18%
326	1.1	8	0	0.5	45.1	3,942,451.5	3,012,895.3	5.11%
327	1.1	8	0	0.6	45.1	3,946,629.2	(26,444,486.5)	4.05%
328	1.1	8	0	0.7	45.0	3,951,513.8	(56,170,614.7)	3.02%
329	1.1	8	4500	0.1	42.6	1,227,404.7	(102,364,623.1)	-0.76%
330	1.1	8	4500	0.2	42.5	2,896,662.3	(1,780,982.0)	4.92%
331	1.1	8	4500	0.3	42.5	4,175,324.5	63,480,280.6	7.33%
332	1.1	8	4500	0.4	42.5	4,181,906.9	31,958,996.1	6.15%
333	1.1	8	4500	0.5	42.5	4,187,776.0	(77,417.3)	5.00%
334	1.1	8	4500	0.6	42.5	4,183,929.9	(33,105,403.7)	3.86%
335	1.1	8	4500	0.7	42.4	4,189,162.2	(65,810,836.4)	2.76%
336	1.1	8	9000	0.1	39.9	1,385,581.7	(101,848,142.7)	-0.53%
337	1.1	8	9000	0.2	39.9	3,224,815.7	7,928,862.4	5.32%
338	1.1	8	9000	0.3	39.9	4,423,269.5	63,565,672.3	7.26%
339	1.1	8	9000	0.4	39.9	4,432,611.2	28,389,666.6	5.99%
340	1.1	8	9000	0.5	39.9	4,434,434.7	(7,602,122.1)	4.74%
341	1.1	8	9000	0.6	39.8	4,430,016.8	(44,224,541.9)	3.53%
342	1.1	8	9000	0.7	39.8	4,433,979.3	(80,534,867.3)	2.36%
343	1.1	8	13500	0.1	37.6	1,545,185.1	(101,412,985.7)	-0.32%
344	1.1	8	13500	0.2	37.6	3,552,969.1	17,356,321.9	5.68%
345	1.1	8	13500	0.3	37.6	4,675,319.7	63,541,560.5	7.20%
346	1.1	8	13500	0.4	37.6	4,683,800.6	24,647,830.0	5.83%
347	1.1	8	13500	0.5	37.5	4,683,594.0	(14,998,153.5)	4.51%
348	1.1	8	13500	0.6	37.5	4,677,885.1	(55,219,621.6)	3.22%
349	1.1	8	13500	0.7	37.5	4,581,822.2	(103,014,479.4)	1.72%
350	1.1	8	18000	0.1	35.5	1,705,978.5	(101,096,642.6)	-0.14%
351	1.1	8	18000	0.2	35.5	3,881,122.4	26,582,780.4	6.00%
352	1.1	8	18000	0.3	35.5	4,925,348.8	63,219,192.4	7.12%
353	1.1	8	18000	0.4	35.5	4,935,919.9	20,853,033.8	5.68%
354	1.1	8	18000	0.5	35.5	4,929,911.4	(22,571,552.4)	4.28%
355	1.1	8	18000	0.6	35.4	4,927,976.8	(66,274,077.3)	2.94%
356	1.1	8	18000	0.7	35.4	4,932,413.9	(109,799,813.5)	1.66%
357	1.1	8	22500	0.1	33.6	1,867,774.7	(100,372,680.2)	0.05%
358	1.1	8	22500	0.2	33.6	4,209,208.6	36,102,104.6	6.31%
359	1.1	8	22500	0.3	33.6	5,175,186.9	63,321,102.4	7.07%
360	1.1	8	22500	0.4	33.6	5,184,435.6	17,075,128.6	5.54%
361	1.1	8	22500	0.5	33.6	5,179,236.9	(30,281,369.4)	4.07%

362	1.1	8	22500	0.6	33.6	4,820,285.9	(105,080,224.7)	1.74%
363	1.1	8	22500	0.7	33.5	5,180,321.0	(125,127,251.7)	1.32%
364	1.1	12	0	0.1	39.5	1,241,920.1	(109,351,692.7)	-1.03%
365	1.1	12	0	0.2	39.5	2,974,041.7	(4,084,578.4)	4.83%
366	1.1	12	0	0.3	39.5	4,351,060.3	67,499,541.8	7.40%
367	1.1	12	0	0.4	39.5	4,394,050.9	37,921,667.5	6.32%
368	1.1	12	0	0.5	39.5	4,134,184.0	(15,442,756.7)	4.46%
369	1.1	12	0	0.6	39.4	4,407,981.8	(28,206,641.9)	4.06%
370	1.1	12	0	0.7	39.3	4,413,244.7	(62,112,565.0)	2.96%
371	1.1	12	4500	0.1	37.5	1,382,693.9	(107,402,901.0)	-0.74%
372	1.1	12	4500	0.2	37.5	3,269,379.7	6,267,955.2	5.25%
373	1.1	12	4500	0.3	37.4	4,638,140.9	74,271,193.9	7.57%
374	1.1	12	4500	0.4	37.4	4,641,196.1	38,159,458.9	6.29%
375	1.1	12	4500	0.5	37.4	4,648,202.7	2,040,034.9	5.07%
376	1.1	12	4500	0.6	37.4	4,646,691.5	(34,896,255.8)	3.87%
377	1.1	12	4500	0.7	37.3	4,649,374.0	(71,881,378.7)	2.72%
378	1.1	12	9000	0.1	35.4	1,540,571.0	(106,818,032.0)	-0.53%
379	1.1	12	9000	0.2	35.4	3,597,533.1	15,694,327.5	5.60%
380	1.1	12	9000	0.3	35.4	4,887,643.2	74,165,240.1	7.49%
381	1.1	12	9000	0.4	35.4	4,894,482.8	34,720,028.3	6.14%
382	1.1	12	9000	0.5	35.4	4,897,456.5	(5,273,787.2)	4.83%
383	1.1	12	9000	0.6	35.3	4,893,856.5	(45,973,118.0)	3.56%
384	1.1	12	9000	0.7	35.3	4,895,458.7	(86,380,426.0)	2.35%
385	1.1	12	13500	0.1	33.6	1,699,753.4	(106,703,188.4)	-0.35%
386	1.1	12	13500	0.2	33.6	3,925,686.4	25,104,770.1	5.93%
387	1.1	12	13500	0.3	33.5	5,138,363.3	74,046,155.0	7.42%
388	1.1	12	13500	0.4	33.5	5,147,484.9	31,137,180.8	5.99%
389	1.1	12	13500	0.5	33.5	5,143,547.3	(13,033,552.2)	4.60%
390	1.1	12	13500	0.6	33.5	5,142,066.8	(57,123,101.5)	3.27%
391	1.1	12	13500	0.7	33.5	5,143,172.9	(101,273,796.2)	2.00%
392	1.1	12	18000	0.1	31.9	1,860,046.8	(106,290,643.1)	-0.18%
393	1.1	12	18000	0.2	31.9	4,253,790.2	34,461,173.9	6.23%
394	1.1	12	18000	0.3	31.9	5,388,740.9	73,893,850.9	7.35%
395	1.1	12	18000	0.4	31.9	5,394,254.5	26,991,911.6	5.83%
396	1.1	12	18000	0.5	31.9	5,390,699.4	(20,717,819.7)	4.38%
397	1.1	12	18000	0.6	31.8	5,388,486.6	(68,634,099.0)	2.99%
398	1.1	12	18000	0.7	31.8	5,392,799.7	(116,342,031.9)	1.67%
399	1.1	12	22500	0.1	30.4	2,021,293.3	(105,672,242.8)	0.00%
400	1.1	12	22500	0.2	30.4	4,581,623.6	43,907,790.5	6.52%
401	1.1	12	22500	0.3	30.4	5,639,970.4	73,849,167.8	7.29%
402	1.1	12	22500	0.4	30.4	5,644,238.6	23,156,484.0	5.70%
403	1.1	12	22500	0.5	30.4	5,643,295.5	(27,940,447.1)	4.19%
404	1.1	12	22500	0.6	30.3	5,637,552.2	(79,716,570.1)	2.74%

405	1.1	12	22500	0.7	30.3	5,642,408.6	(131,217,902.1)	1.36%
406	1.1	16	0	0.1	35.1	1,397,326.2	(115,064,253.2)	-1.04%
407	1.1	16	0	0.2	35.1	3,346,759.1	3,159,261.3	5.12%
408	1.1	16	0	0.3	35.1	4,847,659.8	80,123,458.1	7.69%
409	1.1	16	0	0.4	35.1	4,844,929.0	42,779,714.6	6.40%
410	1.1	16	0	0.5	35.0	4,850,998.7	5,481,301.3	5.18%
411	1.1	16	0	0.6	35.0	4,855,530.7	(31,831,774.7)	4.00%
412	1.1	16	0	0.7	34.9	4,864,241.9	(69,658,260.2)	2.86%
413	1.1	16	4500	0.1	33.5	1,538,008.3	(112,757,206.7)	-0.76%
414	1.1	16	4500	0.2	33.5	3,642,097.1	13,814,651.9	5.52%
415	1.1	16	4500	0.3	33.5	5,092,206.1	83,915,368.0	7.75%
416	1.1	16	4500	0.4	33.5	5,092,172.6	43,520,076.0	6.39%
417	1.1	16	4500	0.5	33.4	5,096,813.2	2,956,435.9	5.09%
418	1.1	16	4500	0.6	33.4	5,097,279.4	(37,696,562.0)	3.85%
419	1.1	16	4500	0.7	33.4	5,103,669.3	(78,504,623.7)	2.66%
420	1.1	16	9000	0.1	31.8	1,695,645.0	(112,480,466.8)	-0.58%
421	1.1	16	9000	0.2	31.8	3,970,250.5	23,279,231.1	5.85%
422	1.1	16	9000	0.3	31.8	5,341,204.7	83,766,538.2	7.67%
423	1.1	16	9000	0.4	31.8	5,346,988.9	40,205,577.5	6.24%
424	1.1	16	9000	0.5	31.8	5,344,045.4	(4,453,110.9)	4.87%
425	1.1	16	9000	0.6	31.8	5,350,617.7	(48,510,885.0)	3.57%
426	1.1	16	9000	0.7	31.7	5,348,587.4	(93,327,079.5)	2.31%
427	1.1	16	13500	0.1	30.3	1,854,483.7	(112,269,936.5)	-0.41%
428	1.1	16	13500	0.2	30.3	4,298,296.6	32,569,421.2	6.15%
429	1.1	16	13500	0.3	30.3	5,591,491.5	83,661,166.0	7.60%
430	1.1	16	13500	0.4	30.3	5,595,786.2	36,088,129.1	6.09%
431	1.1	16	13500	0.5	30.3	5,590,477.7	(12,142,591.3)	4.64%
432	1.1	16	13500	0.6	30.3	5,596,053.1	(59,909,302.9)	3.29%
433	1.1	16	13500	0.7	30.2	5,594,711.1	(108,548,171.4)	1.97%
434	1.1	16	18000	0.1	29.0	2,014,361.9	(111,883,394.7)	-0.24%
435	1.1	16	18000	0.2	28.9	4,625,966.1	41,899,660.7	6.43%
436	1.1	16	18000	0.3	28.9	5,842,370.4	83,390,635.1	7.53%
437	1.1	16	18000	0.4	28.9	5,845,241.2	32,050,241.5	5.94%
438	1.1	16	18000	0.5	28.9	5,842,959.6	(19,808,886.9)	4.44%
439	1.1	16	18000	0.6	28.9	5,842,470.7	(71,604,815.8)	3.01%
440	1.1	16	18000	0.7	28.9	5,845,590.2	(123,435,651.5)	1.66%
441	1.1	16	22500	0.1	27.7	2,175,145.0	(111,899,882.7)	-0.11%
442	1.1	16	22500	0.2	27.7	4,953,589.2	50,777,036.0	6.68%
443	1.1	16	22500	0.3	27.7	6,090,397.8	82,457,625.6	7.44%
444	1.1	16	22500	0.4	27.7	6,092,882.3	27,438,885.1	5.78%
445	1.1	16	22500	0.5	27.7	6,092,958.6	(27,990,554.7)	4.22%
446	1.1	16	22500	0.6	27.7	6,091,811.1	(83,014,667.4)	2.76%
447	1.1	16	22500	0.7	27.6	6,091,738.9	(139,747,997.6)	1.33%

448	1.2	0	0	0.1	69.0	775,704.2	(67,862,880.6)	1.30%
449	1.2	0	0	0.2	68.8	1,855,889.5	(5,094,001.0)	4.76%
450	1.2	0	0	0.3	68.6	2,561,736.1	26,384,823.8	6.12%
451	1.2	0	0	0.4	68.5	2,571,029.3	5,984,649.8	5.25%
452	1.2	0	0	0.5	68.1	2,601,229.5	(15,550,030.5)	4.36%
453	1.2	0	0	0.6	67.6	2,638,139.2	(37,438,922.6)	3.48%
454	1.2	0	0	0.7	67.1	2,683,858.8	(59,691,023.0)	2.61%
455	1.2	0	4500	0.1	63.5	916,957.6	(66,379,587.1)	1.48%
456	1.2	0	4500	0.2	63.3	2,151,227.6	4,925,755.1	5.22%
457	1.2	0	4500	0.3	63.2	2,790,327.2	29,060,641.2	6.19%
458	1.2	0	4500	0.4	63.1	2,805,367.8	5,434,228.6	5.22%
459	1.2	0	4500	0.5	62.8	2,821,436.7	(19,708,589.7)	4.22%
460	1.2	0	4500	0.6	62.5	2,851,012.3	(44,548,825.5)	3.26%
461	1.2	0	4500	0.7	62.1	2,886,567.1	(69,778,448.2)	2.32%
462	1.2	0	9000	0.1	58.2	1,076,030.2	(65,302,655.9)	1.63%
463	1.2	0	9000	0.2	58.1	2,479,380.9	15,147,801.4	5.64%
464	1.2	0	9000	0.3	58.0	3,032,329.1	29,331,097.6	6.16%
465	1.2	0	9000	0.4	57.9	3,048,932.7	2,091,521.1	5.08%
466	1.2	0	9000	0.5	57.7	3,059,909.2	(26,759,334.3)	3.98%
467	1.2	0	9000	0.6	57.5	3,085,586.5	(55,145,045.4)	2.94%
468	1.2	0	9000	0.7	57.1	3,115,970.8	(83,982,618.1)	1.91%
469	1.2	0	13500	0.1	53.8	1,236,840.1	(64,588,366.8)	1.75%
470	1.2	0	13500	0.2	53.6	2,807,534.3	24,816,528.5	6.02%
471	1.2	0	13500	0.3	53.6	3,276,497.4	29,544,133.7	6.13%
472	1.2	0	13500	0.4	53.5	3,294,851.2	(1,543,182.7)	4.94%
473	1.2	0	13500	0.5	53.3	3,305,488.1	(33,924,308.3)	3.75%
474	1.2	0	13500	0.6	53.1	3,328,459.8	(65,978,559.8)	2.62%
475	1.2	0	13500	0.7	52.8	3,357,273.8	(98,566,360.5)	1.51%
476	1.2	0	18000	0.1	49.9	1,399,015.1	(63,961,778.5)	1.86%
477	1.2	0	18000	0.2	49.8	3,135,687.6	34,177,818.5	6.35%
478	1.2	0	18000	0.3	49.8	3,523,819.3	29,319,360.7	6.09%
479	1.2	0	18000	0.4	49.7	3,542,630.4	(5,434,307.2)	4.80%
480	1.2	0	18000	0.5	49.5	3,553,172.4	(41,570,220.6)	3.53%
481	1.2	0	18000	0.6	49.3	3,574,851.5	(77,401,243.8)	2.31%
482	1.2	0	18000	0.7	49.1	3,600,203.1	(114,062,861.9)	1.11%
483	1.2	0	22500	0.1	46.6	1,562,282.1	(63,913,709.4)	1.94%
484	1.2	0	22500	0.2	46.4	3,458,208.7	42,449,168.1	6.62%
485	1.2	0	22500	0.3	46.5	3,774,036.7	28,579,455.6	6.03%
486	1.2	0	22500	0.4	46.4	3,791,926.2	(9,914,789.4)	4.65%
487	1.2	0	22500	0.5	46.2	3,803,200.9	(49,401,969.8)	3.31%
488	1.2	0	22500	0.6	46.0	3,824,557.3	(88,891,059.8)	2.02%
489	1.2	0	22500	0.7	45.8	3,850,107.0	(129,381,506.8)	0.76%
490	1.2	4	0	0.1	57.5	931,108.9	(77,777,209.3)	0.59%

491	1.2	4	0	0.2	57.4	2,228,606.9	(1,793,017.8)	4.92%
492	1.2	4	0	0.3	57.3	3,007,258.7	32,166,901.3	6.32%
493	1.2	4	0	0.4	57.2	3,017,714.6	7,814,768.9	5.32%
494	1.2	4	0	0.5	57.0	3,040,808.3	(17,230,994.9)	4.32%
495	1.2	4	0	0.6	56.8	3,057,030.5	(43,404,573.7)	3.30%
496	1.2	4	0	0.7	56.5	3,087,287.7	(69,310,976.5)	2.31%
497	1.2	4	4500	0.1	53.6	1,072,152.4	(75,616,788.9)	0.85%
498	1.2	4	4500	0.2	53.5	2,523,944.9	8,861,341.6	5.39%
499	1.2	4	4500	0.3	53.5	3,244,666.2	35,451,764.5	6.41%
500	1.2	4	4500	0.4	53.4	3,256,235.1	7,913,306.8	5.31%
501	1.2	4	4500	0.5	53.3	3,264,047.4	(21,110,332.7)	4.19%
502	1.2	4	4500	0.6	53.1	3,280,975.6	(49,833,114.9)	3.12%
503	1.2	4	4500	0.7	52.9	3,305,620.1	(78,804,173.0)	2.07%
504	1.2	4	9000	0.1	49.8	1,230,714.0	(74,723,649.1)	1.03%
505	1.2	4	9000	0.2	49.7	2,852,098.3	19,139,895.1	5.80%
506	1.2	4	9000	0.3	49.7	3,488,813.1	35,872,176.5	6.38%
507	1.2	4	9000	0.4	49.7	3,501,136.3	4,678,959.3	5.18%
508	1.2	4	9000	0.5	49.6	3,507,271.0	(27,976,533.1)	3.97%
509	1.2	4	9000	0.6	49.4	3,520,607.4	(60,395,953.1)	2.81%
510	1.2	4	9000	0.7	49.2	3,541,017.3	(93,130,851.5)	1.68%
511	1.2	4	13500	0.1	46.5	1,390,844.9	(74,194,400.8)	1.18%
512	1.2	4	13500	0.2	46.4	3,180,251.7	28,670,380.0	6.15%
513	1.2	4	13500	0.3	46.4	3,734,893.0	35,734,270.1	6.33%
514	1.2	4	13500	0.4	46.4	3,749,649.0	665,550.2	5.02%
515	1.2	4	13500	0.5	46.3	3,378,590.6	(64,208,245.3)	2.63%
516	1.2	4	13500	0.6	46.1	3,764,120.2	(71,901,422.2)	2.49%
517	1.2	4	13500	0.7	46.0	3,784,045.0	(108,264,959.9)	1.29%
518	1.2	4	18000	0.1	43.6	1,552,251.5	(73,627,247.1)	1.32%
519	1.2	4	18000	0.2	43.5	3,508,405.0	38,102,341.7	6.47%
520	1.2	4	18000	0.3	43.6	3,985,642.7	35,816,331.3	6.29%
521	1.2	4	18000	0.4	43.5	3,999,867.0	(2,886,464.7)	4.90%
522	1.2	4	18000	0.5	43.4	4,001,930.7	(42,926,368.2)	3.53%
523	1.2	4	18000	0.6	43.3	4,013,866.2	(82,655,036.5)	2.22%
524	1.2	4	18000	0.7	43.1	4,031,503.3	(123,120,943.7)	0.94%
525	1.2	4	22500	0.1	41.1	1,714,709.3	(73,112,646.4)	1.45%
526	1.2	4	22500	0.2	41.0	3,836,295.4	47,365,865.9	6.76%
527	1.2	4	22500	0.3	41.0	4,234,808.0	35,595,057.4	6.24%
528	1.2	4	22500	0.4	41.0	4,248,254.7	(6,763,638.4)	4.77%
529	1.2	4	22500	0.5	40.9	4,251,935.6	(50,306,742.7)	3.33%
530	1.2	4	22500	0.6	40.8	4,263,691.0	(93,695,984.0)	1.96%
531	1.2	4	22500	0.7	40.6	4,281,672.4	(137,943,974.8)	0.62%
532	1.2	8	0	0.1	49.3	1,086,514.3	(84,063,021.2)	0.33%
533	1.2	8	0	0.2	49.2	2,601,324.3	4,839,878.4	5.21%

534	1.2	8	0	0.3	49.1	3,475,009.2	42,171,953.7	6.63%
535	1.2	8	0	0.4	49.0	3,484,001.5	13,484,997.8	5.51%
536	1.2	8	0	0.5	48.9	3,502,667.0	(15,640,746.6)	4.42%
537	1.2	8	0	0.6	48.7	3,515,154.3	(45,937,986.4)	3.31%
538	1.2	8	0	0.7	48.5	3,538,528.4	(75,815,140.2)	2.24%
539	1.2	8	4500	0.1	46.4	1,227,404.7	(81,736,903.0)	0.61%
540	1.2	8	4500	0.2	46.3	2,896,662.3	15,763,686.7	5.65%
541	1.2	8	4500	0.3	46.3	3,714,323.7	45,621,030.6	6.71%
542	1.2	8	4500	0.4	46.2	3,722,863.5	13,838,860.7	5.51%
543	1.2	8	4500	0.5	46.1	3,736,074.9	(18,498,516.8)	4.33%
544	1.2	8	4500	0.6	46.0	3,742,828.0	(51,939,963.6)	3.16%
545	1.2	8	4500	0.7	45.8	3,762,177.6	(84,808,650.4)	2.03%
546	1.2	8	9000	0.1	43.5	1,385,581.7	(80,954,540.6)	0.79%
547	1.2	8	9000	0.2	43.4	3,224,815.7	25,897,749.2	6.03%
548	1.2	8	9000	0.3	43.4	3,957,145.4	45,740,403.1	6.66%
549	1.2	8	9000	0.4	43.4	3,970,353.4	10,592,678.8	5.38%
550	1.2	8	9000	0.5	43.3	3,976,608.8	(25,907,452.8)	4.10%
551	1.2	8	9000	0.6	43.2	3,981,761.2	(62,829,941.0)	2.85%
552	1.2	8	9000	0.7	43.1	3,998,402.1	(99,562,092.9)	1.65%
553	1.2	8	13500	0.1	41.0	1,545,185.1	(80,509,819.2)	0.94%
554	1.2	8	13500	0.2	40.9	3,552,969.1	35,489,031.3	6.36%
555	1.2	8	13500	0.3	40.9	4,206,118.1	45,895,632.3	6.62%
556	1.2	8	13500	0.4	40.9	4,221,772.6	7,014,102.0	5.24%
557	1.2	8	13500	0.5	40.8	4,223,067.1	(33,425,864.9)	3.88%
558	1.2	8	13500	0.6	40.7	4,227,651.0	(73,934,581.4)	2.56%
559	1.2	8	13500	0.7	40.6	4,242,442.4	(114,559,043.6)	1.29%
560	1.2	8	18000	0.1	38.7	1,705,978.5	(80,226,116.3)	1.07%
561	1.2	8	18000	0.2	38.6	3,880,859.3	44,938,570.3	6.66%
562	1.2	8	18000	0.3	38.7	4,456,833.5	46,194,995.5	6.58%
563	1.2	8	18000	0.4	38.6	4,468,795.7	3,321,022.5	5.11%
564	1.2	8	18000	0.5	38.5	4,468,922.9	(40,758,453.5)	3.67%
565	1.2	8	18000	0.6	38.5	4,477,409.3	(84,532,652.2)	2.31%
566	1.2	8	18000	0.7	38.4	4,491,386.1	(128,998,045.7)	0.98%
567	1.2	8	22500	0.1	36.7	1,867,774.7	(79,452,024.6)	1.22%
568	1.2	8	22500	0.2	36.6	4,208,290.4	54,084,071.4	6.93%
569	1.2	8	22500	0.3	36.6	4,707,738.8	45,814,315.5	6.52%
570	1.2	8	22500	0.4	36.6	4,715,514.6	(1,108,920.7)	4.96%
571	1.2	8	22500	0.5	36.5	4,718,638.2	(48,539,367.2)	3.47%
572	1.2	8	22500	0.6	36.4	4,725,669.8	(96,083,156.7)	2.04%
573	1.2	8	22500	0.7	36.3	4,741,300.9	(144,621,418.7)	0.64%
574	1.2	12	0	0.1	43.1	1,241,920.1	(88,821,531.4)	0.32%
575	1.2	12	0	0.2	43.0	2,974,041.7	13,077,525.5	5.53%
576	1.2	12	0	0.3	42.9	3,937,093.0	52,860,149.1	6.92%

577	1.2	12	0	0.4	42.9	3,943,614.7	19,837,993.8	5.70%
578	1.2	12	0	0.5	42.8	3,960,323.9	(13,399,900.1)	4.53%
579	1.2	12	0	0.6	42.6	3,975,744.3	(47,280,200.9)	3.38%
580	1.2	12	0	0.7	42.5	3,994,072.2	(81,315,617.0)	2.26%
581	1.2	12	4500	0.1	40.8	1,382,693.9	(86,433,942.2)	0.58%
582	1.2	12	4500	0.2	40.8	3,269,379.7	24,124,601.9	5.94%
583	1.2	12	4500	0.3	40.7	4,174,504.9	56,269,218.8	6.98%
584	1.2	12	4500	0.4	40.7	4,180,469.8	20,048,106.4	5.69%
585	1.2	12	4500	0.5	40.6	4,191,488.1	(16,440,249.4)	4.45%
586	1.2	12	4500	0.6	40.5	4,200,247.4	(53,552,891.0)	3.23%
587	1.2	12	4500	0.7	40.4	4,211,958.8	(91,590,259.4)	2.01%
588	1.2	12	9000	0.1	38.6	1,540,571.0	(85,691,531.0)	0.74%
589	1.2	12	9000	0.2	38.5	3,597,533.1	33,869,229.7	6.27%
590	1.2	12	9000	0.3	38.5	4,420,692.3	56,681,999.8	6.94%
591	1.2	12	9000	0.4	38.5	4,430,583.9	17,132,574.9	5.57%
592	1.2	12	9000	0.5	38.4	4,436,095.7	(23,447,528.3)	4.24%
593	1.2	12	9000	0.6	38.3	4,442,087.2	(64,342,311.5)	2.94%
594	1.2	12	9000	0.7	38.2	3,771,171.1	(159,947,977.2)	-0.36%
595	1.2	12	13500	0.1	36.6	1,699,753.4	(85,591,268.7)	0.87%
596	1.2	12	13500	0.2	36.5	3,925,280.0	43,295,835.5	6.57%
597	1.2	12	13500	0.3	36.5	4,669,006.4	56,679,108.4	6.89%
598	1.2	12	13500	0.4	36.5	4,679,340.0	13,273,509.9	5.43%
599	1.2	12	13500	0.5	36.4	4,682,425.5	(30,964,995.0)	4.02%
600	1.2	12	13500	0.6	36.4	4,688,752.2	(75,312,024.9)	2.67%
601	1.2	12	13500	0.7	36.3	4,702,806.6	(119,757,600.1)	1.37%
602	1.2	12	18000	0.1	34.8	1,860,046.8	(85,177,327.2)	1.00%
603	1.2	12	18000	0.2	34.7	4,252,831.5	52,583,693.7	6.85%
604	1.2	12	18000	0.3	34.7	4,919,368.5	56,438,479.6	6.83%
605	1.2	12	18000	0.4	34.7	4,928,110.4	9,286,700.3	5.29%
606	1.2	12	18000	0.5	34.6	4,928,793.8	(38,803,347.1)	3.81%
607	1.2	12	18000	0.6	34.6	4,936,974.1	(86,782,013.4)	2.40%
608	1.2	12	18000	0.7	34.5	4,948,853.8	(135,410,341.4)	1.04%
609	1.2	12	22500	0.1	33.1	2,021,293.3	(84,600,956.3)	1.13%
610	1.2	12	22500	0.2	33.1	4,580,337.7	61,954,769.7	7.11%
611	1.2	12	22500	0.3	33.1	5,169,658.4	56,206,848.6	6.77%
612	1.2	12	22500	0.4	33.0	5,176,166.6	5,114,968.2	5.16%
613	1.2	12	22500	0.5	33.0	5,179,019.2	(46,764,680.0)	3.61%
614	1.2	12	22500	0.6	32.9	5,185,374.9	(97,837,100.5)	2.16%
615	1.2	12	22500	0.7	32.8	5,200,273.0	(150,245,907.5)	0.75%
616	1.2	16	0	0.1	38.2	1,397,326.2	(94,334,718.1)	0.26%
617	1.2	16	0	0.2	38.2	3,346,759.1	20,556,339.6	5.79%
618	1.2	16	0	0.3	38.1	4,391,213.7	62,179,690.8	7.12%
619	1.2	16	0	0.4	38.1	4,390,950.1	24,506,381.5	5.82%

620	1.2	16	0	0.5	38.0	4,402,405.0	(13,308,034.6)	4.56%
621	1.2	16	0	0.6	37.8	4,420,405.4	(51,267,663.5)	3.35%
622	1.2	16	0	0.7	37.7	4,441,887.5	(89,240,904.7)	2.18%
623	1.2	16	4500	0.1	36.5	1,538,008.3	(91,591,166.4)	0.51%
624	1.2	16	4500	0.2	36.4	3,641,867.8	31,851,812.9	6.18%
625	1.2	16	4500	0.3	36.4	4,629,873.9	66,323,479.1	7.21%
626	1.2	16	4500	0.4	36.4	4,633,894.3	25,957,526.5	5.84%
627	1.2	16	4500	0.5	36.3	4,640,591.0	(15,066,724.3)	4.52%
628	1.2	16	4500	0.6	36.2	4,654,660.6	(56,005,744.1)	3.26%
629	1.2	16	4500	0.7	36.1	4,668,195.4	(97,231,817.4)	2.03%
630	1.2	16	9000	0.1	34.7	1,695,645.0	(91,170,934.8)	0.65%
631	1.2	16	9000	0.2	34.6	3,969,561.4	41,503,311.1	6.48%
632	1.2	16	9000	0.3	34.6	4,874,058.4	66,495,300.7	7.16%
633	1.2	16	9000	0.4	34.6	924,705.1	(307,814,219.5)	-14.93%
634	1.2	16	9000	0.5	34.5	4,883,250.4	(22,375,860.1)	4.31%
635	1.2	16	9000	0.6	34.5	4,895,737.1	(66,730,735.5)	2.99%
636	1.2	16	9000	0.7	34.4	4,908,271.1	(111,722,143.3)	1.71%
637	1.2	16	13500	0.1	33.1	1,854,483.7	(90,940,197.2)	0.78%
638	1.2	16	13500	0.2	33.0	4,297,214.6	50,808,117.6	6.76%
639	1.2	16	13500	0.3	33.0	5,121,488.8	66,098,358.6	7.09%
640	1.2	16	13500	0.4	33.0	5,126,852.6	18,168,037.9	5.56%
641	1.2	16	13500	0.5	32.9	5,135,263.7	(29,470,146.5)	4.12%
642	1.2	16	13500	0.6	32.9	5,142,194.8	(78,019,551.6)	2.73%
643	1.2	16	13500	0.7	32.8	5,153,314.4	(126,918,058.7)	1.38%
644	1.2	16	18000	0.1	31.6	2,014,361.9	(90,593,780.6)	0.90%
645	1.2	16	18000	0.2	31.5	4,624,795.3	60,117,584.5	7.02%
646	1.2	16	18000	0.3	31.5	5,371,386.3	65,940,476.4	7.03%
647	1.2	16	18000	0.4	31.5	5,377,028.9	14,141,877.2	5.42%
648	1.2	16	18000	0.5	31.4	5,383,173.3	(37,363,714.3)	3.92%
649	1.2	16	18000	0.6	31.4	4,650,623.9	(147,811,521.9)	0.57%
650	1.2	16	18000	0.7	31.3	5,401,039.8	(142,219,024.3)	1.07%
651	1.2	16	22500	0.1	30.2	2,175,145.0	(90,657,655.1)	1.00%
652	1.2	16	22500	0.2	30.1	4,952,202.8	68,936,877.5	7.24%
653	1.2	16	22500	0.3	30.1	5,621,331.7	65,089,348.1	6.95%
654	1.2	16	22500	0.4	30.1	5,621,437.1	9,102,823.3	5.26%
655	1.2	16	22500	0.5	30.1	5,631,301.6	(45,471,868.6)	3.72%
656	1.2	16	22500	0.6	30.0	5,636,284.3	(101,623,457.1)	2.21%
657	1.2	16	22500	0.7	29.9	5,639,840.2	(159,234,519.8)	0.73%

Table 21: Full results from UO subsidized case.

Scenario	Peak Load:SMR	WTG Number	PV Nameplate (kW)	PEM Ratio	HES CF (%)	H2 Production (kg)	NPV ($)	Irr (%)
1	1	0	0	0.1	56.5	793430.0	-111435489.7	-1.72%
2	1	0	0	0.2	56.4	1898298.8	-40528186.7	3.01%
3	1	0	0	0.3	56.4	2777998.2	6776442.6	5.29%
4	1	0	0	0.4	56.4	3699630.2	56404275.5	7.21%
5	1	0	0	0.5	56.4	3778448.5	42019514.3	6.61%
6	1	0	0	0.6	56.4	3765067.0	20185618.6	5.76%
7	1	0	0	0.7	56.4	3767883.7	-499453.4	4.98%
8	1	0	4500	0.1	51.8	937911.2	-110876030.1	-1.48%
9	1	0	4500	0.2	51.8	2200385.6	-31065911.8	3.55%
10	1	0	4500	0.3	51.8	3220076.5	23223635.4	5.95%
11	1	0	4500	0.4	51.8	3966037.9	56373593.7	7.13%
12	1	0	4500	0.5	51.8	3960508.1	31994185.9	6.19%
13	1	0	4500	0.6	51.8	3960776.8	25403419.0	5.94%
14	1	0	4500	0.7	51.8	3962313.9	-15921408.0	4.43%
15	1	0	9000	0.1	47.5	1100618.7	-109807325.0	-1.20%
16	1	0	9000	0.2	47.5	2536037.6	-20731905.8	4.07%
17	1	0	9000	0.3	47.5	3708589.2	41368523.4	6.61%
18	1	0	9000	0.4	47.5	4172766.1	49334113.6	6.81%
19	1	0	9000	0.5	47.5	4158140.0	20633405.1	5.74%
20	1	0	9000	0.6	47.5	4158155.7	-6983610.8	4.75%
21	1	0	9000	0.7	47.5	4158997.3	-34575650.8	3.80%
22	1	0	13500	0.1	43.9	1265103.4	-108644716.6	-0.93%
23	1	0	13500	0.2	43.9	2871689.7	-10582493.7	4.55%
24	1	0	13500	0.3	43.9	4188127.9	58837461.1	7.17%
25	1	0	13500	0.4	43.9	4372956.9	41807716.6	6.49%
26	1	0	13500	0.5	43.9	4355837.5	9278211.5	5.32%
27	1	0	13500	0.6	43.8	4355728.9	-21984028.9	4.25%
28	1	0	13500	0.7	43.8	4356606.1	-53202009.9	3.22%
29	1	0	18000	0.1	40.7	1430984.2	-107478573.4	-0.68%
30	1	0	18000	0.2	40.7	3207341.7	-518034.0	4.98%
31	1	0	18000	0.3	40.7	4556575.7	67756939.4	7.41%
32	1	0	18000	0.4	40.7	4569854.2	33972645.5	6.17%
33	1	0	18000	0.5	40.7	4554466.1	-2062995.5	4.93%
34	1	0	18000	0.6	40.7	4553040.4	-37065477.3	3.78%
35	1	0	18000	0.7	40.7	4554416.7	-71882532.2	2.68%
36	1	0	22500	0.1	38.0	1597982.1	-106292879.7	-0.45%
37	1	0	22500	0.2	38.0	3537232.8	9044461.8	5.36%
38	1	0	22500	0.3	38.0	4760298.4	64025289.7	7.21%

39	1	0	22500	0.4	38.0	4762108.5	25725627.8	5.86%
40	1	0	22500	0.5	38.0	4752189.2	-13538836.0	4.56%
41	1	0	22500	0.6	38.0	4750933.7	-52174171.2	3.33%
42	1	0	22500	0.7	38.0	4752064.3	-90646546.9	2.16%
43	1.1	0	0	0.1	62.1	793430.0	-90307697.5	-0.16%
44	1.1	0	0	0.2	62.0	1898298.8	-21712607.5	3.97%
45	1.1	0	0	0.3	62.0	2777720.5	24731474.7	6.05%
46	1.1	0	0	0.4	62.0	3308069.5	44965686.6	6.78%
47	1.1	0	0	0.5	61.9	3313508.9	24398112.7	5.95%
48	1.1	0	0	0.6	61.9	3311296.7	3031190.7	5.12%
49	1.1	0	0	0.7	61.8	3318068.6	-17786477.9	4.33%
50	1.1	0	4500	0.1	57.0	937911.2	-89478400.3	0.03%
51	1.1	0	4500	0.2	57.0	2200385.6	-12121852.2	4.45%
52	1.1	0	4500	0.3	57.0	3215727.5	41357678.5	6.66%
53	1.1	0	4500	0.4	57.0	3507653.1	39946855.8	6.54%
54	1.1	0	4500	0.5	56.9	3498355.3	15084172.0	5.57%
55	1.1	0	4500	0.6	56.9	3501773.2	-8924759.6	4.67%
56	1.1	0	4500	0.7	56.8	3506368.3	-32971156.2	3.79%
57	1.1	0	9000	0.1	52.3	1100618.7	-88423015.7	0.24%
58	1.1	0	9000	0.2	52.2	2536037.6	-1789269.8	4.92%
59	1.1	0	9000	0.3	52.2	3685319.4	58312383.6	7.22%
60	1.1	0	9000	0.4	52.2	3704032.7	32288029.3	6.20%
61	1.1	0	9000	0.5	52.2	3694117.7	3794958.2	5.14%
62	1.1	0	9000	0.6	52.2	3696569.3	-23829250.2	4.14%
63	1.1	0	9000	0.7	52.1	3700401.3	-51460056.0	3.18%
64	1.1	0	13500	0.1	48.2	1265103.4	-87300494.2	0.44%
65	1.1	0	13500	0.2	48.2	2871689.7	8384183.3	5.35%
66	1.1	0	13500	0.3	48.2	3895855.3	55367603.9	7.05%
67	1.1	0	13500	0.4	48.2	3903292.1	24776969.7	5.90%
68	1.1	0	13500	0.5	48.2	3891166.8	-7492349.0	4.73%
69	1.1	0	13500	0.6	48.2	3893470.6	-38741622.0	3.65%
70	1.1	0	13500	0.7	48.2	3896329.1	-70041313.9	2.61%
71	1.1	0	18000	0.1	44.8	1430984.2	-86164673.9	0.63%
72	1.1	0	18000	0.2	44.8	3205946.0	18380386.6	5.73%
73	1.1	0	18000	0.3	44.8	4096102.2	51587664.5	6.86%
74	1.1	0	18000	0.4	44.8	4096312.5	16686525.8	5.59%
75	1.1	0	18000	0.5	44.8	4088885.5	-18837467.9	4.35%
76	1.1	0	18000	0.6	44.7	4090850.3	-53740951.4	3.19%
77	1.1	0	18000	0.7	44.7	4093543.3	-88764938.9	2.07%
78	1.1	0	22500	0.1	41.8	1597982.1	-85018822.6	0.81%
79	1.1	0	22500	0.2	41.8	3532346.7	27701673.6	6.07%
80	1.1	0	22500	0.3	41.8	4296172.7	47630631.4	6.67%
81	1.1	0	22500	0.4	41.8	4292063.5	8749999.2	5.30%

82	1.1	0	22500	0.5	41.8	4286283.6	-30280214.9	3.99%
83	1.1	0	22500	0.6	41.8	4287767.5	-68848961.6	2.76%
84	1.1	0	22500	0.7	41.7	4290155.4	-107758268.9	1.56%
85	1.2	0	0	0.1	67.6	793430.0	-70412254.6	1.14%
86	1.2	0	0	0.2	67.5	1898298.8	-4179465.1	4.81%
87	1.2	0	0	0.3	67.4	2770581.8	40972813.9	6.70%
88	1.2	0	0	0.4	67.4	2861083.8	27880400.3	6.13%
89	1.2	0	0	0.5	67.3	2860725.4	6400178.0	5.26%
90	1.2	0	0	0.6	67.2	2869911.8	-14502814.1	4.43%
91	1.2	0	0	0.7	67.1	2881373.8	-35457985.5	3.62%
92	1.2	0	4500	0.1	62.1	937911.2	-69135750.0	1.32%
93	1.2	0	4500	0.2	62.1	2200385.6	5725513.5	5.25%
94	1.2	0	4500	0.3	62.0	3041812.7	45845452.4	6.83%
95	1.2	0	4500	0.4	62.0	3047394.9	22464748.6	5.88%
96	1.2	0	4500	0.5	61.9	3046855.9	-2101220.8	4.92%
97	1.2	0	4500	0.6	61.9	3053922.9	-26211817.3	4.00%
98	1.2	0	4500	0.7	61.8	3062766.1	-50402336.3	3.11%
99	1.2	0	9000	0.1	57.0	1100618.7	-67814532.7	1.49%
100	1.2	0	9000	0.2	56.9	2534522.5	16320031.4	5.69%
101	1.2	0	9000	0.3	56.9	3236478.9	42503390.2	6.65%
102	1.2	0	9000	0.4	56.9	3239487.3	14858722.4	5.57%
103	1.2	0	9000	0.5	56.8	3238626.8	-13251508.6	4.51%
104	1.2	0	9000	0.6	56.8	3244363.4	-40991568.8	3.50%
105	1.2	0	9000	0.7	56.7	3251907.1	-68804537.3	2.52%
106	1.2	0	13500	0.1	52.6	1265103.4	-66700049.5	1.65%
107	1.2	0	13500	0.2	52.6	2866604.6	26466802.5	6.08%
108	1.2	0	13500	0.3	52.6	3436379.4	38893833.9	6.47%
109	1.2	0	13500	0.4	52.5	3436065.4	7339385.8	5.27%
110	1.2	0	13500	0.5	52.5	3434207.5	-24407723.9	4.12%
111	1.2	0	13500	0.6	52.4	3439176.0	-55743842.7	3.02%
112	1.2	0	13500	0.7	52.4	3445218.6	-87392184.4	1.96%
113	1.2	0	18000	0.1	48.8	1430984.2	-65604988.2	1.79%
114	1.2	0	18000	0.2	48.8	3197570.7	36280468.8	6.42%
115	1.2	0	18000	0.3	48.8	3634335.7	34855905.9	6.28%
116	1.2	0	18000	0.4	48.8	3631627.7	-443905.3	4.98%
117	1.2	0	18000	0.5	48.8	3630938.1	-35691568.2	3.75%
118	1.2	0	18000	0.6	48.7	3635130.2	-70702562.9	2.57%
119	1.2	0	18000	0.7	48.7	3640977.2	-106290935.7	1.42%
120	1.2	0	22500	0.1	45.6	1597982.1	-64523140.2	1.93%
121	1.2	0	22500	0.2	45.5	3511147.4	44661889.3	6.69%
122	1.2	0	22500	0.3	45.6	3831660.6	30757944.7	6.10%
123	1.2	0	22500	0.4	45.5	3829303.6	-8144226.4	4.72%
124	1.2	0	22500	0.5	45.5	3826886.6	-47164719.2	3.40%

125	1.2	0	22500	0.6	45.5	3830373.4	-85963266.4	2.14%
126	1.2	0	22500	0.7	45.4	3834901.4	-125578894.0	0.91%
127	0.95	0	15750	0.25	40.1	3706726.5	19374145.5	5.76%
128	0.95	0	15750	0.3	40.1	4437369.6	58728831.0	7.14%
129	0.95	0	15750	0.35	40.1	4698956.6	62226491.5	7.19%
130	0.95	0	18000	0.25	38.7	3911392.4	26301152.4	6.01%
131	0.95	0	18000	0.3	38.7	4668005.2	66729092.6	7.37%
132	0.95	0	18000	0.35	38.7	4802532.3	59600817.1	7.07%
133	0.95	0	20250	0.25	37.4	4113959.2	33017061.4	6.24%
134	0.95	0	20250	0.3	37.4	4887341.8	73814483.8	7.57%
135	0.95	0	20250	0.35	37.4	4900805.0	56522022.9	6.94%
136	0.95	0	15750	0.25	40.1	3706726.5	19374145.5	5.76%
137	0.95	0	15750	0.3	40.1	4437369.6	58728831.0	7.14%
138	0.95	0	15750	0.35	40.1	4698956.6	62226491.5	7.19%
139	0.95	0	18000	0.25	38.7	3911392.4	26301152.4	6.01%
140	0.95	0	18000	0.3	38.7	4668005.2	66729092.6	7.37%
141	0.95	0	18000	0.35	38.7	4802532.3	59600817.1	7.07%
142	0.95	0	20250	0.25	37.4	4113959.2	33017061.4	6.24%
143	0.95	0	20250	0.3	37.4	4887341.8	73814483.8	7.57%
144	0.95	0	20250	0.35	37.4	4900805.0	56522022.9	6.94%
145	0.95	1	15750	0.25	38.7	3823032.3	20586780.7	5.80%
146	0.95	1	15750	0.3	38.7	4567214.4	60458314.5	7.17%
147	0.95	1	15750	0.35	38.7	4706540.2	54089768.4	6.90%
148	0.95	1	18000	0.25	37.3	4026580.2	27437644.1	6.04%
149	0.95	1	18000	0.3	37.3	4788660.0	67765026.9	7.38%
150	0.95	1	18000	0.35	37.3	4806832.5	51223432.8	6.78%
151	0.95	1	20250	0.25	36.1	4228999.8	34172359.8	6.27%
152	0.95	1	20250	0.3	36.1	4893023.1	66089692.5	7.29%
153	1	0	13500	0.6	43.8	4355728.9	-21984028.9	4.25%
154	1	0	13500	0.7	43.8	4356606.1	-53202009.9	3.22%
155	1	0	18000	0.1	40.7	1430984.2	-107478573.4	-0.68%
156	1	0	18000	0.2	40.7	3207341.7	-518034.0	4.98%
157	1	0	18000	0.3	40.7	4556575.7	67756939.4	7.41%
158	1	0	18000	0.4	40.7	4569854.2	33972645.5	6.17%
159	1	0	18000	0.5	40.7	4554466.1	-2062995.5	4.93%
160	1	0	18000	0.6	40.7	4553040.4	-37065477.3	3.78%
161	1	0	18000	0.7	40.7	4554416.7	-71882532.2	2.68%
162	1	0	22500	0.1	38.0	1597982.1	-106292879.7	-0.45%
163	1	0	22500	0.2	38.0	3537232.8	9044461.8	5.36%
164	1	0	22500	0.3	38.0	4760298.4	64025289.7	7.21%
165	1	0	22500	0.4	38.0	4762108.5	25725627.8	5.86%
166	1	0	22500	0.5	38.0	4752189.2	-13538836.0	4.56%
167	1	0	22500	0.6	38.0	4750933.7	-52174171.2	3.33%

168	1	0	22500	0.7	38.0	4752064.3	-90646546.9	2.16%
169	1.1	0	0	0.1	62.1	793430.0	-90307697.5	-0.16%
170	1.1	0	0	0.2	62.0	1898298.8	-21712607.5	3.97%
171	1.1	0	0	0.3	62.0	2777720.5	24731474.7	6.05%
172	1.1	0	0	0.4	62.0	3308069.5	44965686.6	6.78%
173	1.1	0	0	0.5	61.9	3313508.9	24398112.7	5.95%
174	1.1	0	0	0.6	61.9	3311296.7	3031190.7	5.12%
175	1.1	0	0	0.7	61.8	3318068.6	-17786477.9	4.33%
176	1.1	0	4500	0.1	57.0	937911.2	-89478400.3	0.03%
177	1.1	0	4500	0.2	57.0	2200385.6	-12121852.2	4.45%
178	1.1	0	4500	0.3	57.0	3215727.5	41357678.5	6.66%
179	1.1	0	4500	0.4	57.0	3507653.1	39946855.8	6.54%
180	1.1	0	4500	0.5	56.9	3498355.3	15084172.0	5.57%
181	1.1	0	4500	0.6	56.9	3501773.2	-8924759.6	4.67%
182	1.1	0	4500	0.7	56.8	3506368.3	-32971156.2	3.79%
183	1.1	0	9000	0.1	52.3	1100618.7	-88423015.7	0.24%
184	1.1	0	9000	0.2	52.2	2536037.6	-1789269.8	4.92%
185	1.1	0	9000	0.3	52.2	3685319.4	58312383.6	7.22%
186	1.1	0	9000	0.4	52.2	3704032.7	32288029.3	6.20%
187	1.1	0	9000	0.5	52.2	3694117.7	3794958.2	5.14%
188	1.1	0	9000	0.6	52.2	3696569.3	-23829250.2	4.14%
189	1.1	0	9000	0.7	52.1	3700401.3	-51460056.0	3.18%
190	1.1	0	13500	0.1	48.2	1265103.4	-87300494.2	0.44%
191	1.1	0	13500	0.2	48.2	2871689.7	8384183.3	5.35%
192	1.1	0	13500	0.3	48.2	3895855.3	55367603.9	7.05%
193	1.1	0	13500	0.4	48.2	3903292.1	24776969.7	5.90%
194	1.1	0	13500	0.5	48.2	3891166.8	-7492349.0	4.73%
195	1.1	0	13500	0.6	48.2	3893470.6	-38741622.0	3.65%
196	1.1	0	13500	0.7	48.2	3896329.1	-70041313.9	2.61%
197	1.1	0	18000	0.1	44.8	1430984.2	-86164673.9	0.63%
198	1.1	0	18000	0.2	44.8	3205946.0	18380386.6	5.73%
199	1.1	0	18000	0.3	44.8	4096102.2	51587664.5	6.86%
200	1.1	0	18000	0.4	44.8	4096312.5	16686525.8	5.59%
201	1.1	0	18000	0.5	44.8	4088885.5	-18837467.9	4.35%
202	1.1	0	18000	0.6	44.7	4090850.3	-53740951.4	3.19%
203	1.1	0	18000	0.7	44.7	4093543.3	-88764938.9	2.07%
204	1.1	0	22500	0.1	41.8	1597982.1	-85018822.6	0.81%
205	1.1	0	22500	0.2	41.8	3532346.7	27701673.6	6.07%
206	1.1	0	22500	0.3	41.8	4296172.7	47630631.4	6.67%
207	1.1	0	22500	0.4	41.8	4292063.5	8749999.2	5.30%
208	1.1	0	22500	0.5	41.8	4286283.6	-30280214.9	3.99%
209	1.1	0	22500	0.6	41.8	4287767.5	-68848961.6	2.76%
210	1.1	0	22500	0.7	41.7	4290155.4	-107758268.9	1.56%

211	1.2	0	0	0.1	67.6	793430.0	-70412254.6	1.14%
212	1.2	0	0	0.2	67.5	1898298.8	-4179465.1	4.81%
213	1.2	0	0	0.3	67.4	2770581.8	40972813.9	6.70%
214	1.2	0	0	0.4	67.4	2861083.8	27880400.3	6.13%
215	1.2	0	0	0.5	67.3	2860725.4	6400178.0	5.26%
216	1.2	0	0	0.6	67.2	2869911.8	-14502814.1	4.43%
217	1.2	0	0	0.7	67.1	2881373.8	-35457985.5	3.62%
218	1.2	0	4500	0.1	62.1	937911.2	-69135750.0	1.32%
219	1.2	0	4500	0.2	62.1	2200385.6	5725513.5	5.25%
220	1.2	0	4500	0.3	62.0	3041812.7	45845452.4	6.83%
221	1.2	0	4500	0.4	62.0	3047394.9	22464748.6	5.88%
222	1.2	0	4500	0.5	61.9	3046855.9	-2101220.8	4.92%
223	1.2	0	4500	0.6	61.9	3053922.9	-26211817.3	4.00%
224	1.2	0	4500	0.7	61.8	3062766.1	-50402336.3	3.11%
225	1.2	0	9000	0.1	57.0	1100618.7	-67814532.7	1.49%
226	1.2	0	9000	0.2	56.9	2534522.5	16320031.4	5.69%
227	1.2	0	9000	0.3	56.9	3236478.9	42503390.2	6.65%
228	1.2	0	9000	0.4	56.9	3239487.3	14858722.4	5.57%
229	1.2	0	9000	0.5	56.8	3238626.8	-13251508.6	4.51%
230	1.2	0	9000	0.6	56.8	3244363.4	-40991568.8	3.50%
231	1.2	0	9000	0.7	56.7	3251907.1	-68804537.3	2.52%
232	1.2	0	13500	0.1	52.6	1265103.4	-66700049.5	1.65%
233	1.2	0	13500	0.2	52.6	2866604.6	26466802.5	6.08%
234	1.2	0	13500	0.3	52.6	3436379.4	38893833.9	6.47%
235	1.2	0	13500	0.4	52.5	3436065.4	7339385.8	5.27%
236	1.2	0	13500	0.5	52.5	3434207.5	-24407723.9	4.12%
237	1.2	0	13500	0.6	52.4	3439176.0	-55743842.7	3.02%
238	1.2	0	13500	0.7	52.4	3445218.6	-87392184.4	1.96%
239	1.2	0	18000	0.1	48.8	1430984.2	-65604988.2	1.79%
240	1.2	0	18000	0.2	48.8	3197570.7	36280468.8	6.42%
241	1.2	0	18000	0.3	48.8	3634335.7	34855905.9	6.28%
242	1.2	0	18000	0.4	48.8	3631627.7	-443905.3	4.98%
243	1.2	0	18000	0.5	48.8	3630938.1	-35691568.2	3.75%
244	1.2	0	18000	0.6	48.7	3635130.2	-70702562.9	2.57%
245	1.2	0	18000	0.7	48.7	3640977.2	-106290935.7	1.42%
246	1.2	0	22500	0.1	45.6	1597982.1	-64523140.2	1.93%
247	1.2	0	22500	0.2	45.5	3511147.4	44661889.3	6.69%
248	1.2	0	22500	0.3	45.6	3831660.6	30757944.7	6.10%
249	1.2	0	22500	0.4	45.5	3829303.6	-8144226.4	4.72%
250	1.2	0	22500	0.5	45.5	3826886.6	-47164719.2	3.40%
251	1.2	0	22500	0.6	45.5	3830373.4	-85963266.4	2.14%